KARADENIZ TECHNICAL UNIVERSITY

THE GRADUATE SCHOOL OF NATURAL ANDAPPLIED SCIENCE

ELECTRICAL AND ELECTRONICS ENGINEERING GRADUATE PROGRAM

ANALYSIS OF EEG SIGNALS IN GAZING AT ROTATING VANES FOR BRAIN COMPUTER INTERFACE

Ph.D. THESIS

Masoud MALEKI, M.Sc.E.

JUNE 2017

TRABZON

KARADENİZ TECHNICAL UNIVERSITY

THE GRADUATE SCHOOL OF NATURAL AND APPLIED SCIENCES

ELECTRICAL AND ELEKTRONICS ENGINEERING GRADUATE PROGRAM

ANALYSIS OF EEG SIGNALS IN GAZING AT ROTATING VANES FOR BRAIN COMPUTER INTERFACE

MASOUD MALEKI, M.Sc.E.

This thesis is accepted to give the degree of
DOCTOR OF PHILOSOPHY
By
The Graduate School of Natural and Applied Sciences at
Karadeniz Technical University

The Date of Submission   : 30 / 05 /2017
The Date of Examination   : 03 / 07 /2017

Thesis Supervisor   : Prof. Dr. Temel KAYIKÇIOĞLU

Trabzon 2017

KARADENİZ TECHNICAL UNIVERSITY

THE GRADUATE SCHOOL OF NATURAL AND APPLIED SCIENCES

ELECTRICAL AND ELEKTRONICS ENGINEERING GRADUATE PROGRAM
Masoud MALEKI

ANALYSIS OF EEG SIGNALS IN GAZING AT ROTATING VANES FOR BRAIN
COMPUTER INTERFACE

Has been accepted as a thesis of

DOCTOR OF PHILOSOPHY

after the Examination by the Jury Assigned by the Administrative Board of the
Graduate School of Natural and Applied Sciences with the Decision Number 1704 dated
03 / 07 / 2017
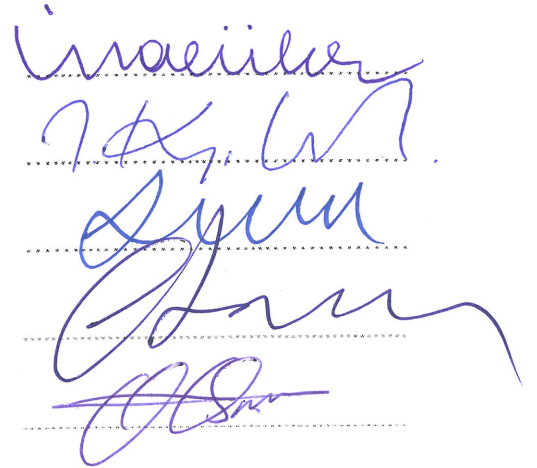
Approved By

Chairman   : Prof. Dr. İnan GÜLER

Member   : Prof. Dr. Temel KAYIKÇIOĞLU

Member   : Prof. Dr. Ali GANGAL

Member   : Prof. Dr. Cemal KÖSE

Member   : Prof. Dr. Onur OSMAN

Prof. Dr. Sadettin KORKMAZ
Director of Graduate School

FOREWORD

Successful completion of this project is the outcome of consistent guidance and assistance from many people, faculty and friends and I am extremely fortunate to have got this all along the completion of the project. I hope this thesis will bring a similar effect on my future studies and it would be benefit for others.

I am very thankful to my supervisor Prof. Dr. Temel KAYIKÇIOĞLU for his valuable help. He is always there to show the right track, when needed his help. It is with the help of his valuable suggestions, guidance and encouragement, that I am able to perform this project work.

Also, special thanks go to my committee members: Prof. Dr. Ali GANGAL and Prof. Dr. Cemal KÖSE for their constructive feedback and timely inspiration in this journey.

I would like to deeply express my sincere thanks to Dr. Mehmet ÖZTÜRK for his support, we would not have been able to finish this project.

Finally, my greatest thanks go to my parents, for their ongoing love and encouragement; I could not have done this without you. This thesis is theirs as well as mine.

Last but not least I most deeply wish to thank my wife Negin and my daughter Roza, for their valuable supports, love and belief in me.

<div align="right">

Masoud MALEKI

Trabzon 2017

</div>

THESIS STATEMENT

I declare that, this PhD thesis, I submitted with the title "Analysis of EEG Signals in Gazing at Rotating Vanes for Brain Computer Interface" has been completed under the guidance of my PhD supervisor Prof. Dr. Temel KAYIKÇIOĞLU. All the data used in this thesis were obtained experimental works done as parts of this thesis in our research labs. All referred information used in the thesis has been indicated in the text and cited in reference list. I have obeyed all research and ethical rules during my research and I accept all responsibily if proven otherwise. 30/05/2017

Masoud MALEKI

TABLE OF CONTENTS

Doktora Tezi

ÖZET

BEYİN BİLGİSAYAR ARAYÜZÜ İÇİN DÖNEN YELKOVANLARIN İZLENMESİ
SIRASINDA EEG SİNYALLERİNİN İNCELENMESİ

Masoud MALEKI

Karadeniz Teknik Üniversitesi
Fen Bilimleri Enstitüsü
Elektrik-Elektronik Mühendisliği Anabilim Dalı
Danışman: Prof. Dr. Temel KAYIKÇIOĞLU
2017, 87 Sayfa, 1 Ek Sayfa

Bir beyin bilgisayar arayüzü insan ve bilgisayar arasındaki iletişimi insan sinir sinyellerini sayısal sinyellere çevirerek sağlamaktadır. Bu tezde EEG tabanlı yeni bir beyin bilgisayar arayüz sistemi dönen yelkovanlara bakarak tasarlanmıştır. Bu sistem beş farklı dönen yelkovanın aynı ekranda gösterimi ve tanımlanmasını öneriyor. Adayların yaş aralığı 20 ila 32 dir. Öznitelikler 0.5, 1 ve 2 saniyelik EEG epoklarından çeşitli yöntemlerle çıkarılmıştır. Bu öznitelikler farklı farklı sınıflandırıcılarla sınıflandırılmış ve sonuçları kıyaslanmıştır. FFT, DWT ve AR model yöntemler özellik çıkarmak için ve SVM, k-NN, LDC ve PLSR ise bu özellikleri sınıflandırmak için kullanılmıştır. PLSR diğer sınıflandırıcılara göre daha iyi sonuç elde etmiştir. T3 kanalının sonuçları ise diğer kanallara göre daha etkilidir. Sadece şu kanalı kullanarak 2 saniyeli epoklarda, önerilen speling sistemi %65 civarında başariya vardı. Önerilen sistemin hızı ise yaklaşik 21 bit/dakika'da dır.

Anahtar Kelimeler: EEG, Beyin bilgisayar arayüzü, Öznitelik çıkarma, Sınıflandırma, Güç spektrumu.

PhD. Thesis

SUMMARY

ANALYSIS OF EEG SIGNALS IN GAZING AT ROTATING VANES FOR BRAIN
COMPUTER INTERFACE

Masoud MALEKI

Karadeniz Technical University
The Graduate School of Natural and Applied Sciences
Electrical-Electronics Engineering Program
Supervisor: Prof. Dr.Temel KAYIKÇIOĞLU
2017, 87 Pages, 1 Appendix Page

A brain computer interface system (BCIs) is a device that translates brain activity into a command for a computer. This thesis proposes a new BCIs based on the gaze on rotating vanes. Our BCIs can identify five different rotating vanes that were shown to the subjects in a screen. The EEG signals were obtained from healthy human subjects in an age group between 20 and 32 years. The features are extracted from the 0.5-sec, 1-sec. and 2-sec. epochs using different methods. These features by different classifiers were classified and the results were compared together. FFT, DWT and AR model to extract features and SVM, k-NN, LDC and PLSR to classify these features were used. PLSR classifier has better classification acuracy in different steps of thesis. Also channel T3 has better results in gazing rotating vanes. By using only this channel, We could classified 2-sec epochs in proposed spelling system, with about %65. Our system's speed is about 21 bits per min.

Key Words: EEG, Brain computer interface, Feature extraction, Classification, Power spectrum

LIST OF FIGURES

LIST OF TABLES

XIII

LIST OF SYMBOLS

BCIs	:	Brain-Computer Interface system
EcoG	:	Electrocorticogram
EEG	:	Electroencephalogram
MEG	:	Magnetoencephalogram
PET	:	Positron Emission Topography
fMRI	:	Functional Magnetic Resonance İmaging
NIRs	:	Near-Infrared Spectroscopy
EMG	:	Electromyogram
MRI	:	Magnetic Resonance İmaging
ADC	:	Analog To Digital Converter
Fp	:	Frontal Pole
C	:	Central
P	:	Parietal
O	:	Occipital
ERS	:	Event-Related Synchronization
Δ	:	Delta
θ	:	Teta
α	:	Alfa
β	:	Beta
γ	:	Gamma
Hz	:	Hertz
μV	:	Micro volt

EOG	:	Electrooculography
ECG	:	Electrocardiography
HCI	:	Human-Computer İnterface
MuCI	:	Muscle-Computer İnterface
MMI	:	Man-Machine İnterface
SSVEP	:	Steady-State Visual Evoked Potential
SCP	:	Slow Cortical Potential
ERP	:	Event Related Potential
ERD	:	Event-Related Desynchronisation
ERS	:	Event-Related Synchronisation
VEP	:	Visual Evoked Potential
SSVEPs	:	Steady-State" Visually Evoked Potentials
K-FCV	:	K-Fold Cross-Validation
CNN	:	Convolutional Neural Network
SMRs	:	Sensorimotor Rhythms
FFT	:	Fast Fourier Transform
DFT	:	Discrete Fourier Transform
DWT	:	Discrete Wavelet Transform
LPF	:	Low Pass Filter
HPF	:	High Pass Filter
cD1	:	Detailed Coefficient Subset
cA1	:	Approximation Coefficient Subset
PLS-DA	:	Partial Least Squares-Discriminant Analysis
PLSR	:	Partial Least Squares Regression

LOO-CV	:	Leave One Out Cross-Validation
SVM	:	Support Vector Machine
K(x,y)	:	Kernel Function
RBF	:	Radial Basis Function
CA	:	Classification Accuracy
TP	:	True Positive
TN	:	True Negative
FP	:	False Positive
FN	:	False Negative
SP	:	Specificity
SE	:	Sensitivity
ITR	:	Information Transfer Rate
CTI	:	Command Transfer Interval
IDWT	:	Inverse Discrete Wavelet Transform
ACA	:	Average Of Classification Accuracy
CAR	:	Common Average Reference
SNR	:	Signal-To-Noise Ratio
LOO-CV	:	Leave One Out Cross-Validation
σ	:	Sigma
LDC	:	Linear Discreaminant Classifier
AD/HD	:	Attention Deficit/Hyperactivity Disorder

1. INTRODUCTION

1.1. Brain Computer Interface System

A Brain-Computer Interface system (BCIs) obtains a straight connection pathway between the brain of a physically disabled patient and an external device or computer. The first aim of BCI research is to create a non-muscular way for physically disabled patients like spinal cord injuries to communicate with and control an external device such as a spelling system for speech or writing a letter [1]. Since the measured activity originates directly from the brain and not from the peripheral systems or muscles, these systems are called a Brain-Computer Interface. In general, there are two categories of BCIs: invasive and non-invasive. Electrocorticogram (ECoG) is an invasive BCI methods that have shown excellent performance in human [2] and monkey [3]. On the other hand, non-invasive BCI methods are more popular because they are lower risk, inexpensive and easily measurable. Non-invasive BCI methods involve electroencephalogram (EEG), magnetoencephalogram (MEG), positron emission topography (PET), functional magnetic resonance imaging (fMRI) and near-infrared spectroscopy (NIRs). Among these non-invasive methods, EEG based BCIs is preferred due to it being practical, cheap and portable. EEG signal provides visual display of the recorded waveform and allows computer aided signal processing techniques to characterize them which further enable us to apply the advanced digital signal processing techniques for analysis of EEG signals [4]. In normal form of peripheral communication or control of a device, we need nerves and muscles. This communication or control starts with the user's intent. This intent triggers a process because certain brain areas are activated by the peripheral nervous system. The signals are sent specifically by the motor pathways to the corresponding muscles. In this case, the user's intent turns perform the movement necessary for the communication or control task. A BCIs provides an alternative way instead of the natural communication and control. A BCIs directly measures brain activity associated with the user's intent and translates them into corresponding control signals for BCI applications. This translation involves signal pre-processing and pattern recognition involve feature extraction and classificatoin, which is typically done by a computer. Many BCI researchers are used the same main identifiers of a BCI system as shown in Figure 1 [5, 6, 7].
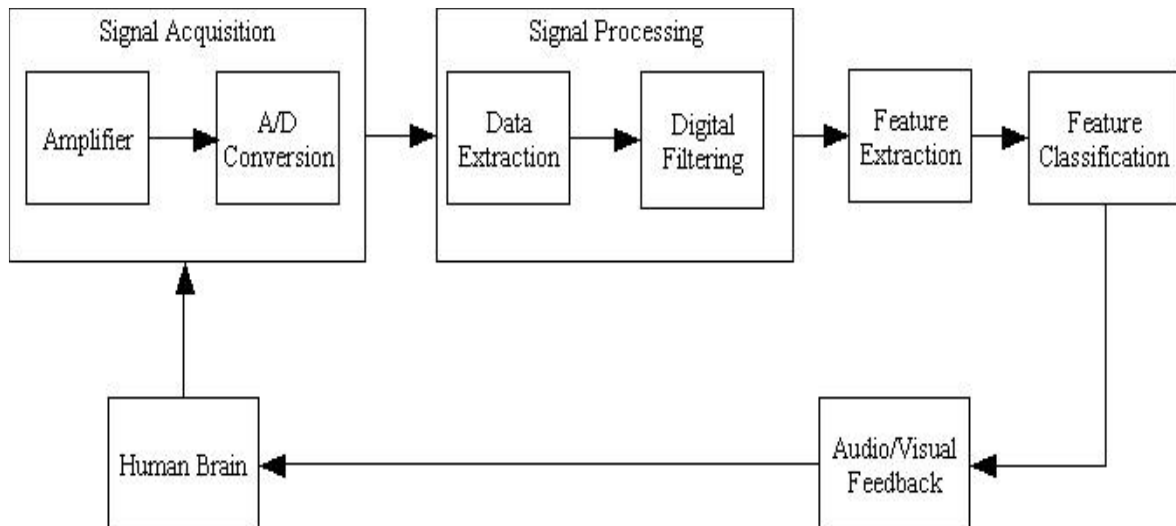
Figure 1. Basic design and operation of any BCI system

In the past few decades, BCI systems have been rapidly developed, because these systems may be the only possible way of communication for people who are unable to communicate via conventional means because of severe motor disabilities. However, in recent years, other industries enter to this area with applications related to biometrics [8], games [9], cursor control [10] etc.

1.2. Our Brain

Our brain is one of the most complex objects that ever studied. In this case, it is still poorly understood. High-level questions such as: "what is a thought?" or "how does the mind work?" remain unanswered, and maybe will remain unanswered for a long time. Instead, the human knowledge about the brain is focused on low-level questions such as: "what kind of cells make up the different parts of the brain?" or "how are these cells interconnected?". The most fundamental component of the brain, and in fact of the whole nervous system, is the neuron. The concept of neuron was introduced by Spanish pathologist Ramon y Cajal in 1911.

1.2.1. Neural Activities

Our Central Nervous System is consist of two types of cells: nerve cells (interneuron) that are the dominant type of neurons in the central nervous system, and glia (output) cells that connect the brain to muscles and sensory organs. Also different areas of the brain connect to each other by these cells. The general structure of most neurons is the same and all of them are consist of axons, dendrites and cell bodies as shown in Figure 2. For transmitting information to other parts of the body, the proteins develope in the cell body. The axon (long cylindrical shaped) transmits the electrical impulse. Dendrites are connected either to the axons or dendrites of other inside cells. They receive the electrical impulse from other nerves cells. Each nerve of human is approximately connected to 10000 other nerves [11]. The electrical activity is mainly due to the current flow between the tip of dendrites and axons, dendrites and dendrites of cells. The level of this signal is in micro-volt range and frequency of it is less than 100Hz [11].
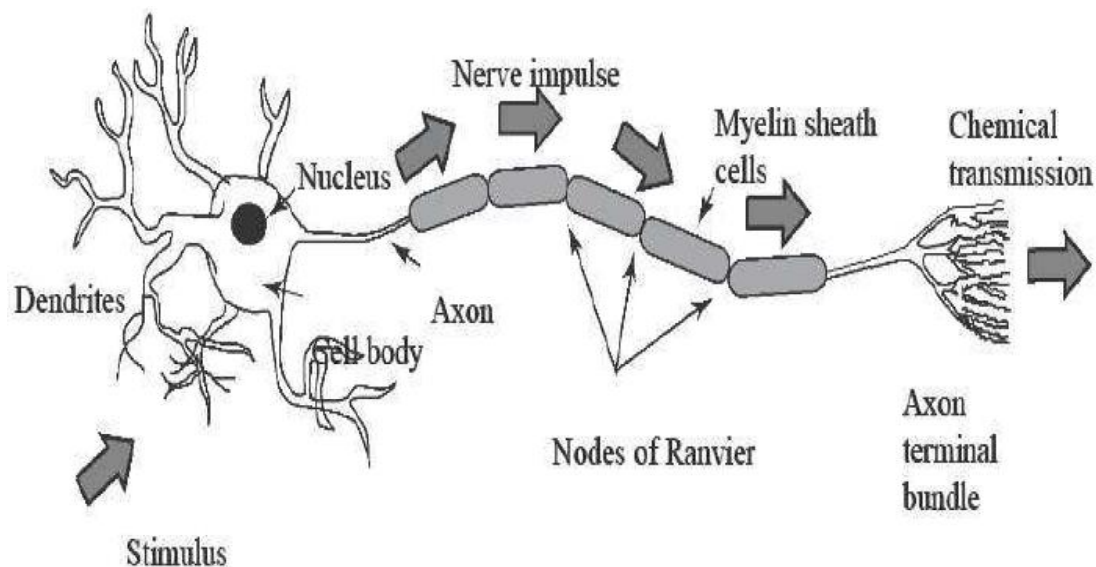
Figure 2. Structure of neuron [11].

This current between the dendrites of nerve cells in the cerebrum region of the brain during their synaptic excitation is called EEG and Current occurs when neurons communicate. This current consists of electric field detected by electroencephalography (EEG) equipment and the magnetic field quantified by electromyogram (EMG) devices [11].

In EEG, brain-related electrical potentials are recorded from the scalp. The simplest event is called action potential, and is a discharge caused by fast opening and closing of Na+ and K+ ion channels in the neuron membrane. If the membrane depolarize to some threshold, the neuron will "fire". Tracking these discharges over time reveals the brain activity. Pairs of conductive electrodes (made of silver) are used to obtain this electricity. The difference in voltage between the electrodes are measured. Since the signals are weak (30-100 microvolt), they have to be amplified.

1.2.2. Brain

There are three distinct parts of the human brain: the large convoluted cerebrum, the rippled cerebellum and the brain stem. These three parts are shown in Figure 3. We are mostly interested in the analysis of electrical signals emanating from the layer surrounding layer of cerebrum as called the cerebral cortex. The cerebrum is divided into two similar structures, the left and the right hemisphere. The left hemisphere senses information and controls movements from the right side of the body and right hemisphere senses information and controls movements from the left side of the body. Two hemispheres weigh (together) is about 1.4 kg and occupy most of the interior of the skull. There are the number at more than 100 billion (10^{11}) neurons in two hemisphere. As is said, each neuron is connected to as many as 10 thousand (10^4) other neurons. The cortex is center for higher order functions of the brain such as vision, hearing, motion control, sensing and planning. Also these functions are localized means that different areas of the cortex are responsible for diferent functions [12]. The cortex has about 5 millimeters thick. Figure 4 shows the map with a few important areas marked out.
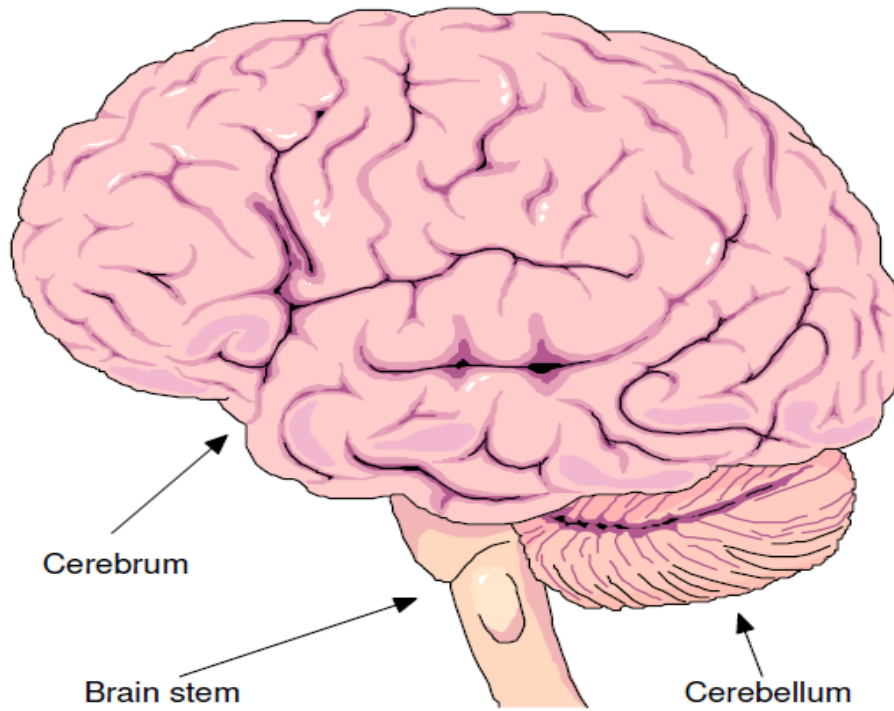
Figure 3. parts of the human brain [11].
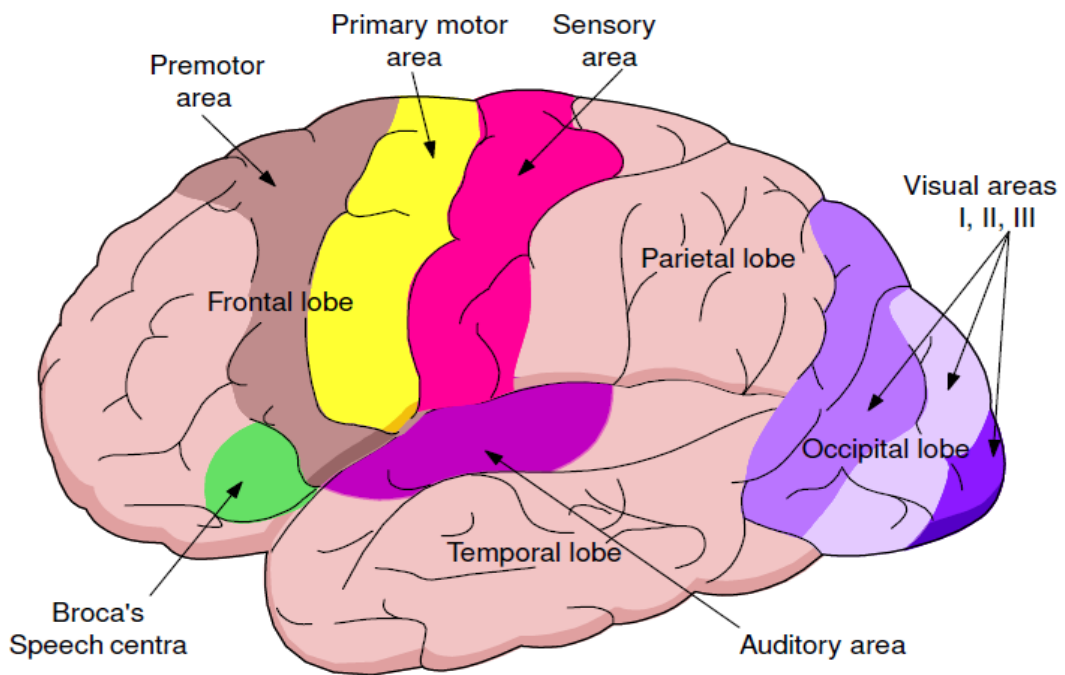
Figure 4. The functionality of different areas of the cerebral cortex [11].

1.3. EEG

Our brain has three different regions namely: cerebrum, cerebellum and brain stem. Each of these regions represent different status of our body. For example the cerebellum region represents initiation of movement, consciousness and state of mind. Also the cerebellum region plays an important role in voluntary action like muscle related movement. The brain stem region control the respiration functioning, heart regulation and neural hormones. In this case, it is very much clear that the EEG signal certainly expresses the status of whole body and brain disorder [11,13].

The English physician Richard Caton, in 1875, discovered that the brain generated electrical potentials. Caton researched about the brains of cats and monkeys using electrodes probing directly on the exposed cortexes of animals. There were no electronic amplifiers at that time and the probes were connected to simple galvanometers with optical magnification. A German psychiatrist named Hans Berger, discovered electroencephalography (EEG) about 80 years ago, in 1929. He said it is possible to record the electric currents generated in the brain, without opening the skull, and to plot them graphically on paper. This form of recording was named electroencephalogram (EEG). Later Berger also found that the EEG varies with the mental state of the patient. After this revolution, new methods for exploring EEG have been found and a new field of medical science as clinical neurophysiology was discoverd. These methods categorize into two main groups: Invasive and non-invasive. An invasive method is based on physical implants of electrodes in humans or animals. Using this method, we can measure single neurons or very local field potentials. A non-invasive method makes use of magnetic resonance imaging (MRI) and EEG technology. Both of these methods give different perspectives and enable us to look inside the brain and to observe what happens in different time and lobe of brain [14].

1.3.1. EEG Signal Recording

The first electrical alteration was distinguished by using a simple galvanometer. But recent EEG systems are consist of multiple electrodes, amplifiers single for each channel to amplify the attenuated signals and followed by filters to remove the system noise and registers [11,13]. EEG is most often recorded from many electrodes on the scalp with a

conductive gel or paste and a common standard for describing position of electrode is the International 10-20 System for most clinical and research applications [15]. The measured signal from the scalp is in the range of microvolt thus amplifier is used. Then analog signal converts to digital signal by using the Analog to Digital Converter (ADC). Finally personal computer or relevant device stores and displays recorded signal. The bandwidth of EEG signal is 0.1-100 Hz, so, the minimum 200 samples/sec are required for sampling to satisfy the Nyquist criterion. Sometimes, the lower sampling rate of 128 samples/sec is used. In this case, only 64 Hz of signal can be used. Sometimes, the higher sampling rate of 2000 samples/sec is used for getting high resolution of EEG signals.

1.3.1.1. Equipment

Electrodes: The purpose of an electrode is to transfer electrical impulses from a recording site to the input of the recorder. In clinical, used electrodes are surface electrodes consisting of small metal discs. The clip electrode is a special form of surface electrode that can be used to detect signals from the earlobes, as shown in Figure 5. The discs of a surface electrode are usually made of gold or silver, coated with a thin layer of silver chloride, platinum or some other metal that does not interact chemically with the scalp. Needle electrodes are another type of electrodes that are inserted under the skin.

The electrical contact is very important issue in recording of EEG. It is desirable to keep the impedance below 10 k-ohm. Clean electrodes and skin (using with alcohol) can be decrease of impedance. To further reduce the impedance several types of contact gels and pastes have been developed that can be applied between the skin and the electrode. The paste increases the conductivity of the skin and helps keeping the electrode in place.
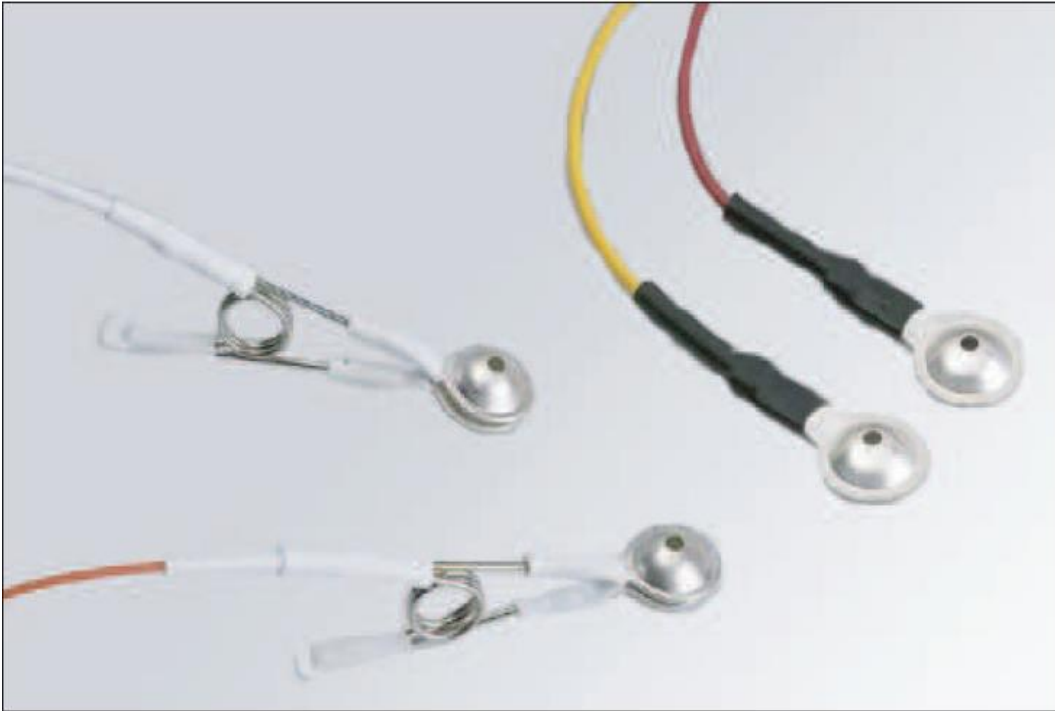
Figure 5. The commonly most used electrodes in clinical EEG are surface electrodes in form of metal discs (attached directly on the skull) or in form of clips (used for earlobes).

Filters: To eliminate the noises, almost any EEG amplifier has a set of filters integrated with the amplifiers. To remove DC-components, a high-pass filter is used. Also to remove high frequency noise, a low-pass filter is used. A notch filter is used to eliminate the most common electrical artifact, interference from equipment powered by alternating current, around 50/60 Hz is provided in EEG amplifier.

Amplifiers: the EEG signals can be detected on the scalp have a few hundred microvolts (maximum amplitude). In this case, the gain of the amplifier has to be very high, such as 10.000 or more. In most EEG amplifiers (called differential amplifiers) the output is generated by the difference between two inputs that are related to the same reference. This property makes the amplifier less sensitive to noise.

1.3.1.2. The 10-20 System

Different regions of the cortex have different functionality because each lobe of brain has a different duty, so the recorded signal by electrodes can vary greatly depending on the

position of the electrode. To compare recordings made by various researchers and be able to repeat previously made experiments, an international group of neurophysiologists in 1947 set out to develop a standard for the placement of EEG electrodes. Four important design principles were agreed upon as following:

- The electrode positions should be measured from standard positions on the skull that can be easily detected in any subject, for example the nasion, the point where the nose meets the forehead.

- All parts of the head should be represented with name-given positions.

- The names should be in terms of brain areas instead of just numbers to make it possible for a non-specialist to understand.

- Studies should be made to determine the functionality of the part of the cortex underlying each electrode. The electrode should be named thereafter.

- Herbert Jasper presented a system at a conference in Paris, [16] and named it "the 10-20 system", and this system is now the most widely used standard for EEG electrode placement. The system works as follows.

The positions in the anterior-posterior direction is based on the distance over the center of the scalp between the nasion, the root of the nose, and the inion, the small protuberance of the skull at the back of the head. The first point is called the frontal pole (Fp) and is placed 10% of the nasion-inion distance from the nasion. The following points are named: frontal (F), central (C), parietal (P) and occipital (O), and are positioned 20% of the distance from each other with the F-point 20% away from the Fp-point. That leaves 10% between the O-point and the inion. Local of electrodes based on this system are shown in Figure 6. Simultaneous recorded EEG from six channels (in various lobe of skull) is shown in Figure 7. These channels involve Fp2, F8, T3, T4, Pz and O2.
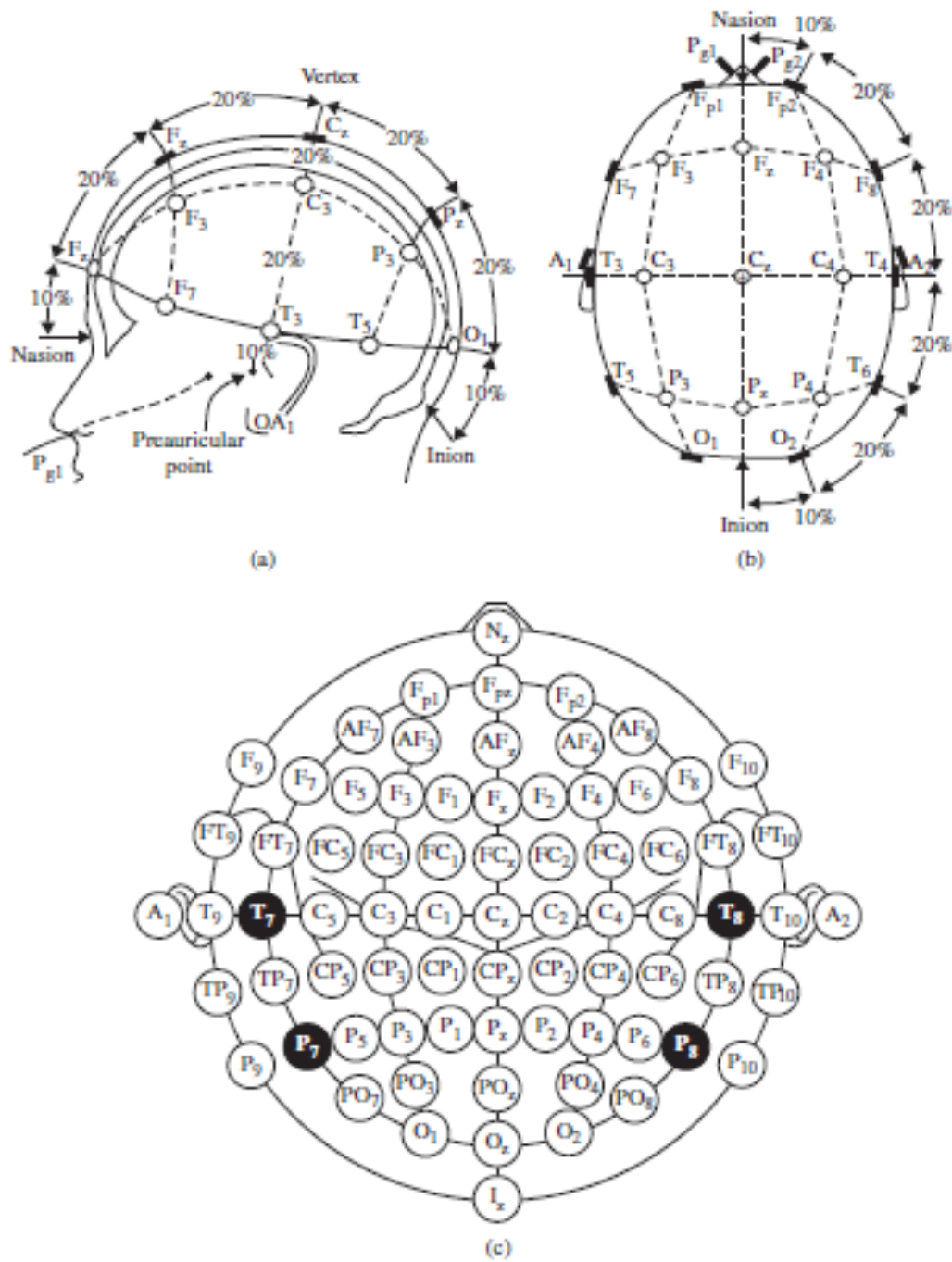
Figure 6. A diagrammatic representation of 10–20 electrode setting, (A) Division of the midline between nasion and inion, (B) Top view of the skull illustrating electrode positions (represent the three-dimensional measures), (C) A two-dimensional view of the electrodes setup configuration [11].
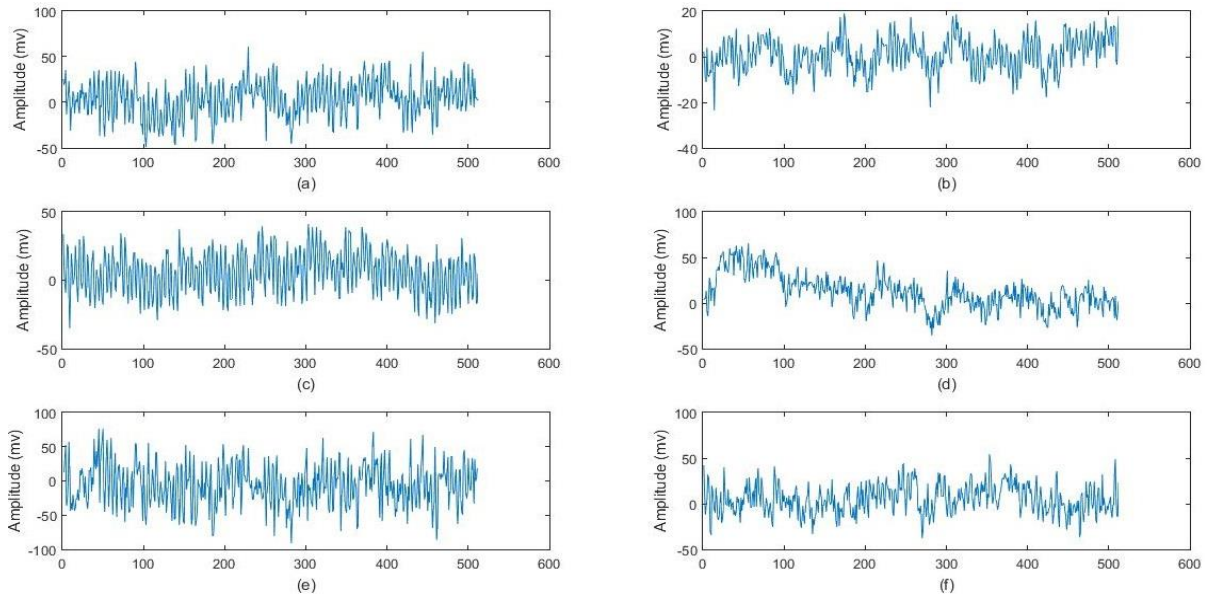
Figure 7. Simultaneous recorded EEG from six channels: (a) Fp2, (b) F8, (c) T3, (d) T4, (e) Pz and (f) O2.

1.3.2. Rhythms of the Brain

The neurons of the cerebral cortex are active any time even when the subject for example is asleep. So it is possible to observe these changes in EEG at any time. The waves are usually categorized based on their frequency content. The first band to be discovered was the alpha band and then followed the beta, theta and delta bands.

Figure 8 shows the most used frequency bands (five typical dominant brain normal rhythms), from low to high frequencies. Also their relations, of the human brain wave activity are shown in Figure 9. A summary of brain rhythms are in below and also we compact them in Table 1.
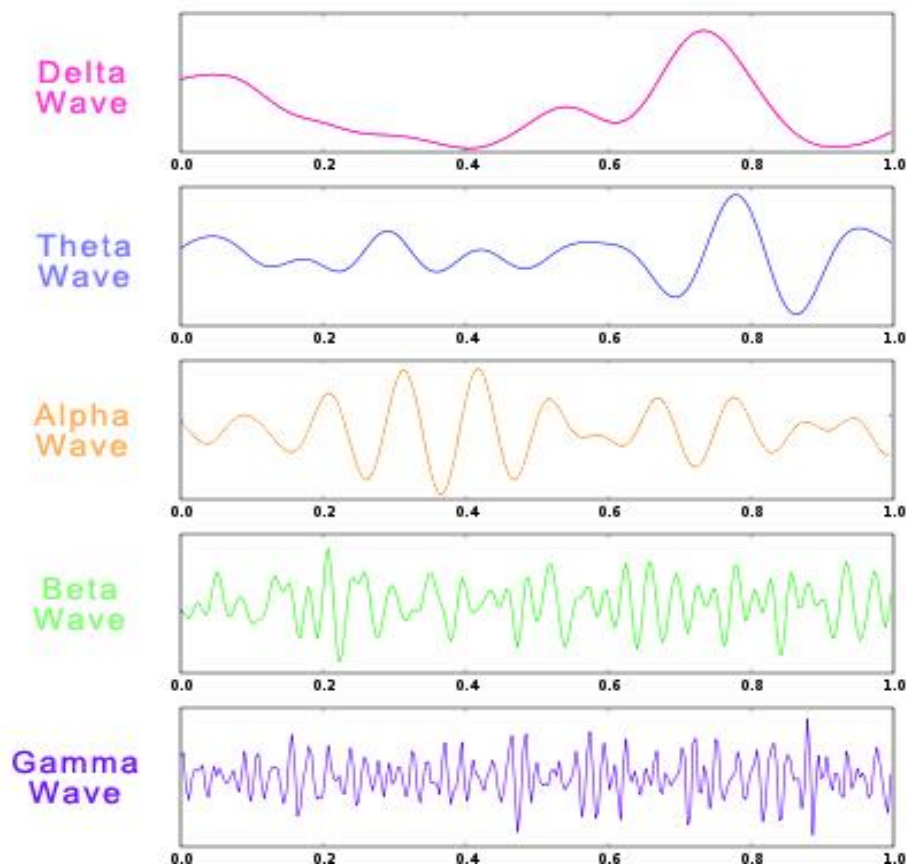
Figure 8. Five typical dominant brain normal rhythms, from low to high frequencies.

Delta waves: Delta waves frequency is between 0.5 and 4 Hz. They are slowest waves with highest amplitude, sometimes over 100 microvolt. They are prevailing rhythm in infants up to one year. Also they occur in adults during deep sleep [17].

Theta waves: It is a slow wave in the frequency range from 4 Hz to 7 Hz. It emerges with closing of the eyes, light sleep and with relaxation. It is normally found in young children or arousal in older children and adults. Most of the waves can be found in the parietal and temporal regions, and their amplitude is usually less than 100 microvolt. Theta waves represent the fine line between being awake or in a sleep state. Theta arises from emotional stress, especially frustration or disappointment [18]. It has also been associated with access to unconscious material, creative inspiration and deep meditation. High levels of theta are considered abnormal in adults, and is, for instance, much related to Attention Deficit/Hyperactivity Disorder (AD/HD) [19].

Alpha waves: Alpha waves have frequency range between 7 Hz until 12 Hz and it is most commonly seen in adults. This activity occurs rhythmically on both sides of the head but are often slightly higher in amplitude on the nondominant side, especially in right-handed individuals. Alpha waves are most profound in the occipital and frontal lobes. Alpha waves are slower and associated with relaxation (disengagement) and closing eyes. It disappears normally with opening eyes or stress position. Thinking of something peaceful with eyes closed should give an increase of alpha activity. Several studies have found a significantly rise in alpha power after smoking marijuana [20].

Beta waves: Beta waves are fast having small amplitude and lie in the frequency range from 12 Hz to 30 Hz. Sometimes, these waves are divided into B1 and B2 to get a more specific range. In the persons who are alert, anxious or who have their eyes open, these waves are the dominant rhythm. When resisting or suppressing movement, or solving a math task, there is an increase of beta activity [21]. Beta waves usually seen on both sides in symmetrical distribution and is most evident in frontal lobe and central portion of the brain. It may be absent or reduced in areas of cortical damage. The amplitude of beta wave is less than 30 µV. It is generally regarded as a normal rhythm and observed in all age groups. In one study by Rangaswamy et al. [22], significantly increased beta power was found in all of the 307 alcohol-dependent subjects, measured across the whole scalp. This leads to an hyper-excitable state which consumption of alcohol temporarily alleviates.

Gamma waves: It is fastest waves of brain having frequency range of 30 Hz and up with very low amplitude. It is also called as fast beta waves. The detection of these rhythms plays an important role in finding the neurological diseases. These waves generally occured in front central part of the brain. It suggests the event-related synchronization (ERS) of the brain [11] because it is thought that reflects the mechanism of consciousness. Beta and gamma waves together have been associated with attention, perception, and cognition [22].

MU: It is associated with motor activities, and is also found in the alpha wave frequency range, but where the maximum amplitude is recorded over motor cortex. So it basically triggers when there is an actual movement or there is an intent to move [23].

Table 1. Summary of EEG bands

Waves	Frequency range (Hz)	Amplitude range (μV)
Delta (δ)	0.5 - 4	over 100 (1 - 120)
Teta (θ)	4 - 7	less than 100 (20 - 100)
Alfa (α)	7 - 12	30-50
Beta (β)	12 - 30	less than 30 (5 - 30)
Gamma (γ)	Up to 30	Variable
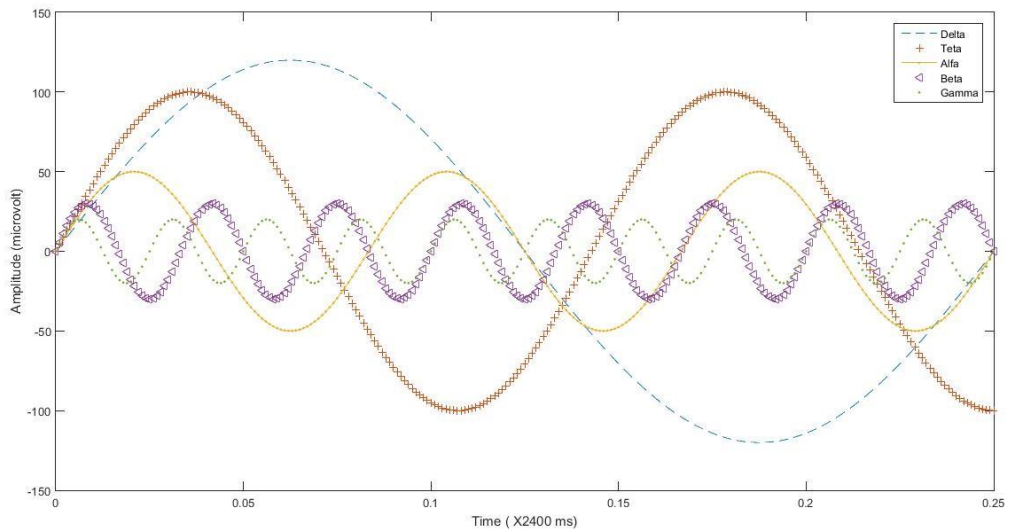
Figure 9. The 5 main frequency bands and their relation to each other.

1.3.3. Artifacts in EEG

Artifacts are undesirable signals that origin is not cerebral but contaminate the EEG signals. Artifacts may reduce the performance of EEG signals, because the shape of neurological phenomenon is affected. Artifacts may be classified into two major categories: physiological artifacts and non-physiological (technical artifacts).

Physiological artifacts are usually due to muscular, ocular and heart activity, known as electromyography (EMG), electrooculography (EOG), and electrocardiography (ECG) artifacts respectively [24].

- EMG artifacts cause large disturbances in brain signals. They come from electrical activity caused by muscle contractions, which occur when subject is talking, chewing or swallowing.

- Blinking and eye movements produced EOG artifacts. Blinking makes generally high-amplitude patterns over EEG signals in contrast to eye movements which produce low-frequency patterns. These electrical patterns are due to the potential difference between the cornea and the retina, as their respective charges are positive and negative. For that reason, the electric field around the eye changes when this dipole moves. EOG artifacts mostly effect in the frontal area, because they are approximately attenuated according to the square of the distance [25].

- ECG artifacts, which reflect heart activity, introduce a rhythmic signal into brain activity [24].

Mainly, line interference, equipment malfunction or result from poor electrode contact create technical artifacts. Incorrect gain, offset or filter settings for the amplifier will cause clipping, saturation or distortion of the recorded signals. We can aviod Technical artifacts by proper apparatus setup, meticulous inspection of equipment and consistent monitoring.

In many studies, researchers, Instead of avoided, rejected or removed artifacts from recordings of EEG signals, try to acquire and process artifacts to offer a communication path that either disabled or healthy people can use in many tasks and in different environments look like a BCIs. These kind of systems are not a BCIs, because communication is not independent of peripheral nerves and muscles. EMG computer interface [26], human-computer interface (HCI) [27], EMG-based human-computer interface [28], EMG-Based Human-Machine Interface [29], EMG-based human-robot interface [30], muscle-computer interface (MuCI) [31], man-machine interface (MMI) [32], and biocontroller interface [33] are different terms that used to name communication interfaces in the scientific literature that can employ artifact signals, among others. These systems usually have greater reliability than BCIs, but they cannot be used by severely disabled people with strong constraints in voluntary movements.

1.4. Brain-Computer Interface System

1.4.1. Application of BCIs

Brain–computer interface (BCI) is a revolutionary new area that is most useful for the severely disabled individuals for hands-off device control and communication as they create a direct interface from the brain to the external environment, therefore circumventing the use of peripheral muscles and limbs. Another mean, providing a straight connection pathway between the brain of a disabled patient and an external device or computer is called brain-computer interface system [34]. The BCI research seeks to generate a non-muscular way for physically disabled patients to communicate with others such as a spelling system for speech, or controlling an external device such as wheelchair, prosthesis, etc. These systems may be the only possible solution for people who are unable to communicate via conventional means because of severe motor disabilities [35, 36, 37].

Moreover, in recent years, other industries have appeared in this field, resulting in the spread of a number of applications such as biometrics [8], games [9], cursor control [10], music, etc. For these reasons, BCI systems have been rapidly developed in recent years. Table 2 gives a non-exhaustive list of possible applications of BCI for both disabled and healthy individuals.

Table 2. Examples of possible BCI applications for disabled and healthy individuals

Disabled individuals	Healthy individuals
• Restoring mobility such as to control wheelchair Movement	• Mainly control of external devices such as: ✓ Mouse control in PC when fingers are on the Keyboard ✓ Playing musical instruments by thoughts
• Environmental control such as to control a TV, power beds, thermostats, etc.	
• Prosthetics control (motor control replacement) such as to control artificial limbs	• Virtual reality such as: ✓ Computer games (e.g. Mind Pacman) ✓ Flight/space control (pilots, astronauts)
• Rehabilitative (assistive) control— to restore motor control (e.g.: strengthen/improve weak muscle)	• Biometrics

1.4.2. Kinds of BCI Systems

In general, there are two categories of Brain-Computer Interface Systems (BCIs): invasive and non-invasive methods. Invasive BCI methods such as electrocorticogram (ECoG) that have a good performance in human [38] and monkey [39] but have a infection risk. Non-invasive approaches based on electroencephalogram (EEG), magnetoencephalogram (MEG), positron emission topography (PET), functional magnetic resonance imaging (fMRI) and near-infrared spectroscopy (NIRs) are more popular as it is safer and have a minimal risk of infection. Among these non-invasive methods, EEG-based BCI is preferred due to it being practical, cheap and portable.

1.4.3. EEG-based BCIs

Electroencephalogram (EEG) signals are useful for diagnosing various mental conditions such as epilepsy, memory impairments and sleep disorders. Also EEG signals are often used in BCIs. EEG benefits from the advantages of having lower risk and being inexpensive and easily measurable, which make them applicable and testable on large human population [36, 40]. Additionally, EEG is electrical signals with high temporal resolution and very small

amplitude (in the µV range) which are generated by neuronal activations in the brain. A BCIs records these brain signals and translates them into artificial outputs or commands. In other words, features of EEG signals have acts in a real world. We will focus on EEG-based BCIs in this thesis. Figure 10 shows a block diagram of the components involved in the processing of EEG data to implement a BCIs. Each of these items will be describe in next subsection.
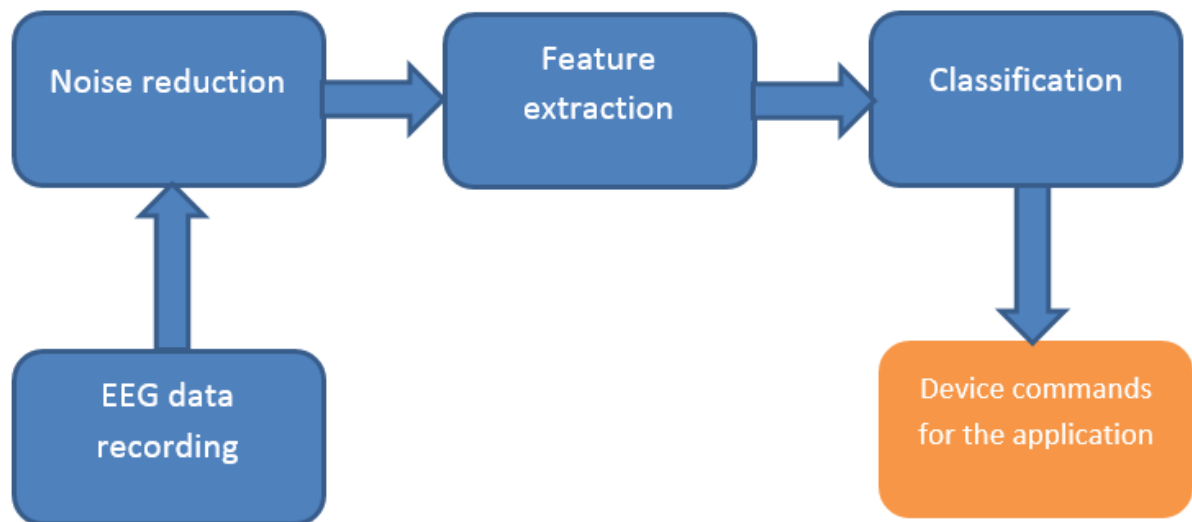
Figure 10. EEG data processing for a BCI

1.4.4. EEG-based BCI Paradigms

In BCI systems, the EEG is obtained based on the system's paradigm. EEG-BCI sytems are generally five types:

- Systems based on visual evoked potential (better known as P300)
- motor imagery
- steady-state visual evoked potential (SSVEP)
- mental tasks
- slow cortical potential (SCP)

Two types of BCI systems are based on Event Related Potential (ERP). Event Related Potentials are specific patterns that occurs in EEG when an auditory or visual stimulus is presented to subject. These include the P300 patterns and Steady State Visual Evoked

Potentials that both of them are used in BCIs. In following, we describe these five systems. Also all these five systems are listed in Table 3, along with some of their main features.

Table 3. Summary of control signals [34]

Signal	Physiological phenomena	Training	Information transfer rate
SSVEP	Brain signal modulations in the visual cortex	No	60–100 bits/min
SCP	Slow voltages shift in the brain signals	Yes	5–12 bits/min
P300 VEP	Positive peaks due to infrequent stimulus	No	20–25 bits/min
Motor Imagery	Modulations in sensorimotor rhythms synchronized to motor activities	Yes	3–35 bits/min
Mental Task	different areas of the brain are activated, so a set of multichannel EEG recordings will have distinct EEG patterns to differentiate the tasks	Yes	3–30 bits/min

1.4.4.1. Paradigm 1- Motor Imagery

Voluntary movements are composed of three steps: planning, execution and recovery. Imaginary movement are known as motor imagery. During motor imagery there is the planning stage that causes a change in EEG. Imagined movements of left side of body (for exapmle left hand) causes a change known as event-related desynchronisation (ERD) in the right motor cortex area, i.e. contralaterally to the imagined movement side and event-related synchronisation (ERS) in the left motor cortex area. Discrimination of these ERD and ERS is used to design a BCIs. ERD and ERS generally occur in alfa (mu 8–12 Hz) and beta (13–20 Hz) frequency bands. ERD is the EEG attenuation in primary and secondary motor cortices during preparatory stage which peaks at movement onset in the contralateral hemisphere while ERS is EEG amplification in ipsilateral hemisphere occurring during the same time [41]. Sometimes, when ERD and ERS occur, there is an increase in EEG energy in gamma frequency band. A simple crude example can be like this: electrode set-up for

measuring motor imagery is consist of two active channels in location C3 and C4. After recording and filtering mu and beta bands of EEG, the energy of EEG from channels C3 and C4 are computed to decide on the movement class:

- if energy of C3EEG > energy of C4EEG: left hand motor imagery
- if energy of C4EEG > energy of C3EEG: right hand motor imagery
- if energy of C3EEG ≈ energy of C4EEG: no motor imagery

1.4.4.2. Paradigm 2 - SSVEP

When our retina is excited by a stimulus flashes at a frequency higher than 6 Hz, our brain generates an electrical activity of the same frequency with its multiples or harmonics. The frequency following effect of the brain that sometimes known as photic response, causes EEG to oscillate in the frequency of the flickering object. This response is spontaneous. The stimulus produces a stable Visual Evoked Potential (VEP) in the human visual system that called as "Steady-State" Visually Evoked Potentials (SSVEPs). In this paradigm, to produce such potentials, the user gazes a target block flickers (for example using LEDs) with a certain frequency on screen [42]. A flickering stimulus of different frequency with a constant intensity can extract SSVEPs with a maximum amplitude in low (5-12 Hz), medium (12-25 Hz) and high (25-50 Hz) frequency bands, separately [43, 44]. It is maximal at the visual cortex, specifically in the occipital region. The detection of the frequency of the EEG is sufficient to detect the focused object. Although there is a recent study that showed the possibility of using SSVEP with eyes closed [45]. In BCI applications, SSVEP are used by presentation of several flickering light sources with different frequencies. In a similar manner, audio-based methods are explored but the results are not as accurate as the visual-based methods.

1.4.4.3. Paradigm 3 - P300 VEP

300–600 ms after visual stimulus a type of EEG occurs that called P300 visual evoked potential (VEP). P300 is maximal in midline locations such as Fz, Cz and Pz and limited to 8 Hz. Therefore a low pass filter is generally used to filter VEP before analyzing. when a target stimulus or a variety of decision making tasks is identified, The wave corresponding

to positive deflection in voltage is evoked. In other words, it means that after an event for example when a picture is recognized, a deflection in the signal should occur after 300ms. Furthermore, the presence, magnitude, topography, and time of P300 are used as metrics of cognitive function in decision making processes. A popular paradigm that used P300 VEP is the Donchin's speller matrix paradigm [46]. It has a screen consists of alphanumeric characters and the rows and columns flash randomly. The row and column containing the target (focused) character will have a higher P300 amplitude compared to row or column that contains the unfocused character. Screenshot of Donchin's speller matrix paradigm are shown in Figure 11. P300 wave is not normally detectable in a single trial of EEG signal, because contamination of EEG signal is high. Hence, detection of P300 wave require averaging from a number of trials. In this Paradigm, the principle is based on the oddball where the frequency of the target stimulus is lower than the non-target stimulus.

A	B	C	D	E	F
G	H	I	J	K	L
M	N	O	P	Q	R
S	T	U	V	W	X
Y	Z	1	2	3	4
5	6	7	8	9	_

Figure 11. Example of P300 VEP paradigm-Donchin's speller matrix

1.4.4.4. Paradigm 4 - Mental Task

In this paradigm, subjects think of different mental tasks. In this case, different areas of the brain are activated, so a set of multichannel EEG recordings will have distinct EEG patterns to differentiate the tasks, which could be used to design a BCI. Mental tasks exhibit inter-hemispheric differences, and hence, the EEG pattern will be separate [47]. For example, computation task such as solving a mathematical problem involves the left hemisphere more while the visual task evoked more activity in the right hemisphere. The separetion of the these activites can be done using asymmetry ratio. The powers of EEG channels in the left and right hemispheres can be compared to decide the activated hemisphere, which can then be used to design a BCIs.

1.4.4.5. Paradigm 5 - SCP

SCP are low frequency potential changes in EEG (about 1–2 Hz) that occur 0.5-10 second after stimulation. Using feedback and reinforcement mechanism we can control SCP. Different tasks can be used to control either the positivity or negativity SCP. For example, cognitive tasks or even inactive relaxed states can generate positivity SCP. Readiness or planning to move can generate negativity SCP. In this case, SCP can be used to generate a binary (On or Off) signal, which can be used as a control mechanism in a BCIs. This Paradigm is not as popular as the other BCIs Paradigms. also in order to give good performance, SCP requires extensive training.

1.4.5. EEG Data Processing for a BCI System

1.4.5.1. Pre-processing

In the pre-processor section, the digital input signal is converted to a form that makes it easier to extract feature and classify. This transformation may include further filtering, noise reduction, normalization, combination of different input channels or other forms of digital signal processing. The objective of noise reduction would be to reduce the noise as much as possible without distorting the signal contents. EEG noises are muscle artifacts, power line

interference and other random noises. Frequency specific filtering using digital filters is commonly used for noise reduction.

1.4.5.2. Feature Extraction

The original EEG signals recorded from the subjects are very large in dimension and also these signals have redundant information that makes complex all signal processing items. To avoid this situation, the original EEG signal is transformed into reduced number of feature vector. Transforming EEG signal into set of feature is called feature extraction. The extracted features give relevant information to the original signal without loss of important information. It means that feauters are successor of EEG signal in low dimensions. The extracted features are classified into respective categories depending on the application.

A minimum number of features always is desirable for the classification. There are two important reasons for this. Firstly, the generalization capability of many classifiers is known to deteriorate when the dimension of the input increases above a certain point. This problem is famous to the curse of dimensionality [48]. Secondly, the training time of classifier (Consequently testing time) normally will grow when the dimension of the input data is large.

Sometimes we need to combine or remove two or more selected features. This is a feature selection. Feature selection means calculating new patterns by combining or removing two or more selected features. Feature selection is as a form of feature extraction. The distinction between selection and extraction is very near, and very often the concepts overlap.

1.4.5.3. Classification

The last section in the BCIs chain is the classifier item. Features, that has been extracted by the mathematical models from raw EEG signals (that pre-processing methods has been implemented about them) are input of classifiers. The classifier is trained to recognize the patterns. In some BCIs feedback of the output to improve the reliability of the system is emploied.

1.4.5.3.1. Binary and Multiple Classifires

Multiclass or multiple classification methods are the methods that can be classified observations into two or more classes. But Some algorithms are by default binary classification algorithms, that means they can only be classified observations into two classes. The binary classification algorithms can be converted to multi class classification by using of two strategies. The training points belong to any one of the M classes used for classification. The basic aim of multiclass classification is to find a function that can classify the data or variables into different classes when used for testing [49]. These two strategies are described in the following subsections.

1.4.5.3.1.1. One-vs-All Classification

In this technique one class is classified to other classes together. If we have N classes, N different binary classifiers have to be built. For the ith classifier, let the positive examples be all the points in class i, and let the negative examples be all the points not in class i. Let fi be the ith classifier. It is classified with Equation 1.

$$f(x) = arg\ max\ f_i(x) \tag{1}$$

1.4.5.3.1.2. All-vs-All Classification

N×(N−1) classifiers are to be built, one classifier for distinguishing each pair of classes i and j. Let fij be the classifier where class i are positive examples and class j are negative. fji=−fji. It is classified using Equation 2.

$$f(x) = arg\ max\left(\sum_j f_{ij}(x)\right) \tag{2}$$

1.4.5.3.2. Classification Training Methods

1.4.5.3.2.1. K-fold Cross-Validation

K-fold cross-validation (K-FCV) is one of the most widely adopted criteria for assessing the performance of a model and for selecting a hypothesis within a class. An advantage of this method, over the simple training-testing data splitting, is the repeated use of the whole available data for both building a learning machine and testing it. Hence, it reduces the risk of (un)lucky splitting [50]. In K-fold cross-validation method, data set is randomly split into K subsets with equal size and the method is repeated K times. Each time, one of the K subsets is used as the validation set and the other K-1 subsets are put together to form the pre-training.

1.4.5.3.2.2. Leave-one-out Cross-Validation

LOO-CV is a particular case of K-FCV with K=N, where N if size of the training set. Hence, the validation sets are all of size one. Like other algorithms, the training data set is divided into two groups. The procedure of LOO-CV method is to take one out of N observations and use the remaining N-1 observations as the training set for deriving the parameters of the classifier [51]. This process is repeated for all N observations to obtain the estimation for the classification accuracy.

1.4.6. BCI in Literature

The main aim of each BCIs is to convert electrophysiological signal (obtained from user) as an input to control external devices as an output [52]. To reach this main aim, different semantic areas have been presented in papers. One of these areas is based on event-related potentials (ERPs), like a P300 wave. Majority of studies based on auditory BCIs have exploited using ERPs as a brain signal [53, 54, 55]. In this BCIs to generate ERPs, Oddball paradigms often are used. The first BCIs based on P300 wave was proposed by Farwell and Donchin in 1988. The detection of P300 visual evoked potential (VEP) by a new method was presented by Hubert et al. [56]. This method is based on a convolutional neural network

(CNN). The proposed method has detected P300 waves in the time domain. The stimulus produces a stable visual evoked potential (VEP) in the human visual system called "steady-state" visually evoked potentials (SSVEPs). Based on this BCIs [42, 43 44], the user gazes a target block flickers with a certain frequency on screen to produce such potentials. In this case, the BCIs can provide many commands. A BCIs based sensorimotor rhythms (SMRs) is another famous method. Based on the SMRs method, a BCIs can offer a high level of control in terms of degrees of freedom as initiated by the intent of users [42]. In a recent study, Rifai et al. [57] used a three-class mental task to control a wheelchair. These three mental tasks were letter composing, arithmetic, and Rubik's cube rolling forward that meant left, right, and forward commands to wheelchair, respectively. The monitoring of eye movement can be used in BCIs. A number of techniques have been used to discern eye movements [58, 59, 60]. Abdelkader et al. [61] proposed an algorithm for recognition of four directions of eye movement from EEG signals. The proposed algorithm obtained the accuracy of %50-85 for twenty subjects using a visual angle of 5°. Another different area in BCIs is tactile BCIs [62, 63, 64].

1.4.7. Challenges in BCI

Comparing the different EEG-based BCIs and their Paradigms show that each method has its strengths and weaknesses. Some of these strengths and weaknesses are given followed at below.

- Motor imagery requires user training and also the response time is slower (the imaginary movement causes changes in EEG to show up typically after a few seconds) but this paradigm circumvents a visual interface and also can be run in the asynchronous mode, thereby allowing the user to turn the system ON/OFF and also use the control mechanism.
- Mental thoughts are similar in this regard but with the brain rapidly changing over time, such EEGbased BCIs will require frequent retraining.
- SSVEP is very robust and requires only a single active channel but require users to gaze at flashing blocks, which is only practical for short periods of time (typically a few minutes). There is also the risk of triggering epilepsy if the flashing frequency is set to be too low.

- P300 VEP also suffers from this risk, though of a lesser degree. Of all the EEG-based BCIs, SCP requires the most extensive training and is less appealing for this reason but gives good performance.

At the moment, the response time of BCI systems and comfort of subjects are two important challenges in the BCI researches. In this case, the BCIs needs to be improved for practical applications in these difficult challenges. SSVEP BCI has relatively good response time with 100 bits/min [34]. However, it cannot be used for long periods of time. Regarding comfort of subjects, gel was commonly used in many studies to improve the conductance between skin and electrode. To solve this problem, dry capacitive electrodes have been proposed, but the quality of the EEG signals in these electrodes is still poor. Using a single channel EEG signal is another way to comfort subjects. Other challenge in this area, is that most of the advances are being tested on healthy subjects and the required adaptation for disabled people. Also many of studies were not in real noisy environments.

As mentioned, in recent years, the focus of BCIs shifted from disabled to other application areas like biometrics, games, virtual reality and indeed music. Many advances in BCIs such as the advent of non-contact electrodes, will allow mind-controlled devices in a future decade because this is very important point that BCIs based EEG still proves to be the most practical, portable and costeffective.

1.5. Object of Thesis

In this thesis, a new fast, simple and comfortable brain–computer interface system is presented based on the gaze on rotating vane-dependent EEG signals. The response time of proposed system when we have four rotating vanes, is about 1 second using a channel EEG signal. This method can be used in application areas such as biomedical (control an electronic device) and clinical engineering (become aware of the subject's state). By using five vanes, we proposed a new spelling system. The present thesis focuses on the following three points:

- Examination and verification of gazing at rotating vanes with different speeds and directions produces different brain waves.

- Proposal of a new fast, simple and convenient BCIs. This system is suitable to be used for real-time applications to control a device.
- Application of proposed system in a novel spelling system

2.   MATERIAL AND METHODS

2.1.   Experimental Setup

2.1.1.   Equipment and Setup of Stimulation Unit

For the development of the BCI system, the EEG signals were acquired by Brain Quick EEG System (Micromed, Italy). The EEG signals were sampled at 512 samples/s and filtered between 0.1 and 120 Hz by a pass-band filter. Also a 50 Hz notch filter, to eliminate line noise, was used. The electrodes were used on the scalp in different locations based on the international 10-20 system. Eighteen EEG electrodes from all lobes of the brain were located according to this system and referenced to the electrode Cz. These electrodes included Fp1, Fp2, F7, F3, Fz, F4, F8, C3, C4, T3, T4, P3, P4, T5, T6, Pz, O1 and O2 as shown in Figure 12. The chair was placed 1 m in front of the monitor. Figure 13 shows the experiment framework and tools.

Using Matlab 2014a, four rotating red vanes in a black screen were designed. Under each vane, the letter of 'A' was written in white. Speed and direction of the rotation could be controlled. Two rotation speeds were defined: one rotation per 5 sec (called slow rotating) and one rotation per 1 sec (called fast rotating). The rotating vanes have these Specifications in order: The first vane rotates slow in an anti-clockwise manner, the second vane rotates slow in an clockwise manner, the third vane rotates fast in anti-clockwise and the forth vane rotates fast in clockwise manners. Screenshot of the rotating vanes is shown in Figure 14.
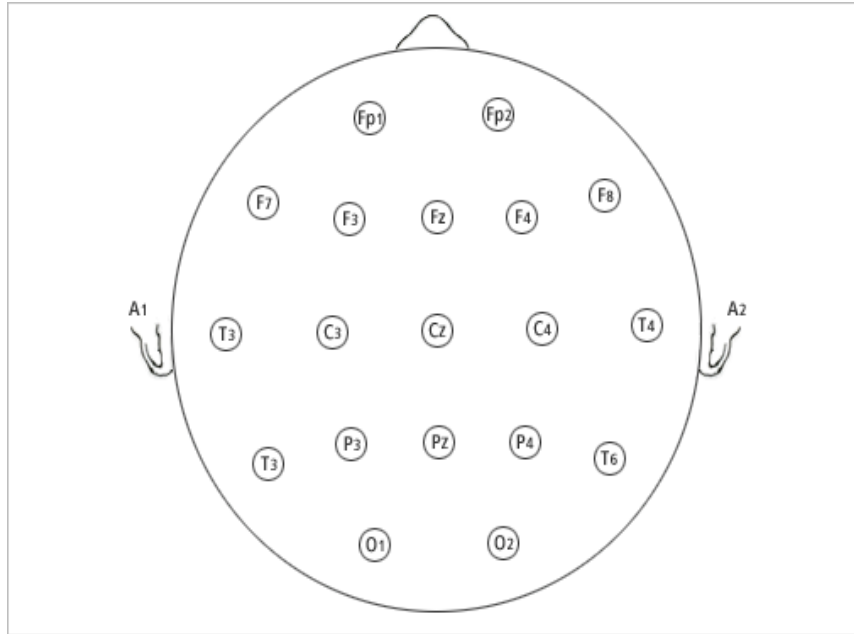
Figure 12. Electrode placement as international 10-20 system and used
electrodes in four different areas of scalp.

(a)
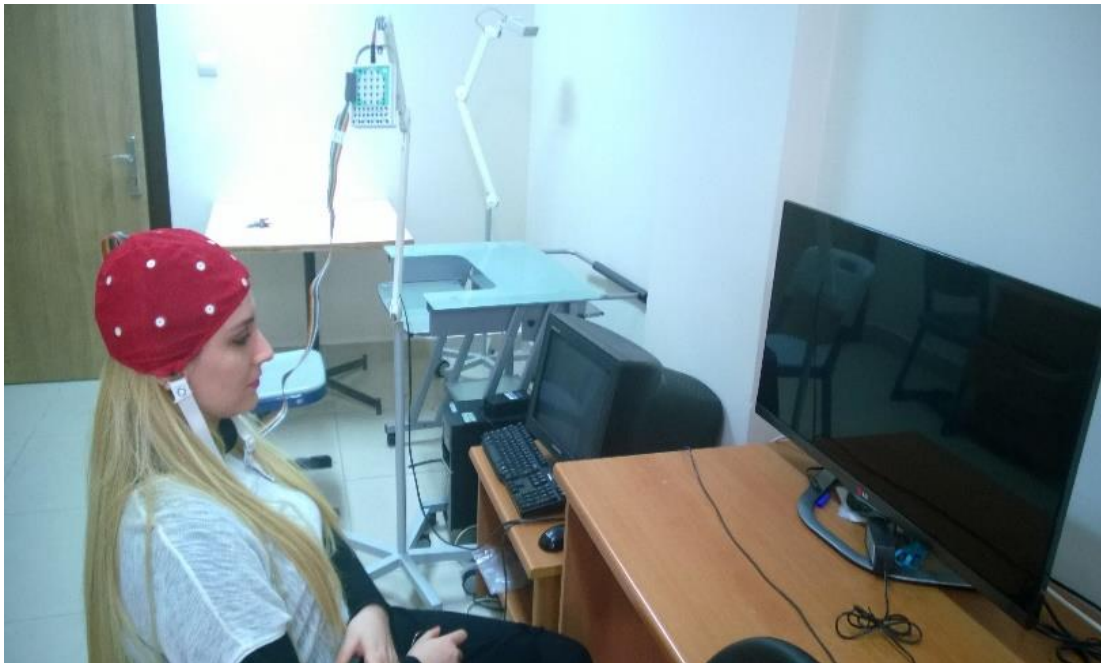
(b)

Figure 13. (a) Brain Quick EEG System (Micromed, Italy), (b) Experiment framework
and tools for EEG recordings.
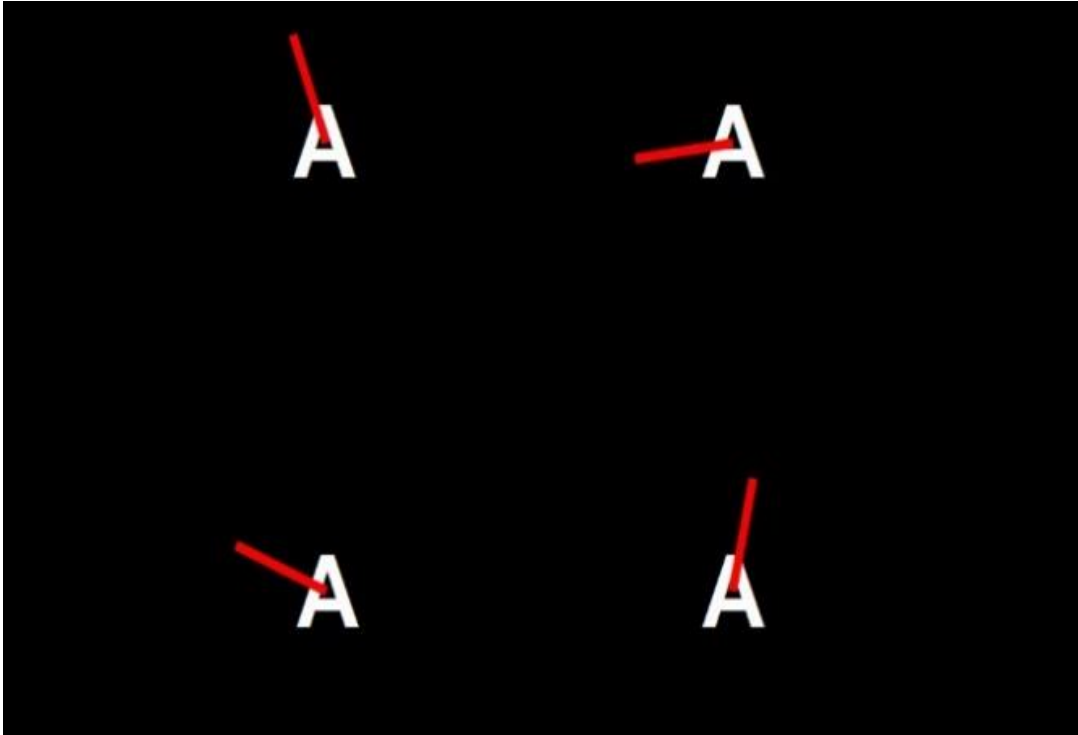
Figure 14. Rotating vanes designed by Matlab

2.1.2. Subjects

EEG signals were obtained from healthy subjects (males and females) in the age groups between 25 and 32 years old at Department of Electrical and Electronics Engineering, Karadeniz Technical University. The volunteers were labeled as: s1, s2, s3… No one had previous experience in using a BCI system. All measurements were in noninvasive method and the volunteers were free to withdraw at any time. Before selection of volunteers, for the precautions, we consulted them about visual problems, headaches, family history with epilepsy and problems related to brain damage. The subjects did not report any problems.

2.1.3. Paradigm

Before beginning to record, the subjects were asked to calm down and relax in a chair for ten seconds. EEG recording was in different sessions. In each session we asked the

subjects that gaze at each vane for 4 min. In each session, each subject gazed at a rotating vane. Afterwards, the subject was asked to gaze the next rotating vane. After each signal recording, there was a 2-min gap for relaxation. To synchronize, before finishing each relaxation time, a beep was issued.

2.1.4. Data Collection Process

In each session, the generated signals (separately for each channel) were divided into 1-sec. and 2-sec. epochs. In this case, we used different window-time to analyze of recording signal. In this way, 240×4 epochs (240 epochs for each speed) were generated per subject. Epochs of each session were divided into two groups, randomly. The first group was called training set (which contained 120 epochs) and the second group was called testing set (which contained 120 epochs). Collection of the data set is described in Table 4. Four raw EEG recorded from four sessions in T3 channel are shown in Figure 15.

Table 4. Selection description of the data set for one subject in a channel

0.5-seconds epochs	1920 epochs in total	480 epochs for session 1, 480 epochs for session 2, 480 epochs for session 3, 480 epochs for session 4,	240 epochs for training set in each session 240 epochs for test set in each session
1-seconds epochs	960 epochs in total	240 epochs for session 1, 240 epochs for session 2, 240 epochs for session 3, 240 epochs for session 4,	120 epochs for training set in each session 120 epochs for test set in each session
2-seconds epochs	480 epochs in total	120 epochs for session 1, 120 epochs for session 2, 120 epochs for session 3, 120 epochs for session 4,	60 epochs for training set in each session 60 epochs for test set in each session
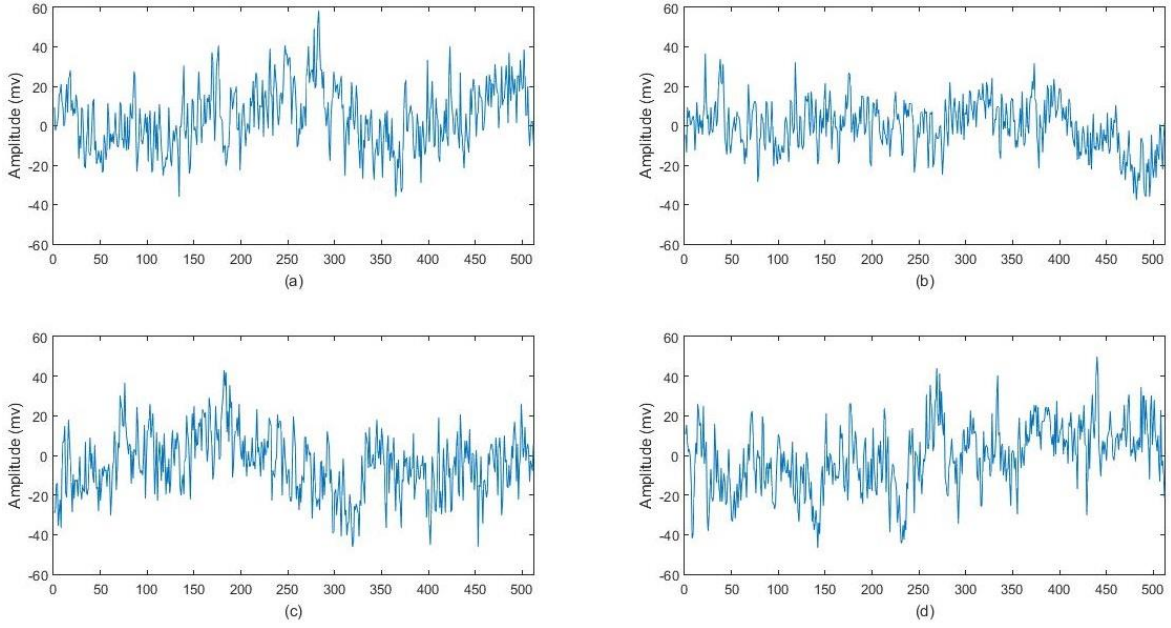
Figure 15. Four raw EEG recorded from four session in T3 channel

2.2. Methods

2.2.1. Pre-prossesing

To be able to compare EEG activity in different individuals or to compare EEG activity between different channels, the signal must be normalized. Moreover, the amplitude of signals can directly influence the classification performance. Therefore, the epochs were normalized between [-1 1] to get similar conditions and to reduce the impact of the magnitude change. In this thesis, a mean normalization process was used for each epoch as Equation 3 [65]. A raw EEG signal and normalized of it based on this method are shown in Figure 16. As we can see, two signals are the same but normalized signal is limited between [-1 1] in amplitude.

$$X_N = \frac{x - \bar{x}}{max|x - \bar{x}|} \tag{3}$$

Here, x, $\bar{x}$, and X_N denote the original epoch, mean of the original epoch and the normalized epoch, respectively.
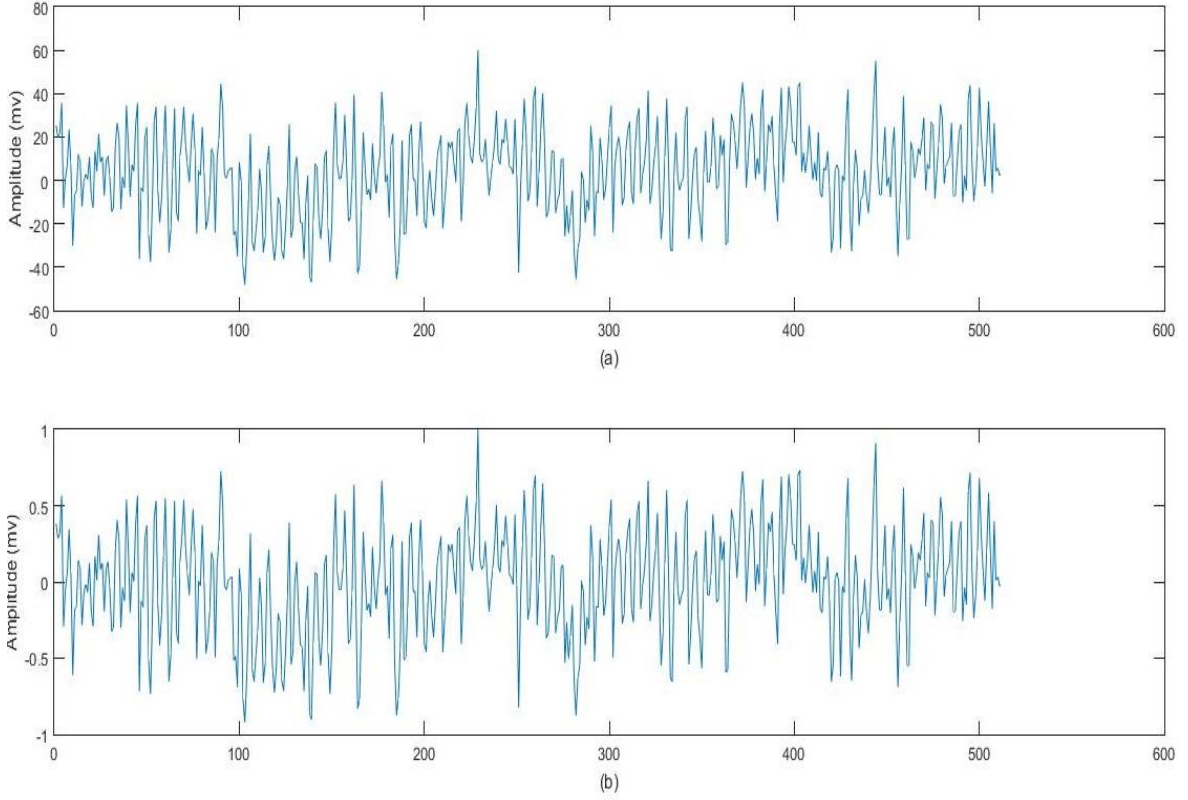
Figure 16. A raw EEG signal and normalized of it, (a) raw EEG signal, (b) normalized EEG signal

2.2.2. Feature Extraction

2.2.2.1. Fast Fourier Transform

The Fourier transform is a method to convert time domain signals into frequency domain that is defined as Equation 4. Discrete Fourier Transform (DFT) converts discrete-time sequences into discrete-frequency versions, which is derived by Equation 5. DFT of discrete-time signals and is widely used for spectrum analysis.

$$X(f) = F\{x(t)\} = \int_{-\infty}^{+\infty} x(t)e^{-j2\pi ft}dt \tag{4}$$

$$X_k = \sum_{i=0}^{n-1} x_i e^{-j2\pi ik/n} \quad \text{for } k=0,1,...,n-1 \tag{5}$$

where in Equation 4, x(t) is the time domain signal and X(f) is its Fourier Transform; in Equation 5, x is the input sequence, X is its DFT, and n is the number of samples [66]. The Fast Fourier Transform (FFT) is an optimized implementation of a DFT, because DFT is computationally very intensive in theory [67].

Since early days, EEG feature extraction and analysis by FFT is known, the representations of the methods based on a Fourier transform have been commonly applied to EEG signals. The disadvantage of the Fourier transform and discrete version of it (FFT), is that they suffer from large noise sensitivity and they need long period data for exactly frequency resolution. In this thesis, non-parametric Welch method to obtain the Power spectrum was used.

This method is consist of the dividing the signal sequence into segments, computing multiplying the segment with an appropriate window and calculation of the periodogram by computing the squared magnitude on the result of its discrete Fourier transform. Individual periodograms obtained are then averaged, resulting in the measurement of power in relation to frequency [68]. Welch method offers reduce noise if compared to the standard periodogram with less computations, but its drawback is the reduction observed in its frequency resolution.

2.2.2.2. Discrete Wavelet Transform

Discrete Wavelet Transform (DWT) has two filters, a low pass filter (LPF) and a high pass filter (HPF). Using these filters, the signal is decomposed into different levels. The output coefficients of the LPF are called Approximation while the output coefficients of the HPF are called Detail. The coefficients of the filters in first level, detailed coefficient subset (cD1) and an approximation coefficient subset (cA1). The Approximation signal can be sent again to the LPF and HPF of the next level for second-level decomposition (cD2 and cA2). This process is repeated until the desired final level is provided. In the wavelet analysis the filter decomposes the signal into frequency bands. In the wavelet synthesis the filter reconstructs the decomposed signal back into the original bands.

The selection of suitable wavelet has an important role in the detection procedure. There are several wavelet families like Harr, Daubechies, Biorthogonal, Coiflets, Symlets, Morlet, Mexican Hat, Meyer etc. and several other Real and Complex wavelets.

2.2.2.3. Auto-Regressive Coefficients

Auto-Regressive Coefficients (AR model) is a powerful and useful tool for signal modelling. In this model, each sample of a given signal is considered a prediction of the previous weighted samples of that signal. The number of coefficients determines the model order. Autoregressive coefficients were estimated with Burg method [69]. The Burg method fits the p'th order AR model to the input signal, x, by minimizing (least squares) the forward and backward prediction errors while constraining AR coefficient, a_i to satisfy the Levinson-Durbin recursion. Equation 6 shows the AR model.

$$x(t) = -\sum_{i=1}^{p} a_i x(t-i) + e(t) \tag{6}$$

2.3. Classification

An algorithm that has to be trained with labelled training samples to be able to distinguish new unlabelled samples in a fixed set of classes is called a classifier. There are many different classifiers that used for classification in BCIs. Three famous classifiers in this area and a new method that are used in this thesis, is described in the following. for visualization of the performance of classifiers, there are many methods. Some performance metrics for classifiers also are defined in the following subsections.

2.3.1. Classifiers

When we have the four-class classification problem it means that chance level is 25%. Four classifiers, involving k-NN, SVM, LDA and PLSR, are used in this thesis. SVM, LDA and PLSR were originally designed for binary classification, so they have to be updated for multi-class problems. For k-NN classifier, we did not have this problem. One way to solve

this problem is to use binary classifier in several items. A multi-class classifier based on the binary classifier is computationally simpler than other methods that investigate classes altogether. To combine the binary classifiers, the one-vs.-one method was used. In this algorithm, a classifier is trained between each pair of classes and in total n×(n-1) binary classifiers are needed for an n-class problem. In testing process, label of a test observation is predicted by majority voting. A summary of four classifiers is given below.

2.3.1.1. Partial Least Squares Regression

Partial least squares regression (PLSR) is a forceful method for multivariate statistical process control when the process variables are highly correlated. Herman Wold developed PLSR in the 1960's as an econometric technique. However, chemical engineers and chemometricians most used this method in their researches. In addition, PLSR has been implemented for monitoring and controlling industrial processes. In prediction area, PLSR does not need to limit the number of measured factors so it can be a useful tool. In 2003, Barker and Rayens proved two points about PLSR:

1) Partial least squares-discriminant analysis (PLS-DA) corresponds to the inverse-least-squares approach to LDA.

2) PLS-DA essentially produces the results of LDA but with the noise reduction and variable selection advantages.

PLSR searches for latent variables with a maximum covariance. These latent variables build a representative model. Selection of the number of latent variables is an important issue. To select the optimal number of latent variables, means of cross validation procedures are usually used by choosing the latent variables which minimise the cross validation error in classification results. The aim of PLSR is firstly to describe a set of such latent variables through the projection of the process and secondly to find quality spaces onto new orthogonal subspaces by maximising the covariance between the two spaces [70, 71].

Data matrix of the process variables is X_{N*M} and data matrix of the quality variables is Y_{N*K}. Data matrixes are recorded for N time points. A number of latent variables is make by linear PLS, say t_j and u_j (j=1,…, A) where A is the number of latent variables and then develop a linear regression model between t_j and u_j by Equation 7.

$$u_j = b_j t_j + e_j \quad (j=1,\ldots, A), \tag{7}$$

where e_j is a vector of errors and b_j is an unknown parameter estimated by Equation 8.

$$\hat{b_j} = (t_j^T t_j)^{-1} t_j^T u_j \tag{8}$$

The latent variables are computed by $u_j = Y_j q_j$, where both w_j and q_j have a unit length and are determined by maximizing the covariance between t_j and u_j. Then, $X_{j+1} = X_j - t_j p_j^T$, where $X_1 = X$ and $p_j = X_j^T t_j/(t_j^T t_j)$, and $Y_{j+1} = Y_j - \hat{b_j} t_j q_j^T$, where $Y_1 = Y$.

If $\hat{u_j} = \hat{b_j} t_j$ be is prediction of u_j, matrices X and Y can be separated into simpler compounds as sum of the following outer products: by Equation 9.

$$X = \sum_{j=1}^{A} t_j p_j^T + E \quad \text{And } Y = \sum_{j=1}^{A} \hat{u_j} q_j^T + F \tag{9}$$

where after extracting the first A pairs of latent variables, E and F are remainders of X and Y [72].

2.3.1.2. k-nearest Neighbor

k-nearest neighbor (k-NN) classification is one of the easy to implement and common algorithms among the existing classification algorithms for statistical pattern recognition [73, 74]. It forms a limited partition X1, X2, . . . , XJ of the sample space X such that an unknown observation x is classified into the jth class if x ∈ Xj. Performance of a nearest neighbor classifier depends on the distance function and value of the neighborhood parameter k. There are several ways for calculating the distance of two points, which include Minkowski distance, Euclidean distance, City block (Manhattan) distance, Canberra

distance, Chebyshev distance, and Bray Curtis distance (Sorensen distance). It is worth mentioning that Euclidean distance method is commonly used in k-NN algorithm. If the observations are not of comparable units and scales, it is meaningful to standardize them before using the Euclidean distance.

The other parameter, which controls the volume of the neighborhood and consequently the smoothness of the density estimates, is k number of neighbors. It plays a very important role in the performance of a nearest neighbor classifier. If k is too small, then the result can be sensitive to noise points; on the other hand, if k is too large, then the neighbors may include too many points from other classes [75]. In many classification studies, selection methods of k have not been stated and, in some studies, k has been selected using trial-and-error method. In the study by Duda et al. [76], the best k was selected using Equation 10 in any data set:

$$m = \sqrt{n} \tag{10}$$

n is the number of observations of training data set and the nearest integer value of m is determined as the best k value. In this algorithm, k is a function of training data set. Enas and Choi [77] accomplished a simulation study and suggested k scaling as $n^{(2/8)}$ or $n^{(3/8)}$. n is also the number of observations of training data set. In this algorithm, value of k also depends on training data set. In brief, no method is dominating the literature and simply setting k=1 or choosing k via cross-validation appears the most popular methods [78]. The advantage of cross-validation is that k-NN classifies testing observations with awareness and acquaintance to training data set; as a result, it influences the misclassification rate. In some papers, empirical algorithms have been used, like K-fold cross validation (K-FCV). The best k value is selected by maximum value of classification accuracy. In some studies k-NN algorithm is trained by K-FCV, in which the best k is selected according to maximum classification accuracy rate [79, 80, 81]. In another paper, Onder A. and Temel K. [82] used leave one out cross-validation (LOO-CV) method to determine optimum k value. They utilized LOO-CV method, since it makes the best use of the available data and avoids the problems of random selections. This algorithm has a high response time when the number of data set is high. In another k selection algorithm, Temel K. and Onder A.[83] used sub-

sampling method. They repeated this method 30 times and computed each classification accuracy for the validation set for different k values. They then selected k of maximum classification accuracy and used it in testing data set. As can be seen from literature, in many studies, the value of k is selected by many trials on the training and validation sets.

2.3.1.3. Linear Discriminant Classifier

Linear Discriminant Classifier (LDC) operates on two classes based on this hypothesis: The classes are under normal distribution with equal covariance matrices. In this case, the separating hyper-plane is generated by finding projection of the labelled training that maximizes the distance between means of the two classes and minimizes the interclass variance. The main aim of LDC is to solve the following problem (Equation 11).

$$y = w^T x + w_0 \tag{11}$$

where x is feature vector. The vectors w^T and w_0 are determined by maximization of the interclass means and minimization of interclass variance [84].

2.3.1.4. Support Vector Machine

Due to its generalization ability among the classifiers, support vector machine (SVM) is one of the most popular supervised learning algorithms [85]. SVM can identify classes using a discriminant hyperplane [86, 87]. The selected hyperplane maximizes the distance from the nearest training points. When SVM classifies through using linear decision boundaries, it is called linear SVM. This classifier has been applied in many synchronous BCI problems [88, 89, 90]. We can create nonlinear decision boundaries by using the kernel trick. It consists to transform input data into a higher-dimensional feature space that can be formulated as a quadratic optimization problem in feature space by using a kernel function K(x,y). In BCI research, the Gaussian or Radial Basis Function (RBF) kernel are generally used with very good results [89, 91]. Equation 12 shows the RBF kernel.

$$K(x,y) = exp(\frac{-|x-y|^2}{2\sigma^2}) \tag{12}$$

As mentioned above, SVM has been applied to multiclass BCI problems using the one-vs.-one strategy. A few parameters of SVM such as width of RBF kernel function σ need to be defined manually. The disadvantage of SVM is that finding optimum σ is highly time consuming. To find best σ value, we searched intervals between 0.1 and 4.5, with step size of 0.2. Moreover, to determine optimum σ value, K-FCV technique was used.

2.3.2. Performance Metrics For Classifier

2.3.2.1. Classification Accuracy

Classification Accuracy (CA) is defined as the number of trials that classified correctly in the test set over the total trials. It is calculated by Equation 13.

$$CA = \frac{TP+TN}{TP+TN+FP+FN} \tag{13}$$

In the binary (two-class) prediction problem, we can define positive and negative classes. In this case a classifier has the following four possible outcomes:

True positive (TP): The number of positive samples correctly predicted.

True negative (TN): The number of negative samples correctly predicted.

False positive (FP): The number of positive samples incorrectly predicted.

False negative (FN): The number of negative samples incorrectly predicted.

2.3.2.2. Sensitivity and Specificity

Sensitivity (SE) and specificity (SP) are calculated by the following formulate, respectively in Equation 14 and Equation 15.

$$\text{Sensitivity} = \frac{TP}{TP+FN} \tag{14}$$

$$\text{Specificity} = \frac{TN}{TN+FP} \tag{15}$$

2.3.2.3. Information Transfer Rate

The Information Transfer Rate (ITR) is one of the most commonly applied metric to assess the overall performance of BCIs [92]. For ITR calculation in BCI research, there are some methods and also new methods are under consideration. The most popular method for ITR calculation in BCI research was defined by Wolpaw et al in 1998. It is a simplified computational model based on Shannon channel theory under several assumptions by Equation 16 [93, 94, 95, 96, 97].

$$B = log_2 N + P log_2 P + (1-P) log_2[(1-P)/(N-1)] \tag{16}$$

where B is the ITR in bit rate means bits per symbol, N is the number of possible choices and P is the probability that the desired choice will be selected, also called target identification accuracy or classifier accuracy. To indicate ITR in bits per min, Equation 17 is used.

$$B_t = B * (60/CTI) \tag{17}$$

The Command Transfer Interval (CTI) was defined as the total experimental time divided by the number of total output digits or letters. In this case, the values of CTI are the Window- length for each epoch and the needed time to convey each symbol.

3. RESULTS AND FINDINGS

This thesis was organized in three section and each section has two subsection. In the first section, we proved that to gaze at rotating vane causes different brain waves. In the second section using this finding we design a new BCIs. And in section three, using this BCIs, we propose a novel spelling system. These three sections are described in the following.

3.1. Demonstrate That To Gaze At Rotating Vane Causes Different Brain Waves

Using Matlab 2014a, a red rotating vane in a black screen was designed. In the center of the screen, the letter of 'A' was written in white. The vane rotated on the letter of 'A'. Speed and direction of the rotation could be controlled. Two rotation speeds were defined: one rotation per 5 sec (called slow rotating) and one rotation per 1 sec (called fast rotating). Screenshot of the rotating vane is shown in Figure 17. To start, EEG signals were obtained from 8 healthy human subjects (5 males and 3 females) in the age groups between 25 and 32 years old at Department of Electrical and Electronics Engineering, Karadeniz Technical University. The electrodes were used on the scalp in different locations based on the international 10-20 system, as mentioned in 2.1.
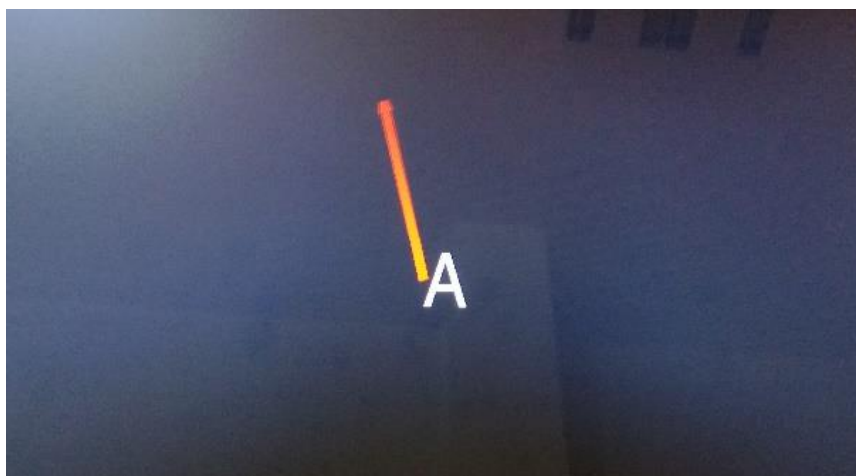
Figure 17. Rotating vane designed by Matlab

EEG recording was in three sessions. In the first session, each subject gazed at the clockwise rotating vane at slow speed for 4 min. There was a 2-min gap for relaxation. Afterwards, the subject was asked to gaze the anti-clockwise rotating vane at fast speed for 4 min and, after 2 min of relaxation, in the third session, the subject gazed at the anti-clockwise rotating vane at slow speed for 4 min. To synchronize, the subject received a beep sound and, at the same time, the vane began to rotate.

Recorded EEG signals in three sessions, were divided into 1 sec. epochs (separately for each channel). In this way, 240×3 epochs (240 epochs for each speed) were generated per subject. Epochs of each session were divided into two groups. The first group was called training set (which contained 120 epochs) and the second group was called testing set (which contained 120 epochs). Also, the proposed method was tested on 2-sec, 3-sec, and 4-sec epochs. Collection of the data set is described in Table 5. We classified the pairwise of three sessions. The results shows the brain waves change in gaze at each rotation vane (in each session). In two approaches, we demonstrate this issue. These approaches are in following.

Table 5. Selection description of the data set for one subject in a channel

1-seconds epochs	720 epochs in total	240 epochs for session 1, 240 epochs for session 2, 240 epochs for session 3,	120 epochs for training set in each session 120 epochs for test set in each session
2-seconds epochs	360 epochs in total	120 epochs for session 1, 120 epochs for session 2, 120 epochs for session 3,	60 epochs for training set in each session 60 epochs for test set in each session
3-seconds epochs	240 epochs in total	80 epochs for session 1, 80 epochs for session 2, 80 epochs for session 3,	40 epochs for training set in each session 40 epochs for test set in each session
4-seconds epochs	180 epochs in total	60 epochs for session 1, 60 epochs for session 2, 60 epochs for session 3,	30 epochs for training set in each session 30 epochs for test set in each session

3.1.1. First Approach; Extracting Feature by FFT and Classification by k-NN

The generated epochs were used for extracting features. As is known, there are 5 frequency rhythms in EEG signals: delta-band, theta-band, alpha-band, beta-band and gamma-band. These bands were extracted by fast Fourier transform method. We used fft( ) function in Matlab for the detection of EEG signal bands. Mean of absolute power of FFT in each epoch was used as features. In this way, for each epoch in one channel, 5 features were extracted and, as mentioned, 18 channels were used. So, 90 (18×5) features were prepared for each epoch.

For classification, k-NN algorithm was used to classify the extracted features from EEG signals. To determine optimum k value, K-fold cross validation (K-FCV) technique was used. Minimum number of epochs in the training set for each speed was 40 (for 4-sec epochs); so, the optimum k value was searched in the interval between 1 and 39 with the

step size of 2. For each subject, we separately trained k-NN classifier. To verify the results, classification was repeated 10 times in each data set with different distributions of training and testing sets. Mean of the classification accuracy and standard deviations for 1-sec, 2-sec, 3-sec, and 4-sec epochs, when vane rotates fast and when it rotates slow in clockwise way, are provided as Table 6. Table 7 shows the classification accuracy when vane rotates fast and slow in anti-clockwise way. Finally, the accuracy of classification, when vane rotated slow in clockwise and slow in anti-clockwise ways, are presented in Table 8.

Table 6. Classification accuracy when vane rotates fast and when it rotates slow in anti-clockwise manner

Subject/Time	1 s	2 s	3 s	4 s
Subject 1	0.816±0.022	0.828±0.029	0.850±0.019	0.866±0.039
Subject 2	0.627±0.019	0.621±0.040	0.585±0.035	0.610±0.069
Subject 3	0.912±0.017	0.945±0.029	0.965±0.005	0.976±0.019
Subject 4	0.784±0.017	0.858±0.026	0.860±0.022	0.890±0.034
Subject 5	0.614±0.030	0.706±0.025	0.702±0.046	0.716±0.011
Subject 6	0.910±0.012	0.915±0.018	0.922±0.022	0.870±0.032
Subject 7	0.565 ±0.026	0.608±0.040	0.592±0.082	0.616±0.042
Subject 8	0.800±0.022	0.808±0.046	0.840±0.036	0.880±0.034

Table 7. Classification accuracy when vane rotates slow in clockwise and fast in anti-clockwise manners

Subject/Time	1 s	2 s	3 s	4 s
Subject 1	0.761±0.042	0.776±0.026	0.780±0.040	0.730±0.044
Subject 2	0.617±0.024	0.623±0.019	0.620±0.054	0.593±0.030
Subject 3	0.864±0.016	0.921±0.029	0.902±0.046	0.906±0.048
Subject 4	0.864±0.016	0.888±0.033	0.887±0.030	0.883±0.021
Subject 5	0.652±0.018	0.700±0.034	0.720±0.050	0.756±0.026
Subject 6	0.887±0.013	0.900±0.029	0.907±0.039	0.930±0.062
Subject 7	0.612±0.030	0.691±0.019	0.675±0.039	0.610±0.095
Subject 8	0.658±0.029	0.731±0.037	0.780±0.014	0.750±0.057

Table 8. Classification accuracy when vane rotates slow in clockwise and slow in anti-clockwise manners

Subject/Time	1 s	2 s	3 s	4 s
Subject 1	0.846±0.013	0.858±0.021	0.827±0.044	0.843±0.069
Subject 2	0.590±0.029	0.595±0.013	0.622± 0.041	0.610± 0.068
Subject 3	0.644±0.017	0.630±0.077	0.675±0.064	0.683±0.082
Subject 4	0.940±0.005	0.941±0.012	0.945±0.019	0.957±0.009
Subject 5	0.806±0.024	0.836±0.049	0.837±0.036	0.907±0.009
Subject 6	0.758±0.020	0.783±0.046	0.837±0.038	0.727±0.058
Subject 7	0.664±0.037	0.691± 0.038	0.695±0.068	0.733±0.021
Subject 8	0.786±0.032	0.801±0.010	0.857±0.027	0.843±0.027

In this first approach we found that:

- Gazing at different rotating vanes cause different brain waves
- Length of Time- window has effect in classification accuracy

3.1.2. Second Approach; Extracting Feature by DWT and Classification by k-NN and LDC

In the second approach, based on findings in the first approach that length of time-window has important effect in classification accuracy, and with considering that time is a important parameter in BCI systems, to increase speed of system, classiffication of 1-sec epochs with another feature extraction and classification methods were presented. Also in this approach, we try to use only five electrodes. Five EEG electrodes from two lobes of brain are selected as shown in Figure 18. These electrodes are involved Fp1 and Fp2 in frontal lobe and Pz, P3 and P4 in parietal lobe. A normalization process was implemented to each epoch in order to reduce the impact of the magnitude change.
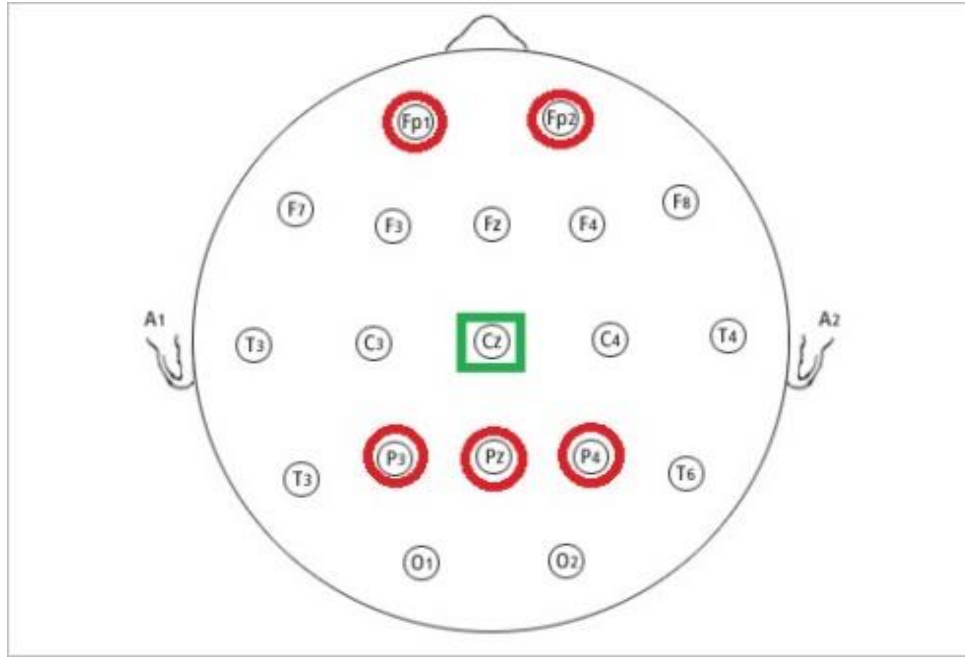
Figure 18. Five used electrodes and a reference electrode Cz.

Discrete wavelet transform was employed to 1-sec as dimensionality reduction technic. The Coiflets wavelet have been chosen for analysis of EEG signal. Seven levels of wavelet decomposition were done in the experiments with consider the fixed sample length at 512 samples. If the decomposition level was set at seven, DWT generates respectively the coefficient subsets at the seventh level approximation (cA7) and the first to the seventh level details (cD1, cD2, cD3, cD4, cD5, cD6 and cD4). After that, each wavelet coefficient subset can be reconstructed to estimate an effective EEG signal component by using the inverse discrete wavelet transform (IDWT). In this approach, the reconstructed EEG signal (D1, D2, ... D7 and A7) were calculated. But we used only D4, D5, D6, D7 and A7 to extract features. Mean, standard deviation, Minimum and Maximum of each these levels were used as featurs. In this case, for each 1-sec epoch, we have provided 20 features from each channel.

Two classifier were implemented for classification of these features, they are k-NN and LDC. The results showed that the LDC classifier is more accurate than k-NN. For each subject, we calculated Performance metrics of each classifier, separately. The classification accuracy of session1&session2 for LDC classifier are provided as Table 9. Table 10 and Table 11 show the classification accuracy of session1&session3 and session2&session3, respectively. In the same as, Table 12, Table 13 and Table 14 show the classification results for k-NN classifier.

Table 9. Classification accuracy of session1 and session2 obtained
from LDC classifier

subjects	CA	SE	SP
Subject 1	83.83	85.13	82.65
Subject 2	75.58	74.43	76.90
Subject 3	77.75	77.90	77.64
Subject 4	93.83	92.78	95.02
Subject 5	94.33	96.38	92.57
Subject 6	80.66	80.00	81.51
Subject 7	84.05	83.99	83.69
Subject 8	82.66	82.52	82.94

Table 10. Classification accuracy of session1 and session3 obtained
from LDC classifier

subjects	CA	SE	SP
Subject 1	78.00	79.67	76.53
Subject 2	82.66	84.09	81.47
Subject 3	68.58	68.88	68.37
Subject 4	87.00	87.34	86.67
Subject 5	75.08	77.19	73.53
Subject 6	80.08	80.03	80.34
Subject 7	77.00	76.65	76.77
Subject 8	74.25	75.53	73.27

Table 11. Classification accuracy of session2 and session3 obtained from LDC classifier

subjects	CA	SE	SP
Subject 1	87.33	89.26	85.76
Subject 2	78.58	79.58	77.70
Subject 3	82.83	82.53	83.18
Subject 4	83.83	85.41	82.71
Subject 5	71.58	71.47	71.77
Subject 6	76.25	75.52	77.09
Subject 7	80.10	81.15	79.00
Subject 8	80.25	80.72	80.14

Table 12. Classification accuracy of session1 and session2 obtained from k-NN classifier

subjects	CA	SE	SP
Subject 1	74.91	81.89	70.90
Subject 2	68.50	65.84	73.36
Subject 3	69.50	74.55	67.00
Subject 4	90.75	85.22	99.22
Subject 5	92.66	93.98	91.94
Subject 6	82.50	79.86	86.20
Subject 7	77.05	79.45	78.56
Subject 8	70.41	72.71	68.76

Table 13. Classification accuracy of session1 and session3 obtained
from k-NN classifier

subjects	CA	SE	SP
Subject 1	70.91	70.79	71.21
Subject 2	73.91	72.44	75.94
Subject 3	58.00	57.38	59.17
Subject 4	82.58	77.34	91.40
Subject 5	75.25	87.58	69.94
Subject 6	78.50	79.57	77.63
Subject 7	72.10	72.55	72.72
Subject 8	62.00	63.44	61.35

Table 14. Classification accuracy of session2 and session3 obtained
from k-NN classifier

subjects	CA	SE	SP
Subject 1	82.41	80.75	84.59
Subject 2	71.58	75.71	68.89
Subject 3	74.00	68.70	85.98
Subject 4	80.50	83.57	78.44
Subject 5	73.83	79.68	70.29
Subject 6	61.83	61.50	62.32
Subject 7	73.80	74.25	74.12
Subject 8	70.41	70.93	70.12

In Table 15, average of each performance metric for seven subject has been calculated.

Table 15. Average of classification accuracy obtained from 8 subjects

	classifiers	CA	SE	SP
Session1 & session2	LDC	**84.09**	84.16	84.17
	k-NN	78.46	79.15	79.63
Session1 & session3	LDC	**77.95**	78.96	77.17
	k-NN	71.95	72.65	72.38
Session2 & session3	LDC	**80.09**	80.64	79.76
	k-NN	73.51	74.41	74.38

In the second approach we found that:

- We can design a new BCIs based on gazing at rotating vane.
- By using different feature extarction and classification methods, we can increase the classification accuracy.
- To comfort subjects, we can decrease electrode numbers.

3.2. Design a Novel BCI System

In this section, based on Experimental Setup in 2.1, we classified four different rotating vanes. In the first approach, we have four subject and in the second approach, we added four other subject to dataset.

3.2.1. First Approach; Extracting Feature by FFT and Classification by k-NN and SVM

In the first approach, we used only 1-sec. Epochs. In this way, 240×4 epochs (240 epochs for each speed) were generated per subject. Collection of the data set is described in Table 4. To verify the results, classification was repeated 10 times and in each time different distributions of training and testing sets was used. Figure 19 shows the flowchart of the proposed classification of EEG method that includes three parts: 1) pre-processing; 2) feature extraction; and 3) classification.

In the proposed novel BCIs, we have the four-class classification problem. For reduction number of channels and the understanding which channels have best performance in the classification, we classified 18 channels, separately. Then based on CA of each channel, seven channels, that they have maximum accuracy, was selected. Using these channels with together, we improved the performance of proposed method.
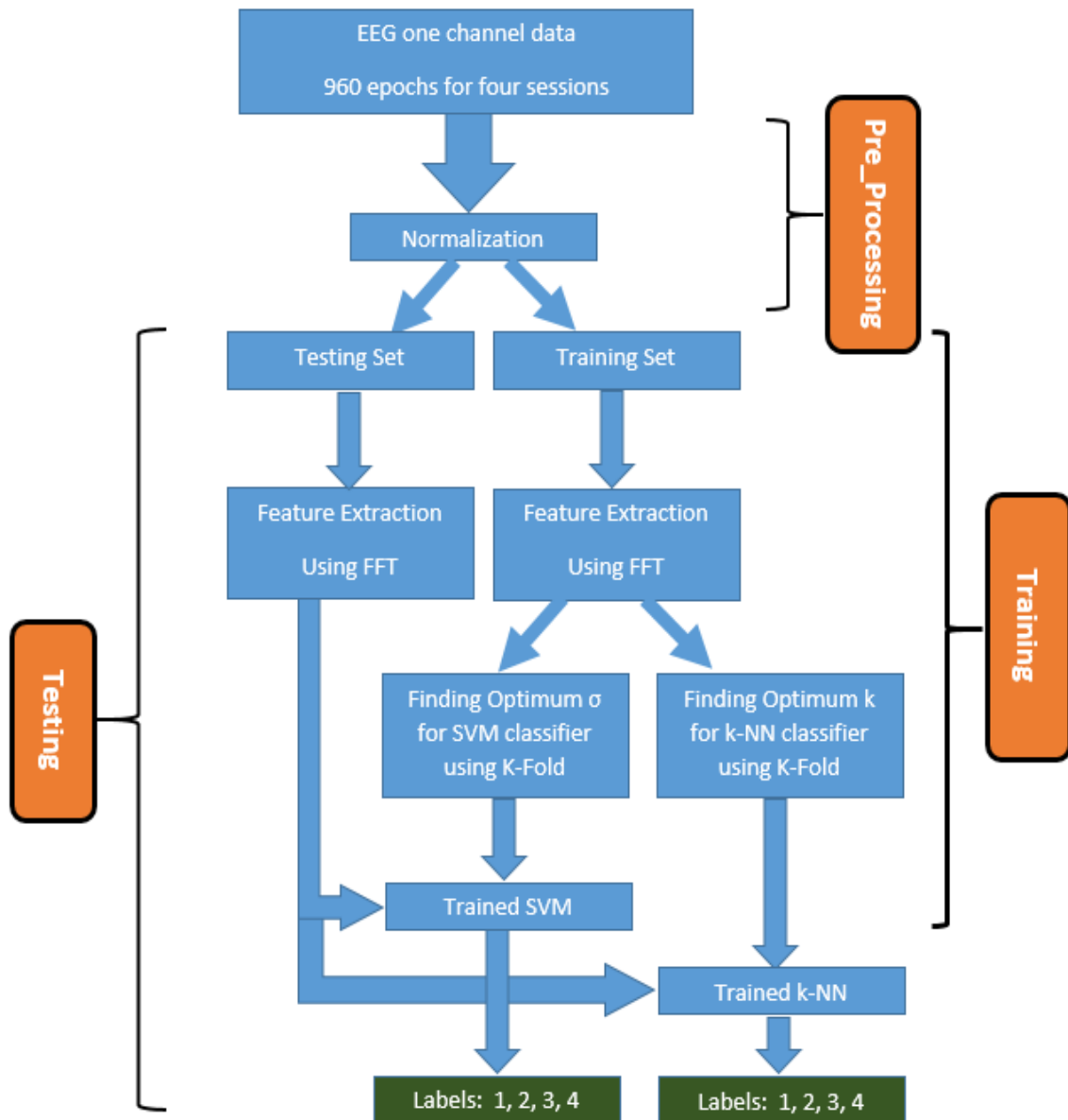
Figure 19. Flow chart of designed System

For each epoch from training set, 5 features using FFT were extracted. SVM and k-NN were selected to classify the features. We separately trained the classifiers using K-FCV to calculate classifiers parameter (k for k-NN and sigma for SVM). Mean of the classification accuracy and standard deviations of classification accuracy for k-NN classifier are provided as Table 16. As is seen in this table, average of classification accuracy (ACA) of each channel for four subjects was calculated. Similarly, Results of Multi-SVM classification are shown in Table 17.

Table 16. Classification accuracy of k-NN for each channel

Channels	Subject 1		Subject 2		Subject 3		Subject 4		Mean of each electrode
	Mean	*std*	*Mean*	*std*	*Mean*	*std*	*Mean*	*std*	
FP1	0.585	0.021	0.504	0.014	0.810	0.014	0.471	0.028	0.592
C3	0.370	0.011	0.439	0.021	0.380	0.012	0.372	0.029	0.390
FZ	0.350	0.020	0.362	0.020	0.500	0.027	0.362	0.021	0.393
C4	0.424	0.011	0.416	0.010	0.363	0.026	0.428	0.023	0.408
F4	0.286	0.018	0.305	0.025	0.540	0.005	0.413	0.027	0.386
F3	0.415	0.017	0.391	0.004	0.486	0.012	0.356	0.016	0.412
F7	0.388	0.023	0.402	0.011	0.487	0.036	0.371	0.013	0.412
F8	0.304	0.022	0.387	0.028	0.620	0.016	0.342	0.023	0.413
FP2	0.357	0.007	0.506	0.018	0.447	0.015	0.377	0.015	0.422
T4	0.385	0.013	0.486	0.015	0.495	0.018	0.373	0.021	0.435
T3	0.371	0.005	0.586	0.012	0.846	0.013	0.356	0.031	0.540
T6	0.407	0.015	0.444	0.011	0.654	0.012	0.346	0.020	0.463
T5	0.335	0.015	0.297	0.026	0.342	0.024	0.353	0.012	0.332
P4	0.668	0.022	0.738	0.013	0.379	0.021	0.360	0.015	0.536
P3	0.310	0.017	0.338	0.023	0.387	0.026	0.368	0.002	0.351
Pz	0.583	0.012	0.612	0.020	0.727	0.009	0.601	0.020	0.631
O2	0.378	0.015	0.378	0.023	0.527	0.015	0.365	0.021	0.412
O1	0.547	0.018	0.479	0.030	0.537	0.013	0.360	0.016	0.481

Table 17. Classification accuracy of Multi-SVM for each channel

Channels	Subject 1		Subject 2		Subject 3		Subject 4		Mean of each electrode
	Mean	*Std.*	*Mean*	*Std.*	*Mean*	*Std.*	*Mean*	*Std.*	
FP1	0.487	0.018	0.362	0.049	0.411	0.025	0.517	0.012	0.444
C3	0.329	0.019	0.412	0.019	0.359	0.056	0.375	0.013	0.369
FZ	0.379	0.012	0.382	0.015	0.478	0.017	0.370	0.005	0.402
C4	0.444	0.015	0.449	0.025	0.397	0.018	0.425	0.007	0.429
F4	0.298	0.009	0.283	0.015	0.467	0.011	0.414	0.021	0.365
F3	0.400	0.008	0.339	0.027	0.445	0.049	0.384	0.020	0.392
F7	0.360	0.021	0.351	0.023	0.518	0.012	0.372	0.011	0.401
F8	0.346	0.024	0.426	0.007	0.493	0.003	0.382	0.011	0.412
FP2	0.402	0.014	0.416	0.088	0.429	0.036	0.371	0.006	0.405
T4	0.412	0.011	0.459	0.012	0.503	0.010	0.378	0.023	0.438
T3	0.472	0.017	0.567	0.024	0.457	0.025	0.477	0.015	0.493
T6	0.392	0.011	0.402	0.022	0.565	0.026	0.404	0.008	0.441
T5	0.317	0.007	0.307	0.014	0.335	0.023	0.378	0.020	0.334
P4	0.485	0.009	0.537	0.002	0.487	0.017	0.457	0.005	0.492
P3	0.339	0.003	0.352	0.011	0.397	0.013	0.360	0.021	0.362
Pz	0.392	0.018	0.505	0.032	0.500	0.018	0.478	0.008	0.469
O2	0.377	0.020	0.374	0.033	0.494	0.015	0.377	0.007	0.415
O1	0.495	0.005	0.430	0.022	0.534	0.013	0.379	0.005	0.460

As can be seen from tables 16 and 17, channels of Fp1, Pz, T3, P4, O1, T4 and T6 for both classifiers have the maximum accuracy. We used these seven channels together, to improve performance of proposed method. We have provided 35 features (7×5) for each 1-sec. In this way, the channel-reduction process is done. We also selected 5, 4, 3 and 2 channels, that they have maximum accuracy. Mean and standard deviations of the classification accuracy for k-NN and SVM are shown in Table 18 and Table 19, separately. As shown in tables, the best seven channels are the same for two classifiers. It shows that these channels may be have more important role in our study. But the best two or three channels for classification are different in each classifier. For example channels Fp1 and Pz in k-NN classifier have better performance, while channels T3 and P4 are better in SVM classifier.

In the other hand, all channels features for an epoch was used. So, 90 (18×5) features were prepared for each epoch. Results of this classifications, also are shown in tables. The best classification accuracy is about 81.51%, when all channels was used for SVM classifier.

Table 18. Classification accuracy of Multi - Channel for k-NN classifier

Channels	Subject 1		Subject 2		Subject 3		Subject 4		Average
	Mean	Std.	Mean	Std.	Mean	Std.	Mean	Std.	
All channels	0.737	0.017	0.644	0.010	0.714	0.024	0.702	0.014	0.699
Fp1,Pz,T3,P4, O1,T4,T6	0.709	0.020	0.585	0.009	0.703	0.019	0.712	0.017	0.677
Fp1,Pz,T3,P4, O1	0.709	0.024	0.625	0.026	0.666	0.022	0.724	0.012	0.681
Fp1,Pz,T3,P4	0.709	0.024	0.807	0.023	0.637	0.020	0.724	0.031	0.719
Fp1,Pz,T3	0.604	0.013	0.767	0.018	0.838	0.003	0.678	0.032	0.721
Fp1,Pz	0.607	0.018	0.717	0.018	0.725	0.012	0.655	0.012	0.675

Table 19. Classification accuracy of Multi - Channel for SVM classifier

Channels	Subject 1		Subject 2		Subject 3		Subject 4		Average
	Mean	Std.	Mean	Std.	Mean	Std.	Mean	Std.	
All channels	0.794	0.014	0.815	0.016	0.916	0.035	0.733	0.019	**0.815**
T3,P4,Pz,O1, Fp1,T4,T6	0.793	0.028	0.809	0.013	0.881	0.005	0.680	0.015	0.791
T3,P4,Pz,O1, Fp1	0.800	0.029	0.781	0.005	0.857	0.016	0.641	0.006	0.770
T3,P4,Pz,O1	0.779	0.017	0.770	0.011	0.787	0.013	0.627	0.015	0.728
T3,P4,Pz	0.676	0.038	0.796	0.001	0.805	0.021	0.656	0.120	0.734
T3,P4	0.655	0.029	0.757	0.021	0.760	0.034	0.640	0.037	0.684

In this approach we found that:

- By using different feature extarction and classification methods, increasing the classification accuracy can be done.
- Channels T3, P4, Pz, O1, Fp1, T4 and T6 are important channels in the gaze at rotating vanes.

3.2.2. Second Approach; Extracting Feature by AR Model and Classification by k-NN, SVM and PLSR

For comforting the subjects and understanding which channels (or lobes) have best performance in the classification accuracy, we tried to classify the EEG by only one channel. Furthermore, three different time-windows were implemented in this approach as mentioned in Table 4. Also 8 subject participated in this approach. After normalization, for each epoch from the training set, 21 features were extracted using by AR method. Then, we selected three classifiers; they are PLSR, SVM and k-NN. After training classifiers, for each epoch from the testing set, 21 features were similarly calculated using AR method. We classified these features and separately calculated classification accuracy for each classifier. Flow chart of this approach is shown in Figure 20.
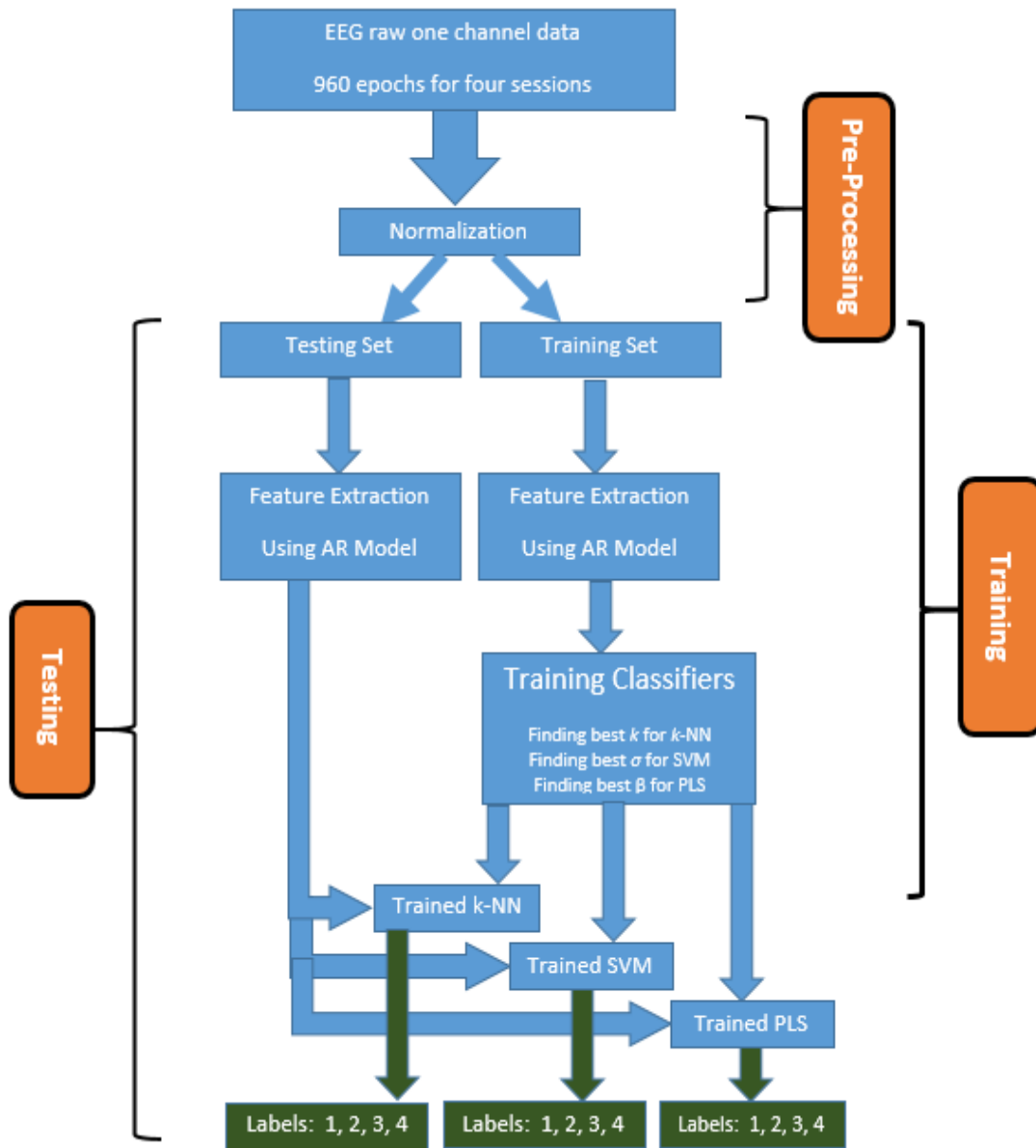
Figure 20. Flowchart of designed System

To verify the results, this method was repeated 10 times with different distributions of training and testing sets. Mean of the classification accuracy in these 10 iterations (for each channel separately) for *k*-NN classifier in three different time-windows are provided in Table 20. Also the average of classification accuracy (ACA) for eight subjects was calculated (for each channel separately) in the last column. Channels of C3, Fp2, T3, T6 and O1 have maximum average of CR in 0.5-sec. epochs and 1-sec. epochs that are bold in the table. In 2-sec. epochs, O2 is instead of Fp2 in this list. The best result of *k*-NN (about 0.8180) is in

the channel C3 when it was used for 2-sec. epochs. The best results of *k*-NN in 0.5 sec. and 1-sec. epochs, are 0.7042 and 0.7799, respectively.

Similarly of *k*-NN, results of Multi-SVM classification, when time-window equals 0.5 second, 1 second and 2 second, were shown in Table 21. ACA of each channel, also was calculated. ACA shows that C3, Fp2, T3, T6 and O2 have the best results in 1-sec. and 2 sec. epochs. In 0.5-sec. epochs, O1 is instead of O2 in this list. The best result of SVM (about 0.8489) is in the channel C3 when it was used for 2-sec. epochs. The best results of SVM in 0.5-sec. and 1-sec. epochs, are 0.7257 and 0.8131, respectively.

Finally, Table 22 shows results of PLSR for three time-windows. ACAs of PLSR show that C3, Fp2, T3, T6 and O2 have the better results in 0.5-sec. and in 1-sec. epochs, instead of O2, there is O1. In 2-sec. epochs, O2, Pz, T3, Fp2 and C3 have the better results. The best result of PLSR (about 0.8848) is in the channel C3 when it used 2-sec. epochs. The best results of PLSR in 0.5-sec. and 1-sec. epochs, are 0.7885 and 0.8621, respectively.

Table 20. Classification accuracy of k-NN for three different time window

0.5 - sec.	Sub. 1	Sub. 2	Sub. 3	Sub. 4	Sub. 5	Sub. 6	Sub. 7	Sub. 8	ACA
FP1	0.5583	0.8472	0.9514	0.6569	0.5694	0.5319	0.5681	0.7056	0.6736
C3	0.7986	0.8708	0.7569	0.7931	0.5653	0.5764	0.6472	0.6250	*0.7042*
FZ	0.5250	0.8222	0.6444	0.5931	0.5333	0.5361	0.6444	0.6833	0.6227
C4	0.5125	0.6958	0.7764	0.5806	0.5500	0.5319	0.5861	0.6625	0.6120
F4	0.6556	0.8486	0.8028	0.6319	0.5014	0.5583	0.5403	0.6611	0.6500
F3	0.5292	0.7472	0.8444	0.5583	0.5278	0.5486	0.7028	0.6903	0.6436
F7	0.5306	0.7403	0.7861	0.5931	0.6167	0.6264	0.6778	0.7486	0.6649
F8	0.5208	0.8167	0.6972	0.5486	0.6597	0.5764	0.5819	0.7458	0.6434
FP2	0.6417	0.8958	0.7819	0.8806	0.5236	0.5139	0.5958	0.7056	*0.6924*
T4	0.5278	0.7194	0.7500	0.5681	0.6431	0.5972	0.5903	0.7028	0.6373
T3	0.7611	0.8333	0.8736	0.7389	0.5125	0.6139	0.6153	0.6194	*0.6960*
T6	0.6417	0.8931	0.9639	0.5319	0.6222	0.6722	0.6125	0.5889	*0.6908*
T5	0.6444	0.8556	0.8278	0.5611	0.5722	0.5500	0.7181	0.5778	0.6634
P4	0.7000	0.8792	0.7069	0.6431	0.5250	0.5208	0.6069	0.6264	0.6510
P3	0.5347	0.8597	0.6750	0.5681	0.5514	0.5472	0.7292	0.5764	0.6302
Pz	0.6875	0.8750	0.7625	0.6417	0.5569	0.5708	0.6556	0.5833	0.6667
O2	0.5708	0.8542	0.7708	0.5417	0.6014	0.6778	0.6986	0.6347	0.6688
O1	0.7917	0.7486	0.7667	0.6083	0.6153	0.7417	0.7208	0.5931	*0.6983*
1 - sec.	Sub. 1	Sub. 2	Sub. 3	Sub. 4	Sub. 5	Sub. 6	Sub. 7	Sub. 8	ACA
FP1	0.5600	0.8854	0.9604	0.6804	0.6475	0.6225	0.7150	0.8133	0.7355
C3	0.8595	0.9000	0.7641	0.8262	0.6725	0.7207	0.7811	0.7151	*0.7799*
FZ	0.5491	0.8287	0.6637	0.6283	0.6040	0.6151	0.7611	0.7846	0.6793
C4	0.5325	0.7387	0.7954	0.5941	0.6050	0.6244	0.7316	0.7568	0.6723
F4	0.7116	0.8662	0.8458	0.6566	0.5920	0.6281	0.6844	0.7337	0.7148
F3	0.5583	0.8137	0.8762	0.5566	0.6429	0.6577	0.8433	0.7781	0.7159
F7	0.5995	0.7787	0.7950	0.5523	0.7087	0.7605	0.7783	0.8550	0.7285
F8	0.4995	0.8750	0.7508	0.5679	0.7577	0.6772	0.6727	0.8466	0.7059
FP2	0.7037	0.9020	0.8012	0.9258	0.6096	0.5966	0.7311	0.7920	*0.7577*
T4	0.5391	0.7266	0.7504	0.5658	0.7253	0.7457	0.6911	0.8040	0.6935
T3	0.8395	0.8662	0.9183	0.8012	0.6031	0.7318	0.7105	0.7207	*0.7739*
T6	0.6937	0.9225	0.9820	0.5150	0.7661	0.8235	0.7350	0.6827	*0.7650*
T5	0.6945	0.8929	0.8212	0.5675	0.6929	0.6272	0.8222	0.7207	0.7299
P4	0.7362	0.8900	0.7262	0.6533	0.6300	0.6124	0.6927	0.7420	0.7103
P3	0.5512	0.8929	0.7333	0.6070	0.6281	0.6624	0.8500	0.6512	0.6970
Pz	0.7283	0.8887	0.7795	0.6795	0.6544	0.7642	0.8005	0.6790	0.7467
O2	0.6500	0.8912	0.8083	0.5283	0.7346	0.8300	0.8222	0.7096	0.7468
O1	0.8120	0.7758	0.7720	0.6020	0.7688	0.8429	0.8600	0.7096	*0.7679*
2 - sec.	Sub. 1	Sub. 2	Sub. 3	Sub. 4	Sub. 5	Sub. 6	Sub. 7	Sub. 8	ACA
FP1	0.5441	0.8966	0.9566	0.6675	0.6529	0.6466	0.7966	0.8404	0.7502
C3	0.9250	0.9266	0.7875	0.8625	0.6945	0.7841	0.8362	0.7279	*0.8180*
FZ	0.5641	0.8600	0.7650	0.6516	0.6425	0.6216	0.8300	0.8112	0.7182
C4	0.5475	0.7516	0.7883	0.6491	0.5987	0.6466	0.7925	0.7883	0.6953
F4	0.7816	0.8916	0.8841	0.6750	0.6237	0.6550	0.7091	0.7925	0.7516
F3	0.6425	0.8158	0.8958	0.5666	0.6737	0.6695	0.9237	0.7904	0.7472
F7	0.6508	0.8083	0.8283	0.5916	0.7570	0.7612	0.8300	0.8529	0.7600
F8	0.5358	0.8900	0.7933	0.5858	0.7779	0.7029	0.7050	0.8425	0.7291
FP2	0.7400	0.9175	0.7933	0.9550	0.6383	0.6570	0.7633	0.8154	0.7850
T4	0.5541	0.7250	0.7441	0.6025	0.7237	0.7612	0.8133	0.8425	0.7208
T3	0.9000	0.8675	0.9200	0.8333	0.5737	0.7258	0.7425	0.7508	*0.7892*
T6	0.7741	0.9241	0.9825	0.5183	0.8237	0.8675	0.8195	0.7008	*0.8013*
T5	0.7333	0.8950	0.8741	0.5766	0.6675	0.6925	0.8987	0.7175	0.7569
P4	0.7716	0.8916	0.7291	0.6525	0.6195	0.6216	0.8175	0.8320	0.7419
P3	0.5816	0.9266	0.7416	0.6166	0.6383	0.6862	0.9341	0.7008	0.7282
Pz	0.7816	0.8925	0.7716	0.6641	0.6695	0.7570	0.905	0.7133	0.7693
O2	0.7008	0.8933	0.8141	0.5533	0.8154	0.8487	0.9404	0.8050	*0.7964*
O1	0.8483	0.7733	0.8033	0.6233	0.7966	0.8904	0.9175	0.7487	*0.8002*

Table 21. Classification accuracy of Multi-SVM for three different time window

0.5 - sec.	Sub. 1	Sub. 2	Sub. 3	Sub. 4	Sub. 5	Sub. 6	Sub. 7	Sub. 8	ACA
FP1	0.5514	0.8903	0.9389	0.6667	0.5764	0.5319	0.5958	0.7403	0.6865
C3	0.8417	0.8944	0.7569	0.7889	0.5486	0.6569	0.6667	0.6514	*0.7257*
FZ	0.5389	0.8194	0.6569	0.6139	0.5361	0.5375	0.6750	0.7139	0.6365
C4	0.5153	0.7403	0.7903	0.5361	0.5514	0.5750	0.6083	0.7222	0.6299
F4	0.7028	0.8569	0.8556	0.5944	0.5125	0.5500	0.5736	0.6903	0.6670
F3	0.5431	0.7833	0.8403	0.5042	0.5514	0.5792	0.7333	0.7333	0.6585
F7	0.5597	0.7625	0.7736	0.5250	0.6278	0.6500	0.6597	0.7611	0.6649
F8	0.5625	0.8417	0.7153	0.5403	0.6431	0.6139	0.5972	0.7319	0.6557
FP2	0.7000	0.9111	0.7861	0.9042	0.5583	0.5417	0.6403	0.7306	*0.7215*
T4	0.5319	0.7306	0.7528	0.5153	0.6597	0.6208	0.6611	0.7278	0.6500
T3	0.7611	0.8569	0.8583	0.7139	0.5375	0.5944	0.6528	0.6486	*0.7030*
T6	0.6250	0.9139	0.9472	0.5250	0.6528	0.7569	0.6347	0.6222	*0.7097*
T5	0.6542	0.8861	0.8514	0.5250	0.5736	0.5792	0.7028	0.6389	0.6764
P4	0.6903	0.8889	0.7236	0.5639	0.5764	0.5319	0.6750	0.6486	0.6623
P3	0.5486	0.8819	0.7056	0.5486	0.5264	0.5750	0.7111	0.6111	0.6385
Pz	0.7000	0.8806	0.7681	0.5736	0.5819	0.5986	0.6944	0.6333	0.6788
O2	0.6014	0.8875	0.7611	0.5347	0.6500	0.6847	0.7417	0.6486	0.6887
O1	0.8014	0.7611	0.7722	0.5625	0.6222	0.6972	0.7361	0.6153	*0.6960*

1 - sec.	Sub. 1	Sub. 2	Sub. 3	Sub. 4	Sub. 5	Sub. 6	Sub. 7	Sub. 8	ACA
FP1	0.5808	0.9200	0.9683	0.7033	0.6900	0.6694	0.7413	0.8294	0.7628
C3	0.8904	0.9258	0.7620	0.8445	0.6905	0.7622	0.8422	0.7874	*0.8131*
FZ	0.5758	0.8550	0.6991	0.6187	0.6494	0.6644	0.8038	0.8133	0.7099
C4	0.5300	0.7875	0.7908	0.5912	0.6494	0.6733	0.7386	0.8090	0.6963
F4	0.7391	0.8841	0.9000	0.6529	0.6155	0.6533	0.7027	0.7938	0.7427
F3	0.6241	0.8491	0.8975	0.5541	0.6730	0.6944	0.8847	0.8179	0.7493
F7	0.6341	0.8404	0.7833	0.5458	0.7505	0.7805	0.7572	0.8327	0.7406
F8	0.5754	0.8741	0.7504	0.5462	0.7613	0.6977	0.7222	0.8327	0.7200
FP2	0.7287	0.9245	0.7941	0.9508	0.6638	0.6205	0.7916	0.8087	*0.7853*
T4	0.5633	0.7566	0.7600	0.5604	0.7505	0.7427	0.7680	0.7948	0.7120
T3	0.8420	0.8875	0.8900	0.7895	0.6450	0.7372	0.7644	0.7874	*0.7929*
T6	0.6616	0.9333	0.9775	0.5291	0.7813	0.8605	0.7930	0.7225	*0.7824*
T5	0.6958	0.9079	0.8650	0.5508	0.6797	0.6877	0.8066	0.7762	0.7462
P4	0.7179	0.9095	0.7350	0.6366	0.6694	0.6266	0.8155	0.7790	0.7362
P3	0.6112	0.9000	0.7379	0.5708	0.6438	0.6800	0.8327	0.7309	0.7134
Pz	0.7391	0.9112	0.8054	0.6470	0.7163	0.7416	0.8511	0.7475	0.7699
O2	0.6941	0.9141	0.8104	0.5483	0.8019	0.7916	0.8866	0.7855	*0.7791*
O1	0.8316	0.7933	0.8095	0.6025	0.7716	0.7888	0.8511	0.7670	0.7769

2 - sec.	Sub. 1	Sub. 2	Sub. 3	Sub. 4	Sub. 5	Sub. 6	Sub. 7	Sub. 8	ACA
FP1	0.5858	0.9166	0.9819	0.7133	0.7133	0.7003	0.7948	0.8207	0.7783
C3	0.9433	0.9388	0.8208	0.8700	0.7170	0.8207	0.8911	0.7892	*0.8489*
FZ	0.5891	0.8625	0.7791	0.6708	0.7170	0.7077	0.8522	0.8429	0.7527
C4	0.5658	0.8152	0.8263	0.6208	0.6855	0.7244	0.7985	0.8300	0.7333
F4	0.8033	0.8777	0.9208	0.6958	0.6374	0.6633	0.7762	0.8003	0.7718
F3	0.6875	0.8750	0.9291	0.5875	0.7096	0.7300	0.9448	0.8300	0.7867
F7	0.6991	0.8444	0.7847	0.5800	0.7966	0.7818	0.8022	0.8540	0.7678
F8	0.5966	0.9125	0.8069	0.5633	0.7966	0.7133	0.7874	0.8485	0.7531
FP2	0.7683	0.9361	0.8166	0.9700	0.7096	0.6651	0.8522	0.8466	*0.8206*
T4	0.5941	0.7611	0.7555	0.5750	0.7966	0.7966	0.8151	0.7929	0.7359
T3	0.9258	0.8958	0.9083	0.8283	0.6503	0.7762	0.8262	0.8022	*0.8266*
T6	0.7150	0.9472	0.9888	0.5408	0.8614	0.9003	0.8374	0.7688	*0.8200*
T5	0.7450	0.9097	0.9000	0.5683	0.6744	0.7337	0.8540	0.8207	0.7757
P4	0.7600	0.9152	0.7555	0.6558	0.6911	0.6725	0.8892	0.8170	0.7695
P3	0.6308	0.9222	0.7444	0.5850	0.6929	0.7096	0.8966	0.7281	0.7387
Pz	0.7916	0.9111	0.8111	0.6391	0.7355	0.7614	0.9522	0.7892	0.7989
O2	0.7466	0.9125	0.8402	0.5691	0.8059	0.8022	0.9318	0.7985	*0.8008*
O1	0.8575	0.7930	0.8152	0.5808	0.8262	0.8040	0.8948	0.7874	0.7949

Table 22. Classification accuracy of PLSR for three different time window

0.5 - sec.	Sub. 1	Sub. 2	Sub. 3	Sub. 4	Sub. 5	Sub. 6	Sub. 7	Sub. 8	ACA
FP1	0.5333	0.8542	0.9056	0.6125	0.5847	0.6125	0.6556	0.7181	0.6845
C3	0.8931	0.8986	0.8097	0.9861	0.5819	0.7167	0.6917	0.6958	*0.7842*
FZ	0.5681	0.8042	0.6819	0.6625	0.5681	0.5736	0.7125	0.7125	0.6604
C4	0.5403	0.7708	0.8361	0.6347	0.5792	0.6153	0.6056	0.6931	0.6594
F4	0.7153	0.8153	0.9236	0.6889	0.5611	0.6042	0.6083	0.7222	0.7049
F3	0.6014	0.7542	0.9139	0.5917	0.5625	0.6236	0.7417	0.7444	0.6917
F7	0.6347	0.7319	0.8278	0.5903	0.6500	0.7028	0.6694	0.7875	0.6993
F8	0.5472	0.8208	0.7611	0.5792	0.7431	0.7264	0.5986	0.7972	0.6967
FP2	0.7014	0.9000	0.7889	0.9764	0.5792	0.6042	0.6944	0.7319	*0.7470*
T4	0.5431	0.7139	0.7583	0.5903	0.6319	0.6236	0.6986	0.7500	0.6637
T3	0.8722	0.8792	0.9403	0.8931	0.6403	0.6917	0.6694	0.7222	*0.7885*
T6	0.6764	0.9194	0.9708	0.5431	0.7028	0.7833	0.6500	0.6444	*0.7363*
T5	0.6889	0.8694	0.8847	0.5694	0.6139	0.6292	0.7764	0.6833	0.7144
P4	0.7792	0.8375	0.7542	0.7042	0.5875	0.5792	0.6736	0.6611	0.6970
P3	0.6389	0.8583	0.7250	0.5861	0.6167	0.6306	0.8028	0.6542	0.6891
Pz	0.7403	0.8611	0.8125	0.7417	0.5722	0.6708	0.7375	0.6528	0.7236
O2	0.6236	0.8528	0.8806	0.6056	0.6986	0.7875	0.7917	0.6903	*0.7413*
O1	0.7986	0.6806	0.7486	0.6042	0.6861	0.7722	0.8014	0.6722	0.7205
1 - sec.	Sub. 1	Sub. 2	Sub. 3	Sub. 4	Sub. 5	Sub. 6	Sub. 7	Sub. 8	ACA
FP1	0.5620	0.8825	0.9345	0.6412	0.7012	0.7466	0.7818	0.8364	0.7608
C3	0.9366	0.9141	0.8233	0.9808	0.7179	0.8503	0.8550	0.8188	*0.8621*
FZ	0.6079	0.8266	0.7070	0.7075	0.6707	0.6938	0.8531	0.8003	0.7334
C4	0.5229	0.8091	0.8425	0.6354	0.7031	0.7587	0.7688	0.8151	0.7319
F4	0.7412	0.8304	0.9312	0.6500	0.6475	0.6837	0.7411	0.8059	0.7539
F3	0.6441	0.7800	0.9412	0.5654	0.6985	0.7244	0.8975	0.8624	0.7642
F7	0.6779	0.7750	0.8570	0.5912	0.7494	0.8040	0.8003	0.8985	0.7692
F8	0.5829	0.8233	0.7933	0.5754	0.8327	0.8633	0.7040	0.8642	0.7549
FP2	0.7537	0.8962	0.8129	0.9845	0.6864	0.7096	0.8364	0.8309	*0.8138*
T4	0.5808	0.6866	0.7720	0.5958	0.7448	0.7466	0.7633	0.8253	0.7144
T3	0.9037	0.9004	0.9408	0.9329	0.7559	0.8253	0.7957	0.7800	*0.8543*
T6	0.7025	0.9245	0.9729	0.5508	0.8568	0.8911	0.7892	0.7318	*0.8024*
T5	0.7087	0.8775	0.8962	0.5750	0.7012	0.7448	0.9262	0.7772	0.7758
P4	0.8000	0.8529	0.7320	0.7425	0.6985	0.6772	0.8031	0.7864	0.7616
P3	0.5887	0.8716	0.7554	0.6108	0.7207	0.7392	0.9411	0.7235	0.7439
Pz	0.7662	0.8845	0.8154	0.7854	0.6864	0.7809	0.9105	0.7651	0.7993
O2	0.7295	0.8816	0.8795	0.6229	0.8587	0.9114	0.9262	0.8151	*0.8281*
O1	0.8212	0.6812	0.7266	0.6241	0.8401	0.8883	0.9420	0.8050	0.7911
2 - sec.	Sub. 1	Sub. 2	Sub. 3	Sub. 4	Sub. 5	Sub. 6	Sub. 7	Sub. 8	ACA
FP1	0.5654	0.9075	0.9416	0.6445	0.7175	0.7883	0.8279	0.8467	0.7799
C3	0.9679	0.9283	0.8325	0.9670	0.7659	0.9008	0.9029	0.8133	*0.8848*
FZ	0.5933	0.8608	0.7470	0.7483	0.6878	0.7070	0.9050	0.8133	0.7578
C4	0.5270	0.8083	0.8354	0.6162	0.7190	0.7758	0.7883	0.8425	0.7391
F4	0.7958	0.8429	0.9454	0.6712	0.6393	0.7300	0.8070	0.8425	0.7842
F3	0.7050	0.7495	0.9491	0.5437	0.7112	0.7550	0.9695	0.8612	0.7805
F7	0.7266	0.7783	0.8570	0.5695	0.8190	0.8612	0.8258	0.9216	0.7949
F8	0.5766	0.8366	0.8258	0.5587	0.8737	0.8800	0.7716	0.8904	0.7767
FP2	0.7645	0.8879	0.8112	0.9770	0.7268	0.7550	0.8445	0.8320	*0.8249*
T4	0.5970	0.7096	0.7804	0.5691	0.7425	0.8091	0.8237	0.8591	0.7363
T3	0.9470	0.9025	0.9583	0.9637	0.7643	0.9154	0.8133	0.8112	*0.8845*
T6	0.7137	0.9125	0.9620	0.5279	0.8800	0.9237	0.8320	0.7779	0.8160
T5	0.7300	0.8941	0.9266	0.5570	0.7128	0.7612	0.9550	0.8258	0.7953
P4	0.8354	0.8625	0.7408	0.7720	0.6909	0.7758	0.8654	0.8529	0.7994
P3	0.6312	0.8791	0.7716	0.6279	0.7534	0.7883	0.9925	0.7487	0.7741
Pz	0.8154	0.8925	0.8275	0.8195	0.7268	0.8550	0.9737	0.7841	*0.8368*
O2	0.7766	0.8683	0.8879	0.6304	0.8846	0.9779	0.9654	0.8508	*0.8552*
O1	0.8279	0.6737	0.7516	0.6145	0.8878	0.9091	0.9425	0.8487	0.8070

For the purposes of comparison and discussion between classifiers, Figure 21, 22 and 23 were designed. These figures show ACA of each channel in different time windows. From these graphs, it is also visible that ACA of PLSR in many channels, is %2-8 better than ACA of SVM. Also we can see that channels of C3 and T3 in all time windows and in all classifiers have a better ACA (T3 is an exception in 0.5-sec epochs for SVM classifier).
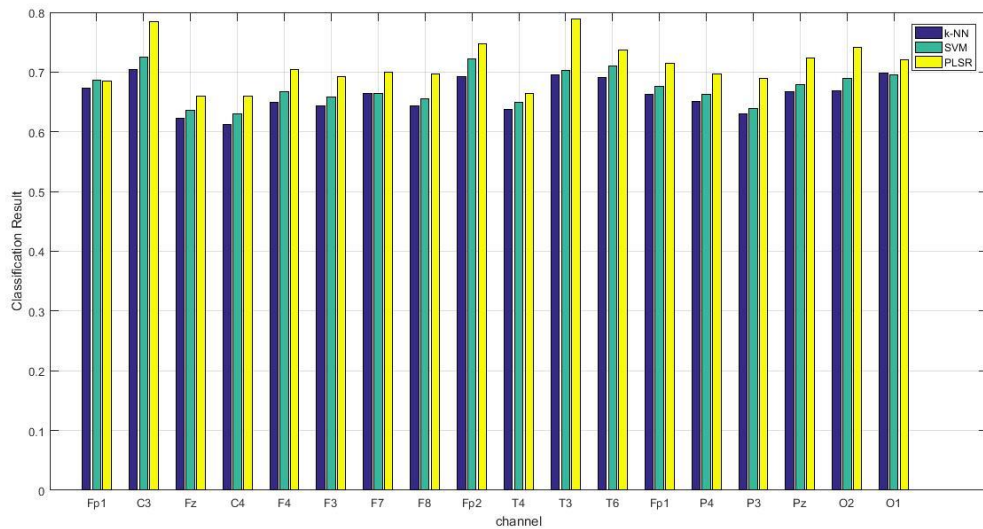

Figure 21. Values of ACA for three classifiers in 0.5-sec epochs
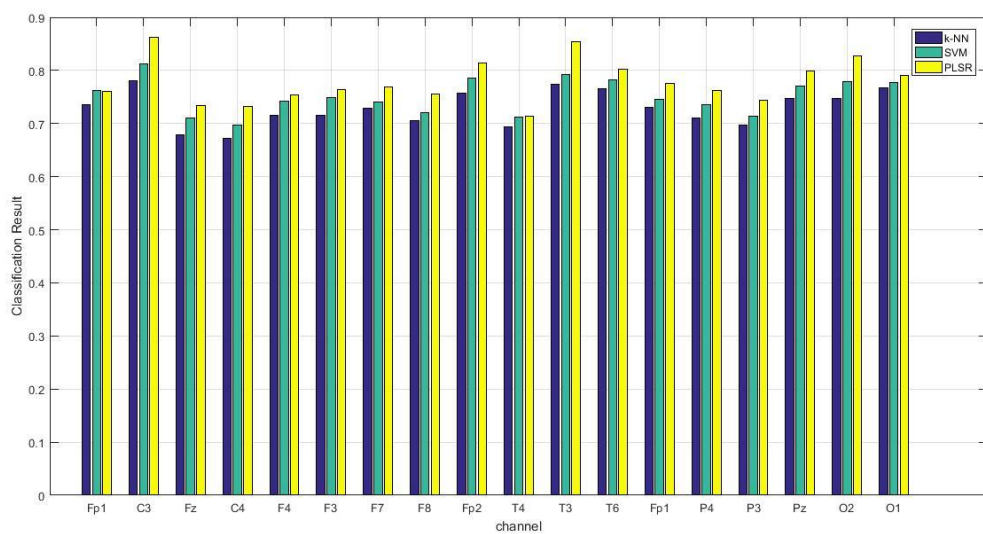

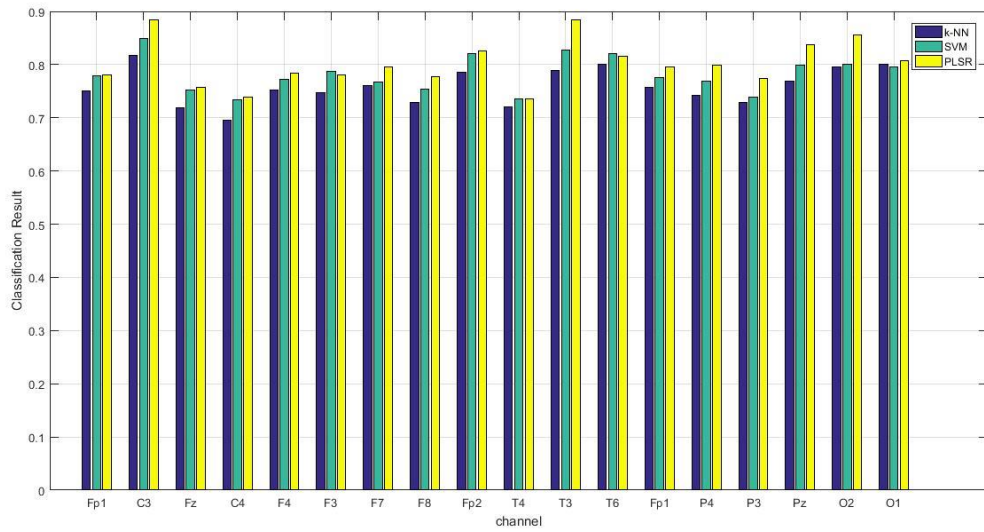Figure 22. Values of ACA for three classifiers in 1-sec epochs

Figure 23. Values of ACA for three classifiers in 2-sec. epochs

In addition, we computed the Information Transfer Rate (ITR) [bits/minute] that it is used as performance metric of BCI systems. Table 23 shows ACAs and related ITRs. It can be seen that the PLSR achieves the best performance among the other classifiers. The maximal ITR is obtained in 0.5-sec epochs in channel T3 about 110.45 bits/min (for ACA 0.7885).

Table 23. Comparison between ACAs and related ITRs for different Time windows

Time window		0.5-sec.			1-sec.			2-sec.		
Channels	*ACA/ITR*	*k*-NN	SVM	PLSR	*k*-NN	SVM	PLSR	*k*-NN	SVM	PLSR
Fp1	*ACA*	0.6736	0.6865	0.6845	0.7355	0.7628	0.7608	0.7502	0.7783	0.7799
	ITR	68.58	72.71	72.06	44.85	50.02	49.63	23.79	26.56	26.72
C3	*ACA*	**0.7042**	**0.7257**	**0.7842**	**0.7799**	**0.8131**	**0.8621**	**0.8180**	**0.8489**	**0.8848**
	ITR	**78.61**	**86.12**	**108.66**	**53.45**	**60.54**	**72.17**	**30.82**	**34.43**	**39.06**
Fz	*ACA*	0.6227	0.6365	0.6604	0.6793	0.7099	0.7334	0.7182	0.7527	0.7578
	ITR	53.51	57.40	64.48	35.20	40.29	44.45	20.87	24.03	24.52
C4	*ACA*	0.6120	0.6299	0.6594	0.6723	0.6963	0.7319	0.6953	0.7333	0.7391
	ITR	50.58	55.52	64.17	34.09	37.97	44.19	18.90	22.22	22.75
F4	*ACA*	0.6500	0.6670	0.7049	0.7148	0.7427	0.7539	0.7516	0.7718	0.7842
	ITR	61.34	66.51	78.85	41.13	46.17	48.29	23.92	25.91	27.17
F3	*ACA*	0.6436	0.6585	0.6917	0.7159	0.7493	0.7642	0.7472	0.7867	0.7805
	ITR	59.46	63.90	74.42	41.32	47.43	50.30	23.51	27.42	26.79
F7	*ACA*	0.6649	0.6649	0.6993	0.7285	0.7406	0.7692	0.7600	0.7678	0.7949
	ITR	65.86	65.86	76.95	43.56	45.78	51.28	24.74	25.51	28.29
F8	*ACA*	0.6434	0.6557	0.6967	0.7059	0.7200	0.7549	0.7291	0.7531	0.7767
	ITR	59.40	63.05	76.08	39.60	42.05	48.49	21.84	24.07	26.39
Fp2	*ACA*	0.6924	**0.7215**	0.7470	0.7577	0.7853	0.8138	0.7850	0.8206	0.8249
	ITR	74.65	**84.62**	93.96	49.04	54.57	60.70	27.24	31.10	31.59
T4	*ACA*	0.6373	0.6500	0.6637	0.6935	0.7120	0.7144	0.7208	0.7359	0.7363
	ITR	57.63	61.34	65.49	37.51	40.65	41.07	21.09	22.45	22.49
T3	*ACA*	**0.6960**	0.7030	**0.7885**	**0.7739**	**0.7929**	**0.8543**	**0.7892**	**0.8266**	**0.8845**
	ITR	**75.85**	78.20	**110.45**	**52.24**	**56.15**	**70.22**	**27.68**	**31.80**	**39.02**
T6	*ACA*	0.6908	0.7097	0.7363	0.7650	0.7824	0.8024	0.8013	0.8200	0.8160
	ITR	74.12	80.49	89.97	50.47	53.96	58.20	28.97	31.04	30.61
T5	*ACA*	0.6634	0.6764	0.7144	0.7299	0.7462	0.7758	0.7569	0.7757	0.7953
	ITR	65.40	69.46	82.12	43.82	46.83	52.63	24.43	26.30	28.33
P4	*ACA*	0.6510	0.6623	0.6970	0.7103	0.7362	0.7616	0.7419	0.7695	0.7994
	ITR	61.64	65.06	76.18	40.36	44.97	49.78	23.01	25.68	28.77
P3	*ACA*	0.6302	0.6385	0.6891	0.6970	0.7134	0.7439	0.7282	0.7387	0.7741
	ITR	55.60	57.97	73.56	38.09	40.89	46.39	21.76	22.71	26.13
Pz	*ACA*	0.6667	0.6788	0.7236	0.7467	0.7699	0.7993	0.7693	0.7989	0.8368
	ITR	66.42	70.23	85.37	46.93	51.43	57.52	25.66	28.71	32.98
O2	*ACA*	0.6688	0.6887	0.7413	0.7468	0.7791	0.8281	0.7964	0.8008	0.8552
	ITR	67.07	73.43	91.82	46.94	53.28	63.94	28.44	28.92	35.22
O1	*ACA*	0.6983	0.6960	0.7205	0.7679	0.7769	0.7911	0.8002	0.7949	0.8070
	ITR	76.61	75.85	84.27	51.03	52.85	55.77	28.85	28.28	29.59

Finally, the training and testing times of the each classifier were computed on a PC with an Intel Pentium® 5 processor with 2.67 GHz and 4 GB RAM. Table 24 shows speed of these classifiers for three different Time windows. For example when we used 2-sec. epochs, we have 240 epochs that PLSR can be trained and tested them only in 5.066 seconds. This time for *k*-NN and SVM is about 12.106 and 24.168 seconds. In 0.5-sec epochs, 960 epochs generated that PLSR can be trained and classified them only in 7.303 seconds that this time for *k*-NN and SVM is about 17 and 122 seconds. Therefore, the results show that PLSR has better training and testing time and it is faster than other classifiers.

Table 24. Speed of three classifiers

Time window/Algorithms	PLSR	*k*-NN	SVM
2-sec. (240 epochs)	~5.066 seconds	~12.106 seconds	~ 24.168 seconds
1-sec. (480 epochs)	~7.011 seconds	~13.848 seconds	~55.066 seconds
0.5-sec. (960 epochs)	~7.303 seconds	~17.399 seconds	~122.408 seconds

In this approach we found that:

- By using different feature extarction and classification methods, the classification accuracy can be increased.
- Channels T3 and C3 are important channels in the gaze at rotating vanes.
- By using 2-sec epochs, we can classified about 89% accuracy.
- PLSR is very fast and accurate classifier.
- By using 0.5-sec epochs, we can achive about 110 bit/sec ITR.

3.3. A Novel Spelling System

By considering the results of previous sections, in this section we propose a new spelling system. Besides four rotating vanes, a constant vane (with no rotation) was added to vanes. This section has two approaches; in the first approach, we have 4 subject and in the second, we have 9 subject. In the first approach, by using welch method, we confirm findings of previous sections, for five different vanes. And in the second approach, by using this confirmation, we propose a new spelling system.

3.3.1. First Approach; Analysis of EEG Signals By Welch Method

Using Matlab 2016b, five rotating red vanes in a black screen were designed. Under each vane, five letters of alphabet were written in white (in total 25 letters). Speed and direction of the rotation could be controlled. The rotating vanes have these specifications in order:

- Vane 1 has the slow mode in an anti-clockwise manner.
- Vane 2 has the slow mode in a clockwise manner,
- Vane 3 has the constant mode (no rotation),
- Vane 4 has the fast mode in an anti-clockwise manner,
- Vane 5 has the fast mode in a clockwise manner.

Screenshot of the rotating vanes is shown in Figure 24.
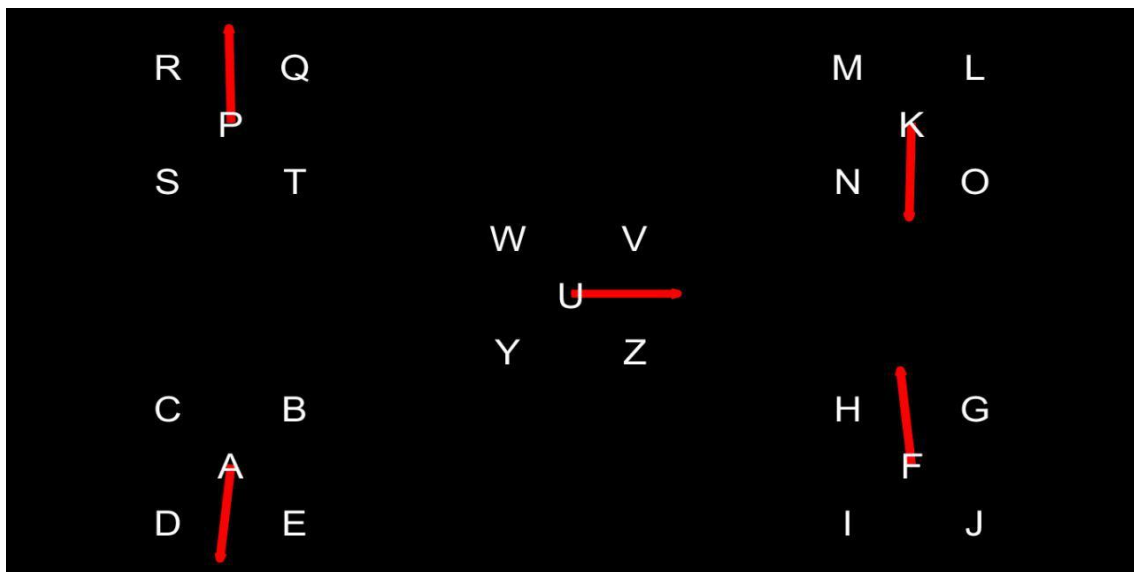
Figure 24. Rotating vanes designed by Matlab

EEG signals were obtained from four healthy subjects (males) in the age groups between 20 and 25 years old. Each one of the subjects was asked to gaze at each vanes for 2-min. There was a 1-min gap for relaxation between gazing at each vanes. After this 10-min (each vane 2-min) EEG recording, we asked the subjects that gaze at each vane 8-sec. for each vane, 4 times was repeated. Paradigm of this approach is described as following.

With using a beep sound, the subjects started to gaze at the Intended vanes. In the end of 8-sec, with using another beep sound, subjects stopped to gaze at the vanes. In the analyzing step, first 3-sec was not used. This duration is for finding the vane in the screen. The next 4-sec was used to analyze. Figure 25 is shown this paradigm.
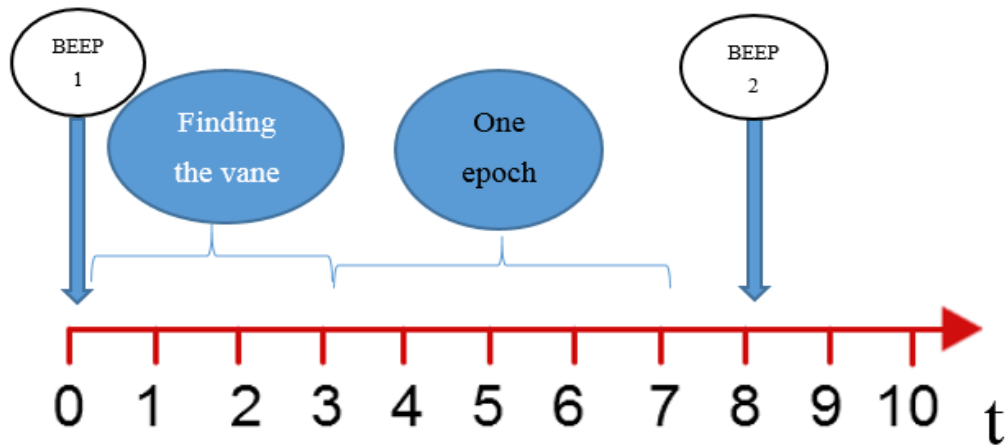

Figure 25. Used paradigm for generated one epoch

For analysis the signal, We divided 2 min signals to 4-sec epochs. In this case, for each vane, we have 30 epoch (in a channel). By using Common Average Reference (CAR), the mean of all the channels is removed for each channel. It works such as a filter, a spatial filter which could further increase the signal-to-noise ratio (SNR) of data [98]. For example for channel O1, we have Equation 18.

$$(O1, CAR)=O1 - (Fp1+Fp2+F7+\ldots+Fz+O1+O2)/18 \tag{18}$$

For these new signals, we implemented welch method to calculate the power spectrum. We use hamming window with length of 256 and 128 samples overlapping. After implementation of Welch method to each 4-sec epoch, mean of power for all epochs of each channel calculated. For all four subjects, we found that, in some channels, for vane 3 (constant vane), the power spectrum shows a significant increase between 6-14 Hz. The channels that are common in four subjects are T3, C3 and O1. For example, Figure 26 shows the power spectrum of channel T3 for five vanes for subject 4.
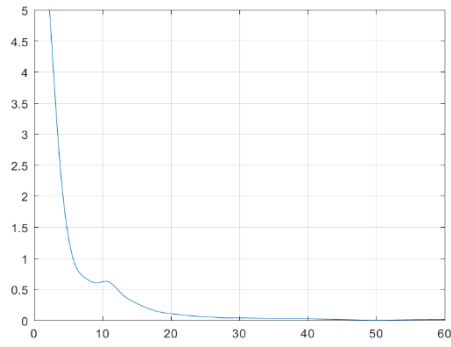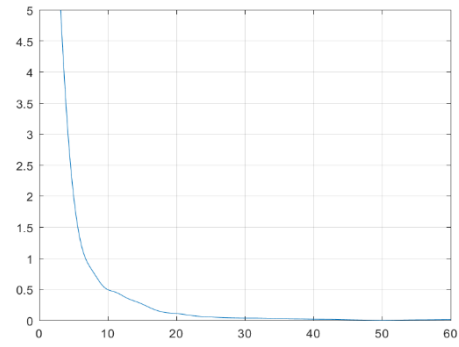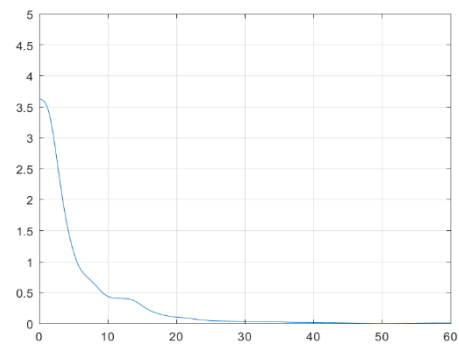
(a)   (b)
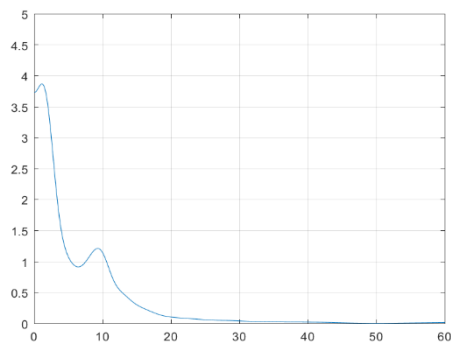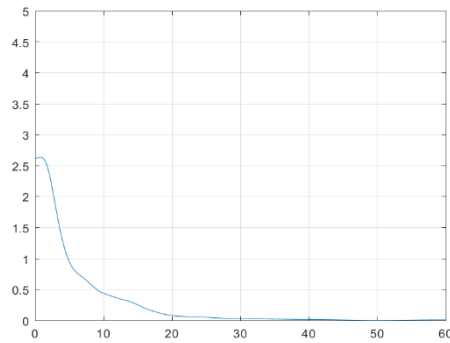
(c)   (d)

(e)

Figure 26. Power spectrum of five different vanes; (a) Vane 1,(b) Vane 2, (c) Vane 3 (constant vane),(d) Vane 4, (e) Vane 5.

As can be seen from Figure 26 (c), there is a significant increase between 6-14 Hz that we cannot see any increasing in the other powers. For confirmation this finding, we implemented the Equation 19.

$$K = A/C - B/C \qquad\qquad (19)$$

That A, B and C are integrals of power between 6-14 Hz, integral of 14-22 Hz and integral of total power (0-60 Hz), respectively. Equation 19 was used for all channels and it confirmed three selected channels. Value of K for vane 3 is maximum in three channels. Figure 27 shows the value of K for channel T3, in subject 4.
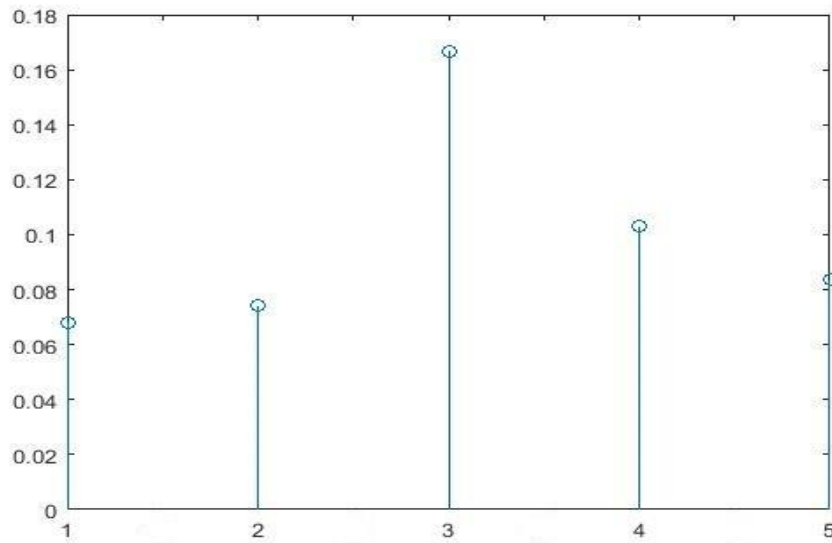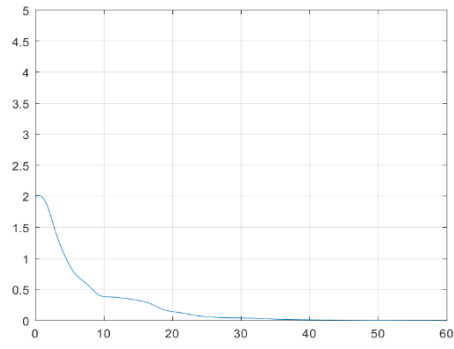

Figure 27. Value of K for each vane

In continue, we repeated these steps for 8-sec epochs. After selection 4-sec epochs and implementation of Equation 18, welch method was used. Results of previous approach was repeated. Power spectrum of channel T3, for subject 4 is shown in Figure 28. Also value of K was computed that is seen in Figure 29.

(a)
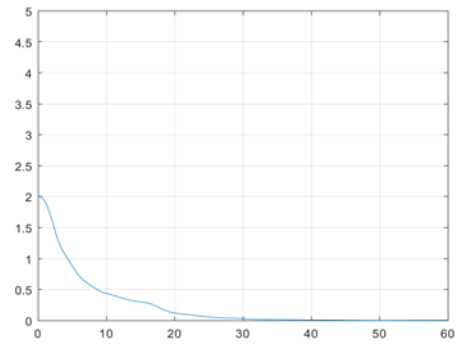
(b)
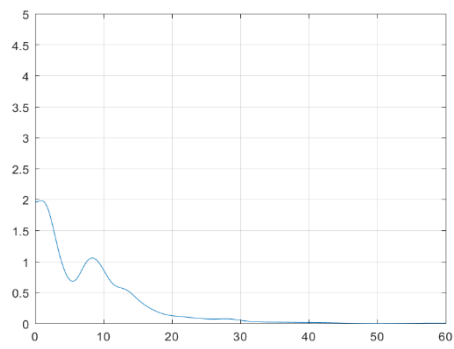
(c)

(d)

(e)

Figure 28. Power spectrum of five different vanes; (a) Vane 1,(b) Vane 2, (c) Vane 3 (constant vane),(d) Vane 4, (e) Vane 5.
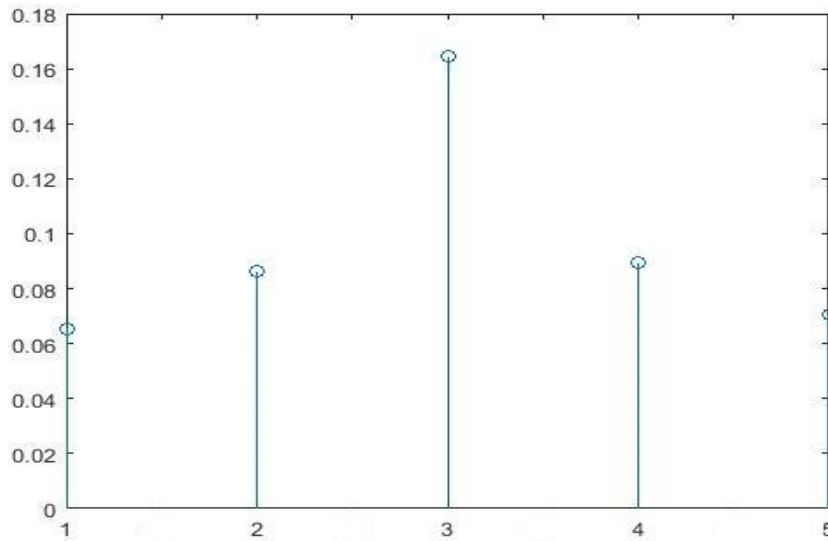
Figure 29. Value of K for each vane for channel T3

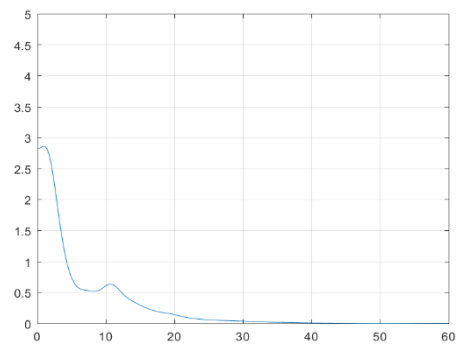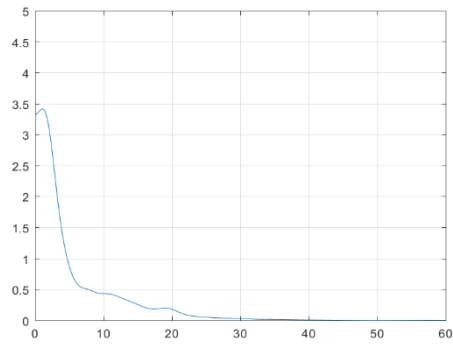In summary, by using welch method to access power spectrum, we found that frequency of between 6-14 Hz EEG signal in three channel is important when the subjects are gazing at rotating vanes. These channels are T3, C3 and O1. By the way, we know from the previous sections (when we had four rotating vanes or when we had only one rotating vane) these channels had better performance in comparing others. By knowing this information, in the next approach, we propose a new spelling system.

3.3.2. Second Approach; Extracting Feature by AR Model and Classification by PLSR

In this approach with using findings of previous approach, we propose a new spelling system in the offline mode. To confirm the results, 9 subjects participated in this approach. Our proposed spelling system has two screen. At first screen, to spell of a letter such as "M", all alphabet are shown to subject. In the middle of screen letter of "M" was written in red. Screenshot of first screen are shown in Figure 30. In the second screen, five letter that are in group of letter "M" ("L","K","N" and "O") are shown to the subject. Screenshot of second screen are shown in Figure 31.
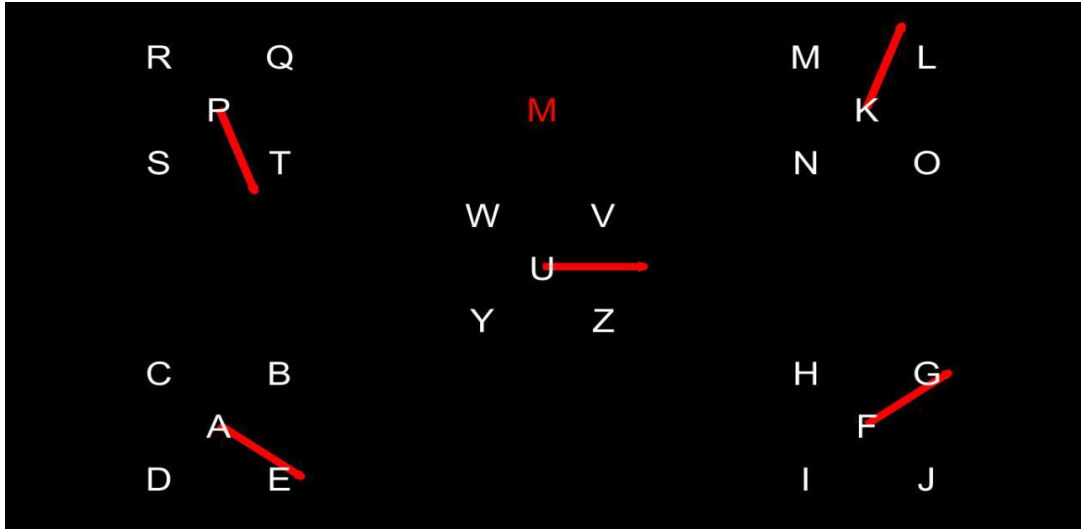
Figure 30. First screen of the proposed spelling system
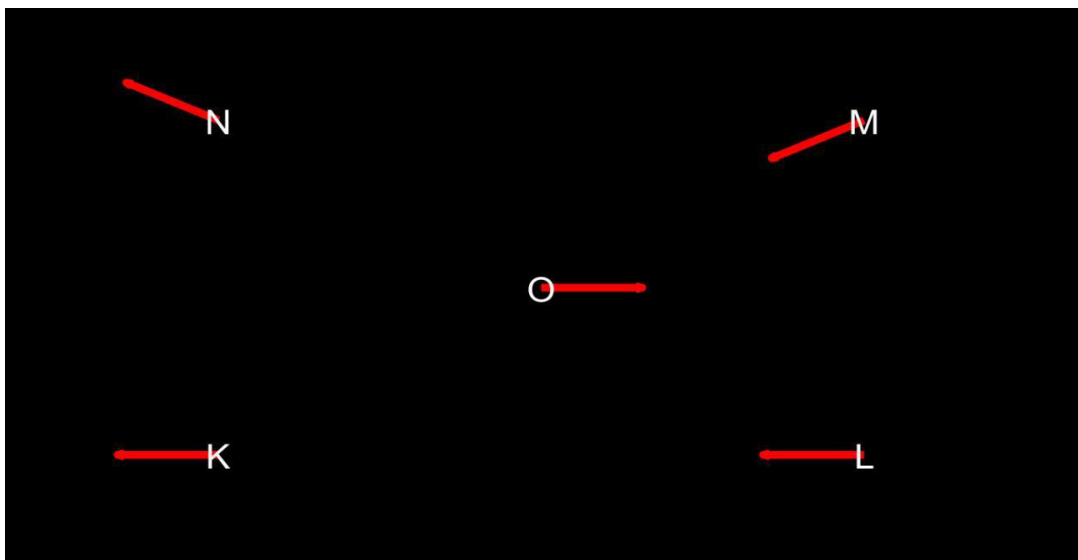
Figure 31. Second screen of the proposed spelling system

To test the proposed spelling system, five words involve five letters were selected for spelling. They are: 'alpha', 'pizza', 'quick', 'paper' and 'apple'. These words are shown to subject automatically. Each screen was shown 7 sec., that we used only 4 second of end. Nine subjects are selected with a mean age of 22 years. The task is to perform the selected words to a cue. After a 2-min relaxation, the task was repeated. In this case, each subject gazing at each vane 10 times in each period. First period's epochs was used as a training

dataset and second period's epochs was used as a testing dataset. We divided 4-sec epochs to 2-sec epochs to extract features.

After normalization the epochs between [-1, 1], by using two Butterworth band pass filters in the order of three for 6-14 Hz and 14-22 Hz, the epochs were ready to extract features. We used AR model for extracting features. 10 AR coefficients were the whole of features in each frequency band, which meant that the present feature vector had 20 dimensions for any epoch. Now features are ready for classification. PLSR used as powerful classifier. The classification accuracy of each channel for 9 subjects were given in Table 25. Also ACA is seen in the table. In the last column, ITR of any ACA was computed.

Table 25. Classification accuracy, ACA and ITR for proposed spelling system

CH.	S.1	S.2	S.3	S.4	S.5	S.6	S.7	S.8	S.9	ACA	ITR
O1	0.650	0.616	0.933	0.441	0.691	0.458	0.783	0.608	0.458	*62.6*	*18.6*
O2	0.408	0.583	0.683	0.491	0.391	0.475	0.966	0.566	0.541	56.7	14.1
Fz	0.558	0.625	0.825	0.508	0.416	0.458	0.750	0.566	0.541	58.3	15.2
Pz	0.616	0.633	0.550	0.491	0.600	0.425	0.825	0.516	0.558	57.9	14.9
P3	0.466	0.616	0.733	0.550	0.550	0.433	0.633	0.525	0.533	56.0	13.5
P4	0.466	0.625	0.783	0.500	0.491	0.466	0.716	0.508	0.491	56.1	13.6
T5	0.450	0.625	0.691	0.491	0.433	0.475	0.716	0.483	0.758	56.9	14.2
C3	0.425	0.575	0.725	0.450	0.441	0.691	0.883	0.566	0.650	*60.0*	*16.5*
C4	0.458	0.608	0.783	0.508	0.408	0.583	0.791	0.575	0.591	58.9	15.7
T6	0.616	0.608	0.725	0.525	0.416	0.475	0.700	0.516	0.675	58.4	15.3
T4	0.475	0.683	0.883	0.516	0.483	0.641	0.908	0.475	0.491	*61.7*	*17.9*
T3	0.783	0.525	0.833	0.558	0.550	0.591	0.883	0.616	0.533	*65.2*	*20.8*
F7	0.500	0.475	0.600	0.400	0.458	0.541	0.875	0.841	0.508	57.7	14.8
F8	0.508	0.791	0.700	0.458	0.433	0.575	0.725	0.600	0.516	58.9	15.7
F3	0.525	0.550	0.550	0.466	0.550	0.516	0.716	0.508	0.458	53.7	12.0
F4	0.508	0.525	0.708	0.558	0.533	0.591	0.683	0.608	0.458	57.5	14.6
Fp2	0.583	0.741	0.816	0.691	0.650	0.641	0.800	0.858	0.633	*71.2*	*26.4*
Fp1	0.750	0.625	0.891	0.766	0.558	0.641	0.700	0.875	0.575	*70.9*	*26.1*

4. DISCUSSION

As mentioned above, these thesis was done in three sections and each section has two subsection. By using each section's results, we designed the next section's paradigm. In each section different subjects were participated to our EEG recording.

In the first section, we had one rotating vane. Two rotation speeds were defined: one rotation per 5 sec and one rotation per 1 sec. To start, EEG signals were obtained from 8 healthy human subjects. EEG recording was in three sessions. In the first session, each subject gazed at the clockwise rotating vane at slow speed for 4 min. Afterwards, the subject was asked to gaze the anti-clockwise rotating vane at fast speed for 4 min and the anti-clockwise rotating vane at slow speed for 4 min, respectively. We classified the pairwise of three sessions. For first approach of this section, EEG bands were extracted by FFT. For classification, k-NN was used. Recorded EEG signals in three sessions, were divided into 1 sec., 2-sec., 3-sec. and 4-sec.. In this case, we can test different length of time- windows. The results were shown in Tables 6, 7, and 8. For 1-sec epochs CA is between %59 and %94. Also in 4-sec epochs CA is between %59 and %97. Results show length of time- window has effect in classification accuracy. This section brought us closer to this fact that gazing at different rotating vanes causes different brain waves. In the second approach of this section, we treid to test diffrent methods for feature extraction and classification. Also we tried to decrease the using electrode numbers to five. We used DWT for feature extraction and k-NN and LDC for classification. Five EEG electrodes from two lobes of brain are selected. These electrodes are involved Fp1 and Fp2 in frontal lobe and Pz, P3 and P4 in parietal lobe. A normalization process was implemented to each epoch before extracting features. In this approach only 1-sec. epochs was used. In 1-sec epochs CA is between %61 and %92. Mean of CA for 8 subjects in Session1 & session2 is about %84, in Session1 & session2 is about %84 and in Session1 & session2 is about %84 by LDC. In this approach we found that we can design a new BCIs based on gazing at rotating vane. Also by using different feature extaraction and classification methods, we can increase the classification accuracy. To comfort subjects, we can decrease electrode numbers until one channel.

In the second section using this finding, we designed a new BCIs. We classified four different rotating vanes. In the first approach of this section, we have four subject. Extracting

feature was done by FFT and Classification by k-NN and SVM. For reduction number of channels and the understanding which channels have best performance in the classification, we classified 18 channels, separately. Then based on CA of each channel, seven channels, that they have maximum accuracy, was selected. Using these channels with together, we improved the performance of proposed method. As can be seen from Table 16 and Table 17, channels of Fp1, Pz, T3, P4, O1, T4 and T6 for both classifiers have the maximum accuracy. Also the best seven channels are the same for two classifiers. We used these seven channels together, to improve performance of proposed method. We have provided 35 features (7*5) for each 1-sec. In this way, the channel-reduction process is done. We also selected 5, 4, 3 and 2 channels, that they have maximum accuracy. Mean and standard deviations of the classification accuracy for k-NN and SVM are shown in Table 18 and Table 19, separately. It shows that these channels may be have more important role in our study. But the best two or three channels for classification are different in each classifier. For example channels Fp1 and Pz in k-NN classifier have better performance, while channels T3 and P4 are better in SVM classifier. The best classification accuracy is about 81.51%, when all channels was used for SVM classifier. By using only two channels, we can solve four classification problom about %68.4 by SVM classifier. These channels are T3 and P4. In this approach, we found that by using different feature extarction and classification methods, increasing the classification accuracy can be done. In the second approach of this section, extracting feature was done by AR Model and Classification by k-NN, SVM and PLSR. In this approach, we added four other subject to dataset (total 8 subjects). Normalization and feature extraction were implemented on 1-sec epochs of each channel separately. PLSR exhibited better performance in compare two others. Table 22 shows results of PLSR for three time-windows. ACAs of PLSR show that C3, Fp2, T3, T6 and O2 have the better results in 0.5-sec. and in 1-sec. epochs, instead of O2, there is O1. In 2-sec. epochs, O2, Pz, T3, Fp2 and C3 have the better results. Excetpt Fp2 and C3, other channels are in best list of the previous aproach. The best result of PLSR (about %88) is in the channels of C3 and T3. Also we can see that channels of C3 and T3 in all time windows and in all classifiers have a better ACA (T3 is an exception in 0.5-sec epochs for SVM classifier). We computed the Information Transfer Rate (ITR) [bits/minute] that it is used as performance metric of BCI systems. Table 23 shows ACAs and related ITRs. It can be seen that the PLSR achieves the best performance among the other classifiers. The maximal ITR is obtained in 0.5-sec epochs in channel T3 about 110.45 bits/min (for ACA 0.7885). That it is a good speed for a BCI

system. In this approach we found that by using different feature extarction and classification methods, the classification accuracy can be increased more than ago. Now, we can say that channels T3 and C3 are important channels in the gaze at rotating vanes.

In section three, using previous section, we propose a novel spelling system. As can be seen from Table 25, the channels of Fp2 and Fp1 have maximum of ACA, that it is may be because of eyes moving. They have about %72 and %71 accuracy in 9 subjects. Also ITRs of these channels are 26.4 and 26.1 bits/min. In order to calculate ITR, we consider ACA for 9 subjects. After these two channels, channels of T3, O1, T4 and C3 have the better ACA. Except the channel T4, the other channels are channels that we forecasted them in the previous approaches. Also by using 2-sec epochs our proposed spelling system has ITR about 20.8 bits/min for channel T3. as can be seen for channel T3 ACA is %65.2. The subject S.2 has the lowest CA (0.525) and the subject S.7 has the highest CA (0.883) in channel T3.

It is not possible to compare all studies in BCIs, because they have different experimental setup, methods and data sets. But in summary, by using Table 3, we can compare our study with others. As mentioned in previous sections, BCIs based on SSVEP methods have a good ITR (about 60-100 bits/min). ITR of BCIs based on P300 is about 20-25 bits/min. Our proposed system's ITR is about 21 with using only a channel. Accuracy of it is about %65. With considering that the subjects use only one channel, their eyes will not bother in using the proposed system and they achieve the goal only in one trial, we can ignore from accuracy that seems to be a little. Also we want to highlight this point that in using four rotating vane, the proposed BCIs has %78 accuracy and 110 bits/min in 0.5-sec epochs in only using one channel.

5.   CONCLUSION AND FUTURE WORK

BCI is a kind of communication system that enables the control of devices or communication with others only through the brain's signal activities without using motor activities. This thesis presented a novel approach for brain-computer interface systems. A simple algorithm was developed for the offline identification of different rotating vanes from EEG signals without any training phase. The results showed that the proposed algorithm could be used for different applications such as control of a wheelchair, flying a helicopter or driving a car. We implemented this system by using in a novel spelling system.

In the future, we would like to design a suitable BCI system based on rotating vanes for real-time applications. Reduction channels to make the user more comfortable and using different methods for feature extraction and classification to improve the classification result will be pursued in our future works. The goal is non-invasive, asynchronous, fast, and simple BCI system based on EEG, because a BCI system with these properties is very suitable for practical machine control, inexpensive, and potentially portable. Real-time control of a wheelchair, flying a helicopter, or driving a car, and even designing a spelling system are our aims by using the proposed algorithm.

6. REFERENCES

1. Bernhard G., Brendan A. and Gert P., Brain–computer interfaces: A gentle introduction, The Frontiers Collection Springer Berlin Heidelberg, (2010) 1-27.

2. Langhenhove Av., Bekaert MH., and Guyen, N., Using a brain-computer interface for rehabilitation: a case study on a patient with implanted electrodes. 4th International Brain-Computer Interface Workshop and Training Course, Graz, Austria, 2008.

3. Borton DA., Yin M., Aceros J., and Nurmikko A., An implantable wireless neural interface for recording cortical circuit dynamics in moving primates, J Neural Eng 10, 2, (2013) 026010.

4. Lotte, F., Congedo, M., Lecuyer, A., Lamarche F. and Arnaldi, B., A Review of Classification Algorithms for EEG-Based Brain-Computer Interfaces, Journal of Neural Engineering, 4, (2007) 1-13.

5. Wolpaw, J.R., McFarland, D.J., Vaughan, T.M. and Schalk, G., The Wadsworth Center Brain-Computer Interface (BCI) Research and Development Program, IEEE Transactions on Neural Systems and Rehabilitation Engineering, 11, 2, (2003) 1-4.

6. Mason, S.G. and Birch, G.E, A General Framework for Brain-Computer Interface Design, IEEE Transactions on Neural Systems and Rehabilitation Engineering, 11, 1, (2003) 70-85.

7. Cincotti, F., Bianchi, L., Birch, G., Guger, C., Mellinger, J., Scherer, R., R.N. Schmidt, Suarez O.Y. and Schalk G., BCI Meeting 2005 – Workshop on Technology: Hardware and Software, IEEE Transactions on Neural Systems and Rehabilitation Engineering, 14, 2, (2006) 128-31.

8. Palaniappan, R., Two-stage biometric authentication method using thought activity brain waves. Int J Neural Syst, 18, 1, (2008) 59–66.

9. Hasan, B. and Gan, J.Q., Hangman BCI: an unsupervised adaptive self-paced brain-computer interface for playing games, Comput Biol Med, 42, 5, (2012) 598–606.

10. Wilson, J.J. and Palaniappan, R., Analogue mouse pointer control via an online steady state visual evoked potential (SSVEP) brain–computer interface, J Neural Eng, 8, 2, (2011) 025026.

11. Saeid S. and Chambers, J.A., EEG Signal Processing, John Wiley and Sons Ltd, England, 2008.

12. Luria, A.R., Higher Cortical Functions in Man, Basic Books, New York, 1966.

13. Teplan, M., Fundamentals of EEG measurements, <u>Measmt Sci Rev.</u>, 2, 2, (2002).

14. Kropotov, J. D., Quantitative EEG, Event-Related Potentials And Neurotherapy Elsevier Inc., 2009.

15. Towle, L., Vernon, B.J., Suarez D., Tan K. and Robert G., The spatial location of EEG electrodes: locating the best-fitting sphere relative to cortical anatomy, <u>Electroencephalography and clinical neurophysiology</u>, 86, 1, (1993) 1- 6.

16. Jasper, H., The ten-twenty electrode system of the international federation. <u>Electroencephalography and Clinical Neurophysiology</u>, 20, (1958) 371-375.

17. Hammond, D. C., What is Neurofeedback? <u>Journal of Neurotherapy</u>, 10, 4, (2006) 11.

18. Zhang, L., He, W., Miao, X. and Yang, J., Dynamic EEG Analysis via the Variability of Band Relative Intensity Ratio: A Time-Frequency Method, Annual International Conference of the IEEE Engineering in Medicine and Biology Society. IEEE Engineering in Medicine and Biology Society, New York City, New York, 2006.

19. Heinrich, H., Gevensleven, H., and Strehl, U., Annotation: Neurofeedback - train your brain to train behaviour, <u>Journal of Child Psychology and Psychiatry</u>, 48, 1, (2007) 3–16.

20. Lukas, S. E., Mendelson, J. H., and Benedikt, R., Electroencephalographic correlates of marihuana-induced euphoria, <u>Drug and alcohol dependence</u>,), 37, 2, (1995) 131–40.

21. Zhang, Y., Chen, Y., Bressler, S. L., and Ding, M., Response preparation and inhibition: The role of the cortical sensorimotor beta rhythm, <u>Neuroscience</u>, 156, 1, (2009) 238–246.

22. Rangaswamy, M., Porjesz, B., Chorlian, D. B., Wang, K., Jones, K. a. and Bauer, L. O., Beta power in the EEG of alcoholics, <u>Biological psychiatry</u>, 52, 8, (2009) 831–42.

23. Bernier, R., Dawson, G., Webb, S., and Murias, M. EEG mu rhythm and imitation impairments in individuals with autism spectrum disorder, <u>Brain and cognition</u>, 64, 3, (2009) 228–37.

24. Fatourechi, M., Bashashati, A., Ward, R.K. and Birch, G.E., EMG and EOG artifacts in brain computer interface systems: A survey, <u>Clin. Neurophysiol</u>, ,118, 2007, 480–494.

25. Croft, R.J. and Barry, R.J., Removal of ocular artifact from the EEG: A review, <u>Neurophysiol</u>, 30, (2000) 5–19.

26. Changmok, C., Micera, S., Carpaneto, J. and Jung, K., Development and quantitative performance evaluation of a noninvasive EMG computer interface, IEEE Trans. Biomed. Eng., 56, (2009) 188–191.

27. Nojd, N., Hannula, M. and Hyttinen, J., Electrode Position Optimization for Facial EMG Measurements for Human-Computer Interface, 2nd International Conference on Pervasive Computing Technologies for Healthcare (PCTH 11), Dublin, 2008.

28. Inhyuk, M., Myoungjoon, L. and Museong, M., A Novel EMG-Based Human-Computer Interface for Persons with Disability, IEEE International Conference on Mechatronics (ICM'04), Tunisia, 2004.

29. Gomez-Gil, J., San-Jose-Gonzalez, I., Nicolas-Alonso, L.F. and Alonso-Garcia S., Steering a tractor by means of an EMG-based human-machine interface, Sensors 11, (2011) 7110–7126.

30. Nan, B., Okamoto, M. and Tsuji, T., A hybrid motion classification approach for EMG-based human-robot interfaces using bayesian and neural networks, IEEE Trans. Robot, 25, 2009 502–511.

31. Zhang, X., Chen, X., Lantz, V., Yang, J.H. and Wang, K.Q., Exploration on the Feasibility of Building Muscle-Computer Interfaces Using Neck and Shoulder Motions, Annual International Conference of the IEEE Engineering in Medicine and Biology Society (EMBC'09), Minneapolis, 2009.

32. De la Rosa, R., Alonso, A., Carrera, A., Durán, R. and Fernández, P., Man-machine interface system for neuromuscular training and evaluation based on EMG and MMG signals, Sensors (Basel), 10, 12, (2010) 11100–11125.

33. Eckhouse, R.H. and Maulucci, R.A., A multimedia system for augmented sensory assessment and treatment of motor disabilities., Telemat. Inf, 14, (1997) 67–82.

34. Nicolas Alonso L. F. and Gomez Gil J., Brain computer interfaces, a review. Sensors, 12, 2, (2012) 1211–1279.

35. Wolpaw, J.R., Birbaumer, N., Heetderks, W.J., McFarland, D.J., Peckham, P.H., Schalk, G., Donchin, E., Quatrano, L.A, Robinson, C.J. and Vaughan, T.M., Brain-computer interface technology: a review of the first international meeting, Rehabilitation Engineering, IEEE Transactions, 8, 2, (2000) 164-173.

36. Kelly S.P., Lalor, E.C., Finucane, C., McDarby, G. and Reilly, R.B., Visual spatial attention control in an independent brain-computer interface, IEEE Transactions on Biomedical Engineering, 52, 9, (2005) 1588-1596.

37. Xiaorong G., Dingfeng X., Ming Ch. and Shangkai G., A BCI-based environmental controller for the motion-disabled, IEEE Transactions on Neural Systems and Rehabilitation Engineering, 11, 2, (2003) 137-140.

38. Langhenhove A.V., Bekaert M-H. and N'Guyen J-P. Using a brain-computer interface for rehabilitation: a case study on a patient with implanted electrodes, 4th International Brain-Computer Interface Workshop and Training Course, Graz, 2012.

39. Borton DA., Yin M., Aceros J. and Nurmikko A., An implantable wireless neural interface for recording cortical circuit dynamics in moving primates. J Neural Eng, 10, 2, (2010) 026010.

40. Cheng-Hsuan Ch., Ming-Shan H., Kuo-Kai Sh., Kou-Cheng H., Kuo-Wei W. and Po-Lei L., A noninvasive brain computer interface using visually-induced near-infrared spectroscopy responses, Neuroscience Letters, 580, (2014), 22-26.

41. Ramaswamy P., Electroencephalogram-based Brain–Computer Interface: An Introduction, Guide to Brain-Computer Music Interfacing, (2014), 6584-2.

42. He B., Neural Engineering. Springer. 2nd ed. 2013.

43. Zhenghua, W., Yongxiu L., Yang X., Dan W. and Dezhong Y., Stimulator selection in SSVEP-based BCI, Medical Engineering and Physics, 30, 8, (2008) 1079-88.

44. Zhu D., Bieger J., Garcia Molina G.R. and Aarts M., A survey of stimulation methods used in SSVEP-based BCIs. Computational Intelligence and Neuroscience. Hindawi Publishing Corporation, 2010.

45. Lim J.H., Hwang H.J., Han C.H., Jung K.Y. and Im C.H., Classification of binary intentions for individuals with impaired oculomotor function: 'eyes close' SSVEP-based brain-computer interface (BCI), J Neural Eng, 10, 2, (2013) 026021.

46. Donchin E., Spencer K.M. and Wijesinghe R. The mental prosthesis: assessing the speed of a P300-based brain-computer interface, IEEE Trans Rehabil Eng, 8, 2, (2000) 174–179.

47. Keirn Z.A. and Aunon J.I. A new mode of communication between man and his surroundings, IEEE Trans Biomed Eng, 37, 12, (1990) 1209–1214.

48. Jain, A.K., Duin, R.P.W. and Jianchang, M., Statistical pattern recognition: A review. IEEE Trans. Pattern Anal, 22, (2000), 4–37.

49. Corinna C. and Vladimir V., Support-vector networks, Machine learning, 20, 3, (1995) 273-297.

50. Anguita, D., Ridella, S. and Fabio R., K-Fold Generalization Capability Assessment for Support Vector Classifiers, International Joint Conference on Neural Networks, Montreal, Canada, 2005.

51. Alippi C. and Roveri M., Virtual k-fold cross validation: an effective method for accuracy assessment, IEEE International Joint Conference on Neural Networks (IEEE IJCNN 2010), Barcelona, Spain, 2010.

52. Jonathan R.W., Niels B., William J. H., Dennis J. McFarland, P. Hunter P., Gerwin S., Emanuel D., Louis A. Q., Charles J. R., and Theresa M. V., Brain–Computer Interface Technology: A Review of the First International Meeting, <u>IEEE transactions on rehabilitation engineering</u>, 8, 2, (2000).

53. Hill N. J., Lal T. N., Bierig K., Birbaumer N. and Schölkopf B., Attention modulation of auditory event-related potentials in a brain–computer interface, IEEE Int. Workshop on Biomedical Circuits and Systems, 2004.

54. Hill N. J. and Schölkopf B., An online brain–computer interface based on shifting attention to concurrent streams of auditory stimuli, J. Neural Eng., 9, (2012) 026011.

55. Kanoh S., Miyamoto K. and Yoshinobu T., A brain–computer interface (BCI) system based on auditory stream segregation, <u>J. Biomech. Sci. Eng.</u>, 5, (2012) 32–40.

56. Hubert C. and Axel G., Convolutional Neural Networks for P300 Detection with Application to Brain-Computer Interfaces, <u>IEEE Transactions on Pattern Analysis and Machine Intelligence</u>, 33, 3, (2011) 433-45.

57. Rifai Ch., S. H., Ling, P., Hunter, Y., Tran and H. T. Nguyen, Brain–Computer Interface Classifier for Wheelchair Commands Using Neural Network With Fuzzy Particle Swarm Optimization, <u>IEEE Journal Of Biomedical And Health Informatıcs</u>, 18, 5, (2014).

58. Ji Q., Wechsler H., Duchowski A. T. and Flickner M., Special issue: eye detection and tracking, <u>Comput. Vis. Image Underst</u>., 98, (2005) 1-3.

59. Kawato S. and Tetsutani N., Detection and tracking of eyes for gaze-camera control, <u>Image Vis. Comput</u>., 22, (2004) 1031-1038.

60. Kim J., A simple pupil-independent method for recording eye movements in rodents using video , <u>J. Neurosci. Methods</u>, 138, (2004) 165-171.

61. Abdelkader N., Hideaki H., Natsue Y., Duk S. and Yasuharu K., Classification of Four Eye Directions from EEG Signals for Eye-Movement-Based Communication Systems, <u>Journal of Medical and Biological Engineering</u>, 34, 6, (2014) 581-588.

62. Muller-Putz G. R., Scherer R., Neuper C. and Pfurtscheller G., Steady-state somatosensory evoked potentials: suitable brain signals for brain–computer interfaces?, <u>IEEE Trans. Neural Syst. Rehabil. Eng</u>., 14, (2006) 30–7.

63. Zhang D., Wang Y., Maye A., Engel A. K., Gao X., Hong B. and Gao S., A brain–computer interface based on multi-modal attention, 3rd Int. IEEE/EMBS Conf. on Neural Engineering, (CNE '07), Hawaii, 2007.

64. Brouwer A. M. and Van Erp J. B., A tactile P300 brain–computer interface, <u>Front. Neurosci.</u>, 4, (2010) 036003.

65. Dat T.H., Shue L. and Guan C., Electrocorticographic signal classification based on time-frequency decomposition and nonparametric statistical modeling, 28th IEEE EMBS Annual International Conference, New York City, USA 2006.

66. Oppenheim A. V. and Schafer R. W., Discrete-Time Signal Processing, Prentice-Hall, 1989, 611-619.

67. Welch P.D., The use of fast Fourier transform for the estimation of power spectra: a method based on time averaging over short, modified periodograms, <u>IEEE Transactions on Audio and Electroacoustics</u>, (1967).

68. Burrus C.S. and Perks T.W., DFT/FFT and Convolution Algorithms, <u>Wiley Interscience</u>, (1985).

69. Susmakova, K. and Krakovska, A., Discrimination ability of individual measures used in sleep stages classification, <u>Artificial Intelligence in Medicine</u>, 44, 3, (2008) 261–277.

70. Wold H., Non-linear estimation by iterative least squares procedures, in: F. David (Ed.), <u>Research Papers in Statistics, Wiley</u>, (1966) 411– 444.

71. Wold H., Model construction and evaluation when theoretical knowledge is scare. Theory and application of partial least squares, in: J. Kmenta, J.B. Ramsey (Eds.), Evaluation of Econometric Models, <u>Academic Press</u>, (1980) 47–74.

72. Li, B., Morris, J. and Martin, E. B., Model selection for partial least squares regression, <u>Chemometrics and Intelligent Laboratory Systems</u>, 64, (2002) 79–89.

73. Fix, E. and Hodges, J.L., Discriminatory analysis nonparametric discrimination: consistency properties, <u>International Statistical Review</u>, 4, (1951) 261–279.

74. Cover, T.M. and Hart, P.E., Nearest neighbor pattern classification, <u>IEEE Trans. Inform. Theory</u>, 13, (1968) 21–27.

75. Wu X., Kumar V. and Ross Quinlan J., Top 10 algorithms in data mining, <u>Knowledge and Information Systems</u>, 14, 1, (2008) 1, 1-37.

76. Duda R., ET Hart P. E. and Stark D. G., Pattern classification, 2nd edition, John Wiley, 2000.

77. Enas, G. G. and Choi, S. C., Choice of the smoothing parameter and efficiency of k-nearest neighbor classification, <u>Comput. Math.Applic</u>, 12, (1986) 235–244.

78. Ripley, B.D., Pattern Recognition and Neural Networks, Cambridge University Press, Cambridge, 1996.

79. Efron B., Estimating the Error Rate of a Prediction Rule: Improvement on Cross-Validation, <u>Journal of the American Statistical Association</u>, 78, 382, (1983) 316-331.

80. Huang, P. and Lee. C. H., Automatic Classification for Pathological Prostate Images Based on Fractal Analysis, <u>IEEE Transaction on Medical Imaging</u>, 28, 7, (2009) 1037-1050.

81. Onder, A. and Temel. K., Wavelet Transform Based Classification of Invasive Brain Computer Interface Data, <u>Radio engineering</u>, 20, 1, (2011) 31-38.

82. Onder, A. and Temel. K., Comparative Performance Assessment of Classifiers in Low-Dimensional Feature Space Which are Commonly Used in BCI Applications, <u>Elektrorevue</u>, 2, 4, (2011) 58-63.

83. Temel, K. and Onder. A., A Polynomial Fitting and k-NN Based Approach for Improving Classification of Motor Imagery BCI Data, <u>Pattern Recognition Letters</u>, 31, 11, (2010) 1207-1215.

84. Muller K.R., Anderson C.W. and Birch, G. E., Linear and nonlinear methods for brain-computer interfaces, <u>IEEE Trans. Neural Syst. Rehabil. Eng.</u>, 11, 2, (2003) 165–16.

85. Vapnik, V., Statistical Learning Theory, Wiley: New York, NY, USA, 1998.

86. Burges C. J. C., A tutorial on support vector machines for pattern recognition, <u>Knowledge Discovery and Data Mining</u>, 2, (1998).

87. Bennett K. P. and Campbell C., Support vector machines: hype or hallelujah?, <u>ACM SIGKDD Explorations Newsletter</u>, 2, 2, (2000) 1-13.

88. Blankertz B., Curio G., and Muller K. R., Classifying single trial EEG: Towards brain computer interfacing, <u>Advances in Neural Information Processing Systems,</u> 14, (2002) 157-164.

89. Garrett D., Peterson D. A., Anderson C. W. and Thaut M. H., Comparison of linear, nonlinear, and feature selection methods for EEG signal classification, <u>IEEE Transactions on Neural System and Rehabilitation Engineering</u>, 11, (2003) 141-144.

90. Rakotomamonjy A., Guigue V., Mallet G. and Alvarado V., Ensemble of svms for improving brain computer interface p300 speller performances, In International Conference on Artificial Neural Networks, Berlin 2005.

91. Kaper M., Meinicke P., Grossekathoefer U., Lingner T. and Ritter H., Bci competition 2003, data set iib: support vector machines for the p300 speller paradigm. <u>IEEE Transactions on Biomedical Engeneering</u>, 51, 6, (2004) 1073-1076.

92. McFarland D. J. and Krusienski D. J. BCI signal processing: feature translation BCI Principles and Practice (Oxford, NewYork: Oxford University Press) chapter 8, 2012.

93. Wolpaw J. R., Ramoser H., McFarland D. J. and Pfurtscheller G., EEG-Based communication: improved accuracy by response verification, IEEE Trans. Rehabil. Eng., 6, (1998) 326–33.

94. Wolpaw J. R., Birbaumer N., McFarland D. J., Pfurtscheller G. and Vaughan T. M. Brain–computer interfaces for communication and control, Clin. Neurophysiol, 113, (2002) 767–91.

95. Shannon C. E. and Weaver W., The Mathematical Theory of Communication, Urbana, IL: University of Illinois Press, 1964.

96. Pierce J. R., An introduction to information theory, New York, Dover, 1980.

97. Allison B. Z. and Neuper C., Could anyone use a BCI? (B+H)CI: The human in brain–computer interfaces and the brain in human–computer interaction Brain-Computer Interfaces, Springer, London, 1988.

98. McFarland D. J., McCane L. M., David S. V. and Wolpaw J. R., Spatial filter selection for EEG-based communication, Electroencephalography and Clinical Neurophysiology, 103, 3, (1997) 386–394.

7. APPENDİX

The experimental procedures were approved by the Ethical Committee at Karadeniz Technichal University. Number of ethical committee' report is 24237859-164 in date 05/03/2015.

ÖZGEÇMİŞ

16.02.1983 yılında İRAN-Tebriz'de doğdu. İlk, orta ve lise öğrenimini İRAN'da tamamladı. 2002 yılında Azad İslamic Üniversitesi Mühendislik Fakültesi Elektrik-Elektronik (telekomünikasyon) Mühendisliği Bölümünü kazandı. Yüksek lisans Elektrik-Elektronik Mühendisliğini (sinyel işleme) Azad İslamic Üniversitesi Mühendislik Fakültesinde 2010 da bitirdi. 2011' de Karadeniz Teknik Üniversitesi Elektrik-Elektronik Mühendislik Fakültesi Doktora programını Prof. Dr. Temel KAYIKÇIOĞLU danişmanlığında başladı. 2013 mart ayından beri Avrasya Üniversitesinde Öğretim Görevlisi olarak çalışmaktadır. İyi seviyede İngilizce, Farsça, Türkçe, Azerice ve başlangıç seviyesinde Arapça bilmektedir. Örüntü Tanıma ve Sinyal İşleme, Tıbbi Görüntü işleme, Biyomedikal, Görüntü işleme, Anten Tasarımı, Office, programlama, internet, web tasarım konularıyla ilgilidir. Daha önce lise, orta okul ve üniversite öğrencilerine özel ders vermiş olup öğretmenliği çok sevmektedir. Yaratıcı, takım çalışmalarında başarılı, yeniliklere kolay uyum sağlayabilen bir kişiliğe sahiptir.

SCI, SSCI, AHCI indekslerine giren dergilerde yayınlanan makaleler

1. Maleki, M., Manshouri, N., Kayıkçıoğlu, T., A New Brain-Computer Interface System Based on Classification of the Gaze on Four Rotating Vanes, <u>International Journal of Computer Science and Information Security</u>, 15, 2, (2017) 437-443.

2. Manshouri, N., Maleki, M., Kayıkçıoğlu, T., Classification of Human Vision Discrepancy during Watching 2D and 3D Movies Based on EEG Signals, <u>International Journal of Computer Science and Information Security</u>, 15, 2, (2017) 430-436.

3. Maleki, M., Manshouri, N., Kayıkçıoğlu, T., "A Novel Simple Method to Select Optimal k in k-Nearest Neighbour Classifier", <u>International Journal of Computer Science and Information Security</u>, 15, 2, (2017) 464-469.

4. Maleki, M., Kayıkçıoğlu, T., A New Brain-Computer Interface System Using the Gaze on Rotating Vane, <u>Biomedical research</u>, 27, 1, (2016) 186-190.

5. Kayıkçıoğlu, T., Maleki, M., Eroğlu, K., Fast and Accurate PLS-Based Classification of EEG Sleep Using Single Channel Data, <u>Expert Systems with Applications</u>, 42, 21, (2015) 7825–7830.

Hakemli konferans/sempozyumların bildiri kitaplarında yer alan yayınlar

1. Maleki, M., Manshouri, N., Kayıkçıoğlu, T., Application of PLSR with a Comparison of MATLAB Classification Learner App in Using BCI, 25th Signal Processing and Communications Applications Conference (SIU), Antalya 2017.

2. Manshouri, N., Maleki, M., Kayıkçıoğlu, T., Frequency Analysis of EEG Signal During Watching 2D & 3D Movies Based on PLSR Classifier: a Comparison of Methods, 25th Signal Processing and Communications Applications Conference (SIU), Antalya 2017.

3. Manshouri N., Yazgan, A., Maleki, M., A Microstrip-fed Ultra-Wideband Antenna with Dual Band-Notch Characteristics, 39th Telecommunications and Signal Processing (TSP), Vienna 2016.

4. Maleki, M., Kayıkçıoğlu, T., Classification of EEG Signal during Gaze on the Different Rotating Vanes, 24th Signal Processing and Communications Applications Conference (SIU), Zonguldak 2016.

5. Manshouri N., Yazgan, A., Maleki, M., A Novel Semi-Circular Fractal Antenna Design With Single Band-Notch Property for Ultra Wide Band Systems, 38th Telecommunications and Signal Processing (TSP), Berlin 2015.

6. Maleki, M., Manshouri, N., Kayıkçıoğlu, T., A Novel Brain-Computer Interface Based on The Gaze Rotating Vane Independent EEG, 23th Signal Processing and Communications Applications Conference (SIU), Malatya 2015.

7. Manshouri N., Najafpour, M., Yazgan, A., Maleki, M., Kaya, H., A Novel Rectangular Microstrip Antenna for Ultra-Wideband Applications With Dual Band-Notched Characteristic, 22th Signal Processing and Communications Applications Conference (SIU), Trabzon 2014.

8. Eroğlu, K., Maleki, M., Kayıkçıoğlu, T., Uyku EEG'sinin KEKKR Yöntemi Kullanarak Hızlı ve Yüksek Doğrulukta Sınıflandırılması, 21th Signal Processing and Communications Applications Conference (SIU), Kıbrıs 2013.

9. Maleki, M., Aydemir, O., Manshouri, N., Eroğlu, K., Kayıkçıoğlu, T., k-NN Sınıflandırma Algoritmasında Optimum k Değerinin Belirlenmesi İçin Yeni Bir Yöntem, 21th Signal Processing and Communications Applications Conference (SIU), Kıbrıs 2013.

10. Naseriyan, A., haghipour, S., akhlagh, S., Maleki, M., Neonatal Pain Assessment Based on Facial Expression after Minor Outpatient Surgery, Iranian Student Conference on Electrical Engineering, 2009, Tahran IRAN.